TECHNISCHE UNIVERSITÄT
KAISERSLAUTERN

Vom Fachbereich Mathematik der Technischen Universität Kaiserslautern zur Verleihung des akademischen Grades Doktor der Naturwissenschaften (Doctor rerum naturalium, Dr. rer. nat.) genehmigte Dissertation.

Numerical Homogenization for Linear Elasticity in Translation Invariant Spaces

Dennis Merkert

Gutachter:
Prof. Dr. Bernd Simeon, Technische Universität Kaiserslautern
Prof. Dr. Axel Klawonn, Universität zu Köln

Disputation: 29. Juni 2018

D 386

Contents

1 Introduction

Composite materials are designed for specific elastic behavior, durability, or a high strength at low weight. Such materials consist of multiple pure phases that are intermixed. They can take the form of laminate structures, fiber reinforced structures, or woven or non-woven filaments embedded in a surrounding matrix material. Polycrystals consist of the same material everywhere, but different grains have different orientations. Therefore, polycrystals can also be considered as composites.

A simulation of the elastic properties of such composites often precedes experimental measurements or even replaces them. Especially for large geometries, where the changes in material occur on a much smaller scale, simulations get very large and costly. Homogenization simplifies such simulations by replacing the small-scale composite by a homogeneous material that has — viewed from a macroscopic point of view — the same elastic properties.

In this thesis we solve the homogenization problem numerically, introduce a new discretization approach and test the method on examples.

We assume that the typical scale of microstructure features, like fiber lengths, is much smaller than the macroscopic problem. Mathematically, this introduces a scale separation variable which is very small and requires a periodic microstructure [25]. This periodicity means that the microscopic behavior of the composite can be represented by a single reference volume element that is repeated throughout the macroscopic geometry. Homogenization problems lead then to partial differential equations with periodic boundary conditions. In this thesis, we omit the boundary by searching solutions on the multidimensional torus instead. These equations can be discretized and subsequently solved among others by finite element or finite difference methods. For an overview see for example [84].

Given stiffness data on a regular tensor product grid, Moulinec and Suquet [73, 74] introduce an algorithm based on the fast Fourier transform, the so-called basic-scheme. They reformulate the partial differential equation into a Fredholm integral equation of the second kind, where the kernel is the Green operator. Compared to other solution methods, their algorithm can be implemented easily such that the program works efficiently. The only non-local operation is the discrete Fourier transform, for which highly optimized implementations are available [31]. All other operators are pointwise multiplications, which make parallelization simple. A comparison between fast Fourier transform methods, finite element methods, and other approaches is found in [2, 84, 104].

This discretization method using truncated trigonometric polynomials is analyzed in detail: a convergence proof exists for regular coefficients [102, 105] and for Riemann integrable coefficients [89]. The method can also be interpreted and analyzed as an asymptotically consistent Galerkin discretization [22] and is linked to finite element

methods for general history and time-dependent material models [111].

Moulinec and Suquet solve the partial differential equation using a Neumann-series approach. Other solution techniques for the linear system include grid refinement [30], augmented Lagrangians [67], and other methods suited for arbitrarily high contrasts between the material coefficients [68]. The conjugate gradient method [106, 112] and the fast gradient method of Nesterov [88] can solve the resulting linear system, for an overview and comparison of methods see [70, 75].

Nonlinear elasticity and nonlinear material laws are implemented in polarization based methods [72] and solved using conjugate gradients based on the Newton-Raphson method [34]. Homogenization of higher order that give arbitrary derivatives of the strains and the macroscopic elastic coefficients can also be solved by fast Fourier transform based algorithms [14, 26, 98].

For Galerkin-type discretizations [19], bounds on the homogenized coefficients can be computed [71, 103, 107]. Postprocessing of the solution includes the reconstruction of displacements from strain solutions [20] and smoothing techniques to remove artifacts in the solution fields [35].

The established theory for fast Fourier transform based solutions of the elastic homogenization problem is backed by validations and experiments. This includes other material laws like hyperelasticity and large deformation [27, 43, 52], thermoelasticity and non-linear composites [100], piezoelectricity [17], and elastoviscoplasticity in polycrystals [50, 54–59, 63, 76, 81, 85]. FFT-based homogenization methods are applied to metal foams [60, 61] and to complex large-scale problems like transient creeping of ice [38].

Goals of this thesis

For this thesis we have three goals that aim at the discretization of the equations of homogenization. The first goal deals with resolving dominant directions in the geometry and discretizing the partial differential equation on anisotropic grids. The second goal is to unify and generalize several ansatz spaces that have been used to discretize the equation. For the third goal we deal with high-resolution data and reduce the amount of degrees of freedom to a more manageable size. Those three goals are motivated in the following paragraphs and explained in detail.

Geometries, which have a strong dominant direction that is not aligned with a coordinate axis of the reference volume element, are of special interest in this thesis. Such composites can be found in elastomeres with embedded magnetic particles [32, 33] and grids which evolve in the direction of Newtonian fluids to solve multiparticle problems [52]. Such problems suggest that a tensor product grid, where the coordinate axes are the dominant directions of grid refinement, may not always be the best choice. The setting for the discrete Fourier transform is given by an Abelian group structure [1], also called the generalized Fourier transform. On the torus, the tensor product grid structure is relaxed to an arbitrary anisotropic sampling lattice in order to derive periodic wavelets [10, 53]. A corresponding fast Fourier and fast wavelet transform are developed in [4].

The first goal of this thesis is to generalize the basic-scheme introduced by Moulinec

and Suquet to anisotropic periodic lattices. These lattices can be adapted to dominant directions other than the coordinate axes. The number of sampling points in these directions can then be chosen according to the underlying geometry of the problem [6]. We use general anisotropic lattices that require no additional computational effort over tensor product grids. That is because the anisotropic fast Fourier transform algorithm has the same complexity and leading factor as the transform on tensor product grids [4].

The method of Moulinec and Suquet can be applied to other discretization techniques, which adapt the Green operator to the underlying discretization. These approaches can be divided into three groups. The first group replaces the derivative operator by a discretization using rotated finite differences [108], an operator working on a staggered grid [91], and finite elements with full integration [90]. The latter publication also introduces a unified framework for such discretization methods in the context of the basic-scheme. The second group of discretization techniques uses a Fourier-Galerkin approach to compute guaranteed bounds on the macroscopic elastic properties [11, 103, 104, 107]. The third group uses different discrete ansatz spaces and evaluates the derivative operator there. Such an approach uses the Green operator introduced by Moulinec and Suquet and convolves it in frequency domain with the Fourier coefficients of the ansatz function. The approach by Moulinec and Suquet corresponds to truncated trigonometric polynomials as ansatz functions [102, 105]. Piecewise constant finite elements are implemented in [18, 21] using an exact expression of their Fourier coefficients. Periodic translation invariant spaces, meaning spaces generated by translating a single function, are introduced in [78] and their approximation properties are analyzed in the one-dimensional case. In the multivariate case, approximation estimates can be found in [95] for tensor product grids. A generalization of translation invariant spaces to anisotropic lattices was done in [23]. An approximation theory for anisotropic periodic spaces of translates is developed in [5, 9], which makes use of periodic Strang-Fix conditions.

The second goal of this thesis is to generalize the discretization of the partial differential equation for homogenization to anisotropic periodic spaces of translates [7, 8]. Such spaces include truncated trigonometric polynomials in form of the Dirichlet kernel. Piecewise constant finite elements, and more general periodic Box splines [13] of arbitrary smoothness are also contained, unifying the approaches of [74], of [105] and [18, 21]. The framework can be used to adapt the underlying space of translates to enhance the solution fields, for example by using de la Vallée-Poussin means [10], a generalization of the Dirichlet and the Fejér kernel. The de la Vallée-Poussin means provide good localization in space and compact support in frequency domain [37]. Further, they reduce the Gibbs phenomenon in the solution. The Green operator on spaces of translates emerges as a Fourier-space convolution of the Green operator of Moulinec and Suquet with a function of the Fourier coefficients of the function generating the space of translates. We classify the properties of this periodized Green operator and show that it constitutes a projection operator if and only if the space of translates is generated by the Dirichlet kernel. This projection property is crucial to understand the connection between the variational formulation and the Lippmann-Schwinger equation. A convergence analysis yields that the smoothness of the ansatz function drives and limits the convergence of the discretization for regular coefficients. There, a balance between the regularity of the

ansatz function, its localization in space, and the size of its support in frequency domain has to be found.

Homogenization problems from engineering applications often come with large numbers of measurements for the elastic coefficients. Solutions based on data from computer tomography images can be too large to fit into memory or can lead to undesirably long computation times. Using the methods from anisotropic lattices, the data given on a large lattice can be reduced to a smaller sampling set by subsampling. Restricting the computations to a subset of the original set of sampling points, however, leaves large amounts of information on the coefficients and thus the geometry unused. A formula for the elasticity coefficients, that includes data on the sub-voxel level and uses estimated directions of interfaces inside the voxels is introduced in [64–66] for the heat equation and in [46] for tensor product grids based on [18]. Subsequently, this approach, called composite voxel technique, is applied to nonlinear incremental problems [44], adapted to hyperelastic laminates at finite strains [47], and used for inelastic problems [45].

The third and final goal of this thesis is to generalize the composite voxels in [46] to anisotropic sampling lattices.

We demonstrate the effects of the choice of the sampling lattice, the space of translates, and the effectivity of composite voxels on several numerical examples. Those examples are in two and three dimensions, where we use the two-dimensional problems to demonstrate mathematical properties and convergence of the method. The three-dimensional geometries show the applicability of the methods we develop for more realistic applications.

A simple example geometry is the generalized Hashin structure, a two-dimensional problem where the solution is known and the macroscopic elastic properties can be computed explicitly. The approximation results are studied on a problem with piecewise polynomial coefficients and a specific smoothness. In three dimensions, a single fiber geometry serves to study the effects of the lattice and the space of translates. The effect of composite voxels is strongest in the presence of many interfaces. We demonstrate them on a polycrystalline structure.

Structure of this thesis

The thesis is divided into three parts and organized as follows: the first part, found in Chapter 2, contains the preliminaries. They introduce the periodic and non-periodic function spaces, followed by lattices and the discrete Fourier transform on them. We then explain translation invariant spaces and their approximation estimates. We derive the partial differential equation of elasticity in homogenization and explain the Lippmann-Schwinger equation and the variational formulation. Finally, we collect some theoretical results and error estimates for elliptic partial differential equations.

The Chapter 3 starts by defining the periodized Green operator derived by a convolution in Fourier space with the Fourier coefficients of the ansatz function. This operator is subsequently used to discretize the Lippmann-Schwinger equation and the variational equation. We characterize their solution spaces and embed them into the existing methods.

The convergence analysis of this discretization starts with showing the boundedness and ellipticity of several bilinear and linear forms, followed by the convergence result. Afterwards, we prove the convergence of the basic-scheme and the conjugate gradient algorithm.

Finally, in Chapter 4, we comment on the software used for the numerical simulations and explain the example problems used in this thesis. We investigate the effects of the choice of the lattice numerically and study the effects, the underlying space of translates has on the solution. These investigations are both done in two and in three dimensions. We introduce the composite voxel technique as a preprocessor on the stiffness data that reduces a high-dimensional problem to a lower-dimensional system of equations. This is followed by a demonstration of the effectiveness of the composite voxels for a polycrystalline structure.

Acknowledgments

First, I thank Prof. Dr. Bernd Simeon for not only supervising my thesis but also for having my back in difficult times. He gave me the freedom to find my own area of research and guided me towards my academic path. My second supervisor, Prof. Dr. Gabriele Steidl, saw a connection between my work and the dissertation of Dr. Ronny Bergmann and brought us together. This very fruitful cooperation is not least the result of her involvement. Prof. Dr. Axel Klawonn I thank for the comprehensive review of my thesis and for his visit for my defence.

I owe special thanks to Ronny as he accompanied me for most of my time as a PhD student . His knowledge of anisotropic patterns and translation invariant spaces resulted in lengthy, productive and intense discussions and programming sessions. In Ronny I found a tutor, a great scientist and a fellow nerd. His meticulous search for typos and mistakes in my thesis increased its quality substantially.

I am indebted to Clarissa Arioli, Alexander Shamanskiy, Alexander Hunt and especially to Felix Dietrich for correcting my creative uses of the English grammar and LaTeX. Felix — and before him Dr. Anmol Goyal — spent the last two years with me in our office, a difficult task in itself.

The guidance provided by Dr. Heiko Andrä, Dr. Matti Schneider, and Dr. Matthias Kabel gave me great insights into research and the problems industry is interested in. With their knowledge and experience we solved challenging problems. I also thank the Fraunhofer ITWM for giving me access to their resources, software, and computing power.

My friends, Jan Niedermeyer, Jan Sauerwein, Laura Tozzo, and Markus Doktor, helped me to relax in lengthy discussions and extensive bantering. We shared our frustration and success over quite some glasses of beer and plates of homemade food.

Jessika, I thank you for being there when I was stressed or needed moral or immoral support. On you I could lean and unconditionally rely on to be by my side. You have my love.

My sister Jacqueline gives me moral support and is always there to listen to my

problems and worries. My parents, Fred and Susanne, highly involved in my very existence, always have my back. My home with them was my save heaven in troubled times and they always helped me to pursue my PhD relaxed with a deliciously filled stomach. Thank you!

2 Preliminaries

This thesis centers around and connects two separate topics: approximation on periodic anisotropic spaces of translates and periodic homogenization in linear elasticity. Introducing both of them is the aim of this chapter, which summarizes and states relevant concepts and scientific results.

The first part starts with the notation used throughout the remainder of this thesis, which is explained in Section 2.1. The Sections 2.2, 2.3, and 2.4 then deal with the discrete Fourier transform on periodic lattices, translation invariant spaces, and their approximation theory.

Section 2.2 establishes the infinite-dimensional function spaces like Lebesgue and Sobolev spaces, both on subsets of $\mathbb{R}^d$ and on the d-dimensional torus. In the latter case, we draw the connection to Fourier series and anisotropic function spaces.

Those Fourier series are discretized in Section 2.3. To that aim, this section reviews anisotropic lattices and the construction of appropriate point sets in the space and in the frequency domain and provides a discrete Fourier transform on such patterns.

Based on these lattices and the discrete Fourier transform, Section 2.4 describes translation invariant spaces which are a finite dimensional subspace of the periodic Lebesgue space of square integrable functions. As such, they can be used for interpolation and approximation in periodic Sobolev spaces and thus constitute the foundation for the numerical analysis in the following chapters.

The second part of the preliminaries is divided into two sections. In Section 2.5, we explain the mathematical idea of periodic homogenization as a limit process of a scale separation between the macro and the micro scale of a material. This leads to the equation of linear elasticity in periodic homogenization — the focus of the discretization approach in Chapter 3. To aid the discretization, we introduce equivalent formulations of this partial differential equation.

On a more general level, Section 2.6 states results from the theory and numerical analysis of partial differential equations. This includes results dealing with the existence, uniqueness, and smoothness of solutions, followed by a convergence theorem for very general discretization methods by Strang.

2.1 Notation

To ease the journey of the reader through the — sometimes quite involved — notation used in this thesis, the following conventions apply throughout this document, unless stated explicitly otherwise.

With the symbols $a \in \mathbb{C}$, bold $\mathbf{a} \in \mathbb{C}^d$, bold capitals $\mathbf{A} \in \mathbb{C}^{d\times d}$, and calligraphic capitals $\mathcal{A} \in \mathbb{C}^{d\times d\times d\times d}$ we denote (complex-valued) scalars, vectors, matrices, and fourth-order tensors, respectively. Vectors are through this thesis understood as column vectors. For scalar functions, symbols f are reserved. Vector valued functions, and functions mapping onto second-order tensors, i.e. matrices, have bold symbols $\mathbf{f}$ and Greek letters ε, respectively. The capital calligraphic letter $\mathcal{C}$ is reserved for the stiffness distribution and $\mathcal{F}$ denotes the discrete Fourier transform. In general, capital calligraphic letters $\mathcal{S}$ are used for sets. The letter $d \in \mathbb{N}$ is exclusively used for the dimension, in applications we usually have $d = 2$ or $d = 3$.

Vectors, second-order tensors, and fourth-order tensors are indexed by $\mathbf{a}_i$, $\mathbf{A}_{ij}$, and $\mathcal{A}_{ijkl}$ with $i, j, k, l = 1, \dots, d$. The product between a fourth-order tensor $\mathcal{A} \in \mathbb{C}^{d\times d\times d\times d}$ and a second-order tensor $\mathbf{A} \in \mathbb{C}^{d\times d}$ is written as

$$\big(\mathcal{A} : \mathbf{A}\big)_{ij} \coloneqq \sum_{k,l=1}^{d} \mathcal{A}_{ijkl}\mathbf{A}_{kl}.$$

The inner product between two vectors is denoted by $\mathbf{a}^{\mathrm{T}}\mathbf{b} \coloneqq \sum_i a_i b_i$, and $\langle \cdot, \cdot \rangle$ is reserved for the inner product of two functions.

The induced Euclidean norm of a regular matrix $\mathbf{M} \in \mathbb{R}^{d\times d}$ is written as $\|\mathbf{M}\|$, without subscript on the norm, and the condition number of a regular matrix $\mathbf{M}$ is given as $\kappa_{\mathbf{M}} \coloneqq \|\mathbf{M}\|\|\mathbf{M}^{-1}\|$.

The complex conjugate of a complex number $a = b + \mathrm{i}c$ with $b, c \in \mathbb{R}$ is written as $\overline{a} \coloneqq b - \mathrm{i}c$. The imaginary unit i and constants like Euler's number e are set upright.

The Kronecker delta is denoted by $\delta_{ij} \coloneqq 1$, if $i = j$, and $\delta_{ij} \coloneqq 0$ otherwise. With $|\cdot|$ we denote the absolute value of a scalar.

Let $\mathcal{S}$ be an arbitrary set. Then we use the notation

$$\mathrm{Sym}_d(\mathcal{S}) \coloneqq \left\{ s \in \mathcal{S}^{d\times d} : s_{ij} = s_{ji} \in \mathcal{S} \text{ for all } i,j = 1,\dots,d \right\}$$

for the set of symmetric matrices that are componentwise elements of $\mathcal{S}$. If we take the symmetric linear operators between symmetric matrices $\mathrm{Sym}_d(\mathcal{S})$ we get the set

$$\mathrm{SSym}_d(\mathcal{S}) \coloneqq \big\{ s \in \mathrm{Sym}_d(\mathcal{S}) \times \mathrm{Sym}_d(\mathcal{S}) : s_{ijkl} = s_{klij} \in \mathcal{S} \text{ for all } i,j,k,l = 1,\dots,d \big\}.$$

This set consists of fourth-order tensors with minor and major symmetries, i.e. tensors satisfying $s_{ijkl} = s_{jikl} = s_{ijlk} = s_{klij}$ for all $i,j,k,l = 1,\dots,d$.

Further, $\mathbf{Id}_\mathrm{d} \in \mathbb{R}^{d\times d}$ denotes the identity matrix, and for a set $\mathcal{S}$ the operator $\mathrm{Id} : \mathcal{S} \to \mathcal{S}$ is the identity. Let g be a function. Then $\mathcal{O}(g)$ defines the Landau symbol in the limit $a \in \mathbb{R}$ by

$$\mathcal{O}(g) \coloneqq \left\{ f : \limsup_{x\to a} \frac{|f(x)|}{|g(x)|} < \infty \right\}.$$

For a multi-index $\mathbf{a} = (a_1, a_2, \dots, a_b)$ with $b > 0$ and $a_i \in \mathbb{N}$, we denote the sum of $\mathbf{a}$ by

$$|\mathbf{a}| \coloneqq \sum_{i=1}^{b} a_i.$$

2.2 Function spaces and Fourier series

The aim of this section is to introduce the necessary function spaces for the analysis in the following chapters. We do this in two steps: first, function spaces on subsets of the $\mathbb{R}^d$ are defined in detail. With these at hand, we can proceed to periodic function spaces and Fourier series.

Function spaces on subsets of $\mathbb{R}^d$

The definition of the function spaces on subsets of $\mathbb{R}^d$ in this section is done from scratch. Beginning with Lebesgue spaces, we proceed from partial derivatives to weakly partially differentiable functions. These provide the basis to subsequently define Sobolev spaces with their according norm and inner product.

Let $\mathcal{R} \subset \mathbb{R}^d$ be a non-empty and open set, then the *Lebesgue space* $\mathcal{L}^p(\mathcal{R})$ of order $1 \le p \le \infty$ is defined by

$$\mathcal{L}^p(\mathcal{R}) \coloneqq \big\{ f : \mathcal{R} \to \mathbb{C} : \|f\|_p < \infty \big\},$$

where

$$\|f\|_p \coloneqq \left(\int_{\mathcal{R}} |f(\mathbf{x})|^p \,\mathrm{d}\mathbf{x} \right)^{\frac{1}{p}}$$

for $1 \leq p < \infty$ and

$$\|f\|_\infty \coloneqq \operatorname*{ess\,sup}_{\mathbf{x}\in\mathcal{R}} |f(\mathbf{x})|,$$

with ess sup being the essential supremum. For the Lebesgue norms, a single subscript is used. The norm $\|\cdot\|_2$ is induced by the inner product

$$\langle f, g\rangle_2 \coloneqq \int_{\mathcal{R}} f(\mathbf{x})\overline{g(\mathbf{x})}\,\mathrm{d}\mathbf{x}, \quad f, g \in \mathcal{L}^2(\mathcal{R})$$

and thus $\mathcal{L}^2(\mathcal{R})$ is a Hilbert space. If the functions f and g are vector-valued or tensor-valued, e.g. $f, g \in \mathcal{L}^p(\mathcal{R})^{d\times d}$, the above definitions are applied using the inner product on vectors and the Frobenius inner product. For matrices $\mathbf{A}, \mathbf{B} \in \mathbb{C}^{d\times d}$ with entries a_{ij} and b_{ij} for $i, j = 1, \ldots, d$, respectively, we use the *Frobenius inner product*

$$\langle \mathbf{A}, \mathbf{B}\rangle \coloneqq \sum_{i,j=1}^{d} \overline{a_{ij}} b_{ij}.$$

For higher order tensors, the Frobenius inner product is applied similarly.

The *partial derivative* $\frac{\partial f}{\partial x_i}$ of a function $f : \mathcal{R} \to \mathbb{C}^{\tilde{d}}$ with $\tilde{d} \in \mathbb{N}$ at point $\mathbf{x} = (x_1, \ldots, x_d)^{\mathrm{T}} \in \mathcal{R}$ with respect to the component x_i is given as

$$\frac{\partial f}{\partial x_i}(\mathbf{x}) \coloneqq \lim_{h\to 0} \frac{f(x_1, \ldots, x_i + h, \ldots, x_d) - f(x_1, \ldots, x_i, \ldots, x_d)}{h}.$$

For a multi-index $\mathbf{a} = (a_1, a_2, \ldots, a_d)$ we define

$$\partial^{\mathbf{a}} f \coloneqq \frac{\partial^{a_1} f}{\partial_{x_1}^{a_1}} \cdots \frac{\partial^{a_d} f}{\partial_{x_d}^{a_d}},$$

using Schwarz's theorem, assuming all partial derivatives are continuous.

Further, a function $f : \mathcal{R} \to \mathbb{C}^{\tilde{d}}$ is *differentiable* in a point $\mathbf{x} \in \mathcal{R}$ if and only if there exists a linear mapping $\mathbf{J} : \mathcal{R} \to \mathbb{C}^{\tilde{d}}$ with

$$\lim_{\mathbf{h}\to\mathbf{0}} \frac{\|f(\mathbf{x}+\mathbf{h}) - f(\mathbf{x}) - \mathbf{J}(\mathbf{h})\|}{\|\mathbf{h}\|} = 0.$$

If this mapping $\mathbf{J}$ exists, then all partial derivatives of f exist as well and

$$\left(\frac{\partial f}{\partial x_i}\right)_j = \mathbf{J}_{ji}$$

for $i = 1, \ldots, d$ and $j = 1, \ldots, \tilde{d}$.

Let $\mathcal{C}^p(\mathcal{R})$ for $p \in \mathbb{N} \cup \{\infty\}$ with $0 \leq p \leq \infty$ denote the *space of p-times continuously differentiable functions* in the above sense.

For a function $f \in \mathcal{L}^1(\mathcal{R})$, where $\mathcal{R} \subset \mathbb{R}^d$ is open and bounded, the *weak partial derivative* with respect to the multi-index $\mathbf{a}$ is defined as follows. We call $g \in \mathcal{L}^1(\mathcal{R})$ the weak $\mathbf{a}$-derivative of f if and only if

$$\int_{\mathcal{R}} f\partial^{\mathbf{a}}\varphi\,\mathrm{d}\mathbf{x} = (-1)^{|\mathbf{a}|}\int_{\mathcal{R}} g\varphi\,\mathrm{d}\mathbf{x}$$

for all $\varphi \in \mathcal{C}^\infty(\mathcal{R})$ which have compact support in $\mathcal{R}$. We further collect the weak partial derivatives of f in the *Jacobi matrix*

$$\nabla f \coloneqq \left(\frac{\partial f}{\partial_{x_i}}\right)_{i=1,\dots,d}.$$

The *Sobolev space* $\mathcal{W}^{b,p}(\mathcal{R})$ with Sobolev index $b \in \mathbb{N}$ and Lebesgue index $1 \leq p \leq \infty$ is given by

$$\mathcal{W}^{b,p}(\mathcal{R}) \coloneqq \left\{f \in \mathcal{L}^p(\mathcal{R}) : \|f\|_{b,p} < \infty\right\}$$

using the multi-index $\mathbf{a}$ with

$$\|f\|_{b,p} \coloneqq \left(\sum_{\mathbf{a}\colon |\mathbf{a}|\leq b} \left\|\partial^{\mathbf{a}} f\right\|_p^p\right)^{\frac{1}{p}}$$

for $1 \leq p < \infty$ and

$$\|f\|_{b,\infty} \coloneqq \max_{\mathbf{a}\colon |\mathbf{a}|\leq b} \left\|\partial^{\mathbf{a}} f\right\|_\infty.$$

Here, the Sobolev norm has two indices.

For $p = 2$ we also write $\mathcal{H}^b(\mathcal{R}) \coloneqq \mathcal{W}^{b,2}(\mathcal{R})$ and the Sobolev spaces $\mathcal{H}^b(\mathcal{R})$ endowed with the inner product

$$\langle f, g\rangle_{b,2} \coloneqq \sum_{\mathbf{a}\colon |\mathbf{a}|\leq b} \langle \partial^{\mathbf{a}} f, \partial^{\mathbf{a}} g\rangle_2, \quad f, g \in \mathcal{H}^b(\mathcal{R})$$

are Hilbert spaces.

The space $\mathcal{H}_0^b(\mathcal{R}) \subset \mathcal{H}^b(\mathcal{R})$ denotes the set of functions in the Sobolev space that have compact support in $\mathcal{R}$. The space $\mathcal{H}^{-b}(\mathcal{R})$ is the dual space to $\mathcal{H}_0^b(\mathcal{R})$, i.e. the space of bounded linear functionals from $\mathcal{H}_0^b(\mathcal{R})$ to $\mathbb{C}$.

The interested reader can find a more detailed introduction of the function spaces on subsets of $\mathbb{R}^d$ in [3, Section 1.5 and Section 7], or [99, Section 1 and Section 2].

Periodic function spaces on $\mathbb{T}^d$

Fourier series provide the basis for the function spaces used in this thesis. Their theoretical requisite are spaces of p-summable sequences which are introduced at the beginning of this section. These allow for the definition of Fourier coefficients as weights of the Schauder basis of $\mathcal{L}^2(\mathbb{T}^d)$ given by the trigonometric monomials. Among the sequence spaces, the Wiener algebra and the square summable sequences are special in the way, that they have isomorphic counterparts in the Lebesgue spaces.

Similar to the Sobolev spaces, we define next the anisotropic function spaces. They are introduced in [5, 9] and require a certain order of decay of the Fourier coefficients weighted with an elliptic weight function. In the case of square integrable functions and isotropic decay of the Fourier coefficients, they are equivalent to certain Sobolev spaces.

We identify the d-dimensional *torus* $\mathbb{T}^d \coloneqq \mathbb{R}^d/(2\pi\mathbb{Z})^d$ with the interval $\mathbb{T}^d \cong [-\pi, \pi)^d$. With this identification, the definitions for the Lebesgue spaces and Sobolev spaces carry over to the periodic case.

In addition to the Lebesgue spaces $\mathcal{L}^p(\mathbb{T}^d)$ we define the *spaces of p-summable sequences* using the counting measure instead of the Lebesgue measure. For a set $\mathcal{Z} \subseteq \mathbb{Z}^d$ and $1 \leq p \leq \infty$ we define

$$\ell^p(\mathcal{Z}) \coloneqq \left\{ \{c_\mathbf{k}\}_{\mathbf{k}\in\mathcal{Z}} \subset \mathbb{C} : \left\|\{c_\mathbf{k}\}_{\mathbf{k}\in\mathcal{Z}}\right\|_p < \infty \right\}$$

with the norms

$$\left\|\{c_\mathbf{k}\}_{\mathbf{k}\in\mathcal{Z}}\right\|_p \coloneqq \left(\sum_{\mathbf{k}\in\mathcal{Z}} |c_\mathbf{k}|^p \right)^{\frac{1}{p}}$$

for $1 \leq p < \infty$ and

$$\left\|\{c_\mathbf{k}\}_{\mathbf{k}\in\mathcal{Z}}\right\|_\infty \coloneqq \sup_{\mathbf{k}\in\mathcal{Z}} |c_\mathbf{k}|.$$

The space $\ell^2(\mathcal{Z})$ is a Hilbert space endowed with the inner product

$$\left\langle \{c_\mathbf{k}\}_{\mathbf{k}\in\mathcal{Z}}, \{b_\mathbf{k}\}_{\mathbf{k}\in\mathcal{Z}} \right\rangle_2 \coloneqq \sum_{\mathbf{k}\in\mathcal{Z}} c_\mathbf{k}\overline{b_\mathbf{k}}, \quad \{c_\mathbf{k}\}_{\mathbf{k}\in\mathcal{Z}}, \{b_\mathbf{k}\}_{\mathbf{k}\in\mathcal{Z}} \in \ell^2(\mathcal{Z}).$$

For a function $f \in \mathcal{L}^1(\mathbb{T}^d)$ we define the *Fourier coefficients*

$$c_\mathbf{k}(f) \coloneqq \frac{1}{(2\pi)^d} \int_{\mathbb{T}^d} f(\mathbf{x})\, \mathrm{e}^{-\mathrm{i}\mathbf{k}^\mathrm{T}\mathbf{x}}\, \mathrm{d}\mathbf{x}, \quad \mathbf{k} \in \mathbb{Z}^d.$$

For vector-valued or tensor-valued functions this definition applies componentwise. In case of $f \in \mathcal{L}^2(\mathbb{T}^d)$ these Fourier coefficients can be written as $c_\mathbf{k}(f) = \left\langle f, \mathrm{e}^{\mathrm{i}\mathbf{k}^\mathrm{T}\cdot} \right\rangle_2$ and the functions $\mathrm{e}^{\mathrm{i}\mathbf{k}^\mathrm{T}\cdot}$ constitute a Schauder basis of $\mathcal{L}^2(\mathbb{T}^d)$. For $f \in \mathcal{L}^2(\mathbb{T}^d)$ the *Fourier series*

$$f = \sum_{\mathbf{k}\in\mathbb{Z}^d} c_\mathbf{k}(f)\, \mathrm{e}^{\mathrm{i}\mathbf{k}^\mathrm{T}\cdot}$$

converges with equality in $\mathcal{L}^2(\mathbb{T}^d)$-sense, i.e. with equality up to sets of Lebesgue measure zero.

The spaces $\mathcal{L}^2(\mathbb{T}^d)$ and $\ell^2(\mathbb{Z}^d)$ are isomorphic via the Parseval equation, i.e. for functions $f, g \in \mathcal{L}^2(\mathbb{T}^d)$ with Fourier coefficients $\left\{c_\mathbf{k}(f)\right\}_{\mathbf{k}\in\mathbb{Z}^d}$ and $\left\{c_\mathbf{k}(g)\right\}_{\mathbf{k}\in\mathbb{Z}^d}$, respectively, it holds that

$$\langle f, g\rangle_2 = \left\langle \left\{c_\mathbf{k}(f)\right\}_{\mathbf{k}\in\mathbb{Z}^d}, \left\{c_\mathbf{k}(g)\right\}_{\mathbf{k}\in\mathbb{Z}^d} \right\rangle_2. \tag{2.1}$$

For the Banach space $\ell^1(\mathbb{Z}^d)$ an isomorphic space is given by the *Wiener algebra*

$$\mathcal{A}(\mathbb{T}^d) \coloneqq \left\{ f \in \mathcal{L}^1(\mathbb{T}^d) : \|f\|_\mathcal{A} < \infty \right\}$$

with

$$\|f\|_\mathcal{A} \coloneqq \left\|\{c_\mathbf{k}(f)\}_{\mathbf{k}\in\mathbb{Z}^d}\right\|_1,$$

i.e. the space of functions with an absolute convergent sequence of Fourier coefficients.

For a function $f \in \mathcal{A}(\mathbb{T}^d)$ that fulfills

$$f = \sum_{\mathbf{k}\in\mathbb{Z}^d} c_{\mathbf{k}}(f)\, \mathrm{e}^{\mathrm{i}\mathbf{k}^{\mathrm{T}}\cdot}$$

in $\mathcal{L}^2$-sense and that is weakly partial differentiable with respect to x_j with $\frac{\partial f}{\partial x_j} \in \mathcal{A}(\mathbb{T}^d)$ for $j = 1, \dots, d$, the derivative can be characterized via its Fourier series with

$$\frac{\partial f}{\partial x_j} \coloneqq \sum_{\mathbf{k}\in\mathbb{Z}^d} \mathrm{i}k_j c_{\mathbf{k}}(f)\, \mathrm{e}^{\mathrm{i}\mathbf{k}^{\mathrm{T}}\cdot},$$

where $\mathbf{k} = (k_1, \dots, k_d)^{\mathrm{T}}$.

We define for a function $\mathbf{u} \in \mathcal{H}^1(\mathbb{T}^d)^d$ the *symmetric gradient operator*

$$\nabla_{\mathrm{Sym}}\, \mathbf{u} \coloneqq \frac{1}{2}\big(\nabla\, \mathbf{u} + (\nabla\, \mathbf{u})^{\mathrm{T}}\big) \tag{2.2}$$

with $\nabla_{\mathrm{Sym}}\, \mathbf{u} \in \mathrm{Sym}_d\big(\mathcal{L}^2(\mathbb{T}^d)\big)$. In terms of Fourier coefficients, this operator — acting as a Fourier multiplier — is given as

$$c_{\mathbf{k}}\big(\nabla_{\mathrm{Sym}}\, \mathbf{u}\big) \coloneqq \nabla_{\mathrm{Sym}_{\mathbf{k}}}\, c_{\mathbf{k}}(\mathbf{u}) \coloneqq \frac{\mathrm{i}}{2}\big(\mathbf{k}c_{\mathbf{k}}(\mathbf{u})^{\mathrm{T}} + c_{\mathbf{k}}(\mathbf{u})\mathbf{k}^{\mathrm{T}}\big), \quad \mathbf{k} \in \mathbb{Z}^d.$$

The *divergence operator* div is defined as the negative $\mathcal{L}^2$-adjoint of the symmetric gradient operator via

$$\langle \mathbf{u}, \operatorname{div} \gamma\rangle_2 \coloneqq -\langle \nabla_{\mathrm{Sym}}\, \mathbf{u}, \gamma\rangle_2,$$

for all $\mathbf{u} \in \mathcal{H}^1(\mathbb{T}^d)^d$ and $\gamma \in \mathrm{Sym}_d\big(\mathcal{L}^2(\mathbb{T}^d)\big)$.

With these differential operators the space $\mathcal{L}^2(\mathbb{T}^d)$ can be decomposed into a direct sum of constants, divergence-free fields and gradient fields with the help of the Helmholtz decomposition [69, Section 12.1], stated in the following theorem.

Theorem 2.1. *It holds that*

$$\mathrm{Sym}_d\big(\mathcal{L}^2(\mathbb{T}^d)\big) = \mathrm{Sym}_d\big(\mathcal{U}(\mathbb{T}^d)\big) + \mathcal{E}(\mathbb{T}^d) + \mathcal{D}(\mathbb{T}^d),$$

where

$$\begin{aligned}
\mathcal{U}(\mathbb{T}^d) &\coloneqq \big\{f \in \mathcal{L}^2(\mathbb{T}^d) : f \text{ is constant almost everywhere}\big\},\\
\mathcal{E}(\mathbb{T}^d) &\coloneqq \big\{\varepsilon \in \mathrm{Sym}_d\big(\mathcal{L}^2(\mathbb{T}^d)\big) : \exists \mathbf{u} \in \mathcal{H}^1(\mathbb{T}^d)^d,\, \varepsilon = \nabla_{\mathrm{Sym}}\, \mathbf{u}\big\},\\
\mathcal{D}(\mathbb{T}^d) &\coloneqq \big\{\sigma \in \mathrm{Sym}_d\big(\mathcal{L}^2(\mathbb{T}^d)\big) : \int_{\mathbb{T}^d} \sigma(\mathbf{x})\, \mathrm{d}\mathbf{x} = 0 \text{ and } \langle \varepsilon, \sigma\rangle_2 = 0 \text{ for all } \varepsilon \in \mathcal{E}(\mathbb{T}^d)\big\}.
\end{aligned} \tag{2.3}$$

The set U consists of all constant functions, $\mathcal{E}(\mathbb{T}^d)$ collects all gradient fields, and $\mathcal{D}(\mathbb{T}^d)$ all divergence-free functions.

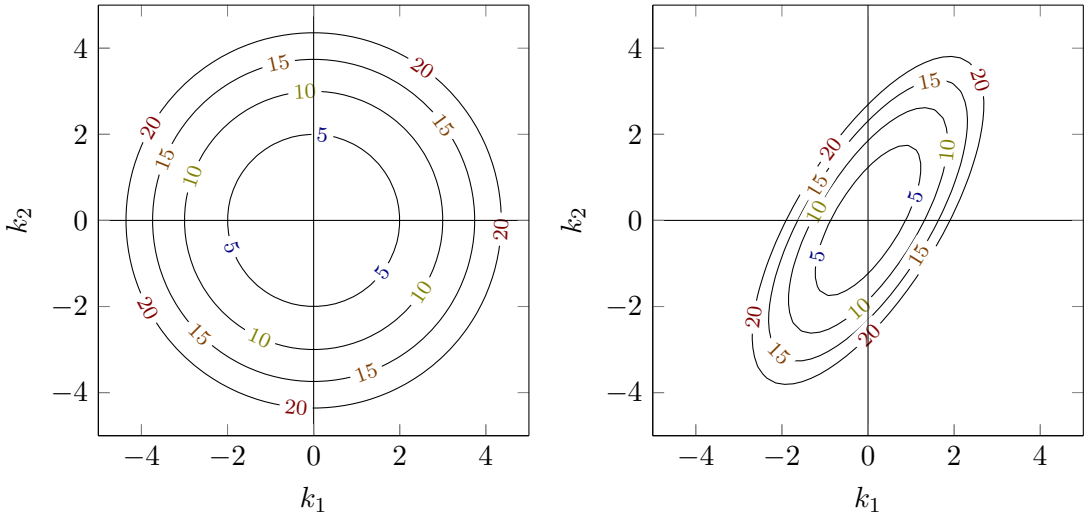

Figure 2.1. Level set plot of the elliptic weight function $\sigma_b^{\mathbf{M}}(\mathbf{k})$ for $b = 2$ and $\mathbf{k} \in \mathbb{R}^2$ with matrix $\mathbf{M}_1$ (left) and matrix $\mathbf{M}_2$ (right) for levels 5, 10, 15, and 20.

Connected to the Sobolev spaces $\mathcal{W}^{a,p}(\mathbb{T}^d)$ are spaces that are characterized by the decline of the Fourier coefficients of their functions. The so-called isotropic function spaces [95, Section 1.1], for example, require a certain decline of the Fourier coefficients in all directions. For the analysis in the following sections, however, we require anisotropic function spaces. These spaces allow for different declines of the Fourier coefficients in directions which are not necessarily aligned with the coordinate axes.

These directions are parametrized by regular matrices $\mathbf{M} \in \mathbb{Z}^{d\times d}$. The directions in frequency domain are then described by ellipsoids via an elliptic weight function. Let $b \in \mathbb{R}$, then the *elliptic weight function* $\sigma_b^{\mathbf{M}}$ is given by

$$\sigma_b^{\mathbf{M}}(\mathbf{k}) \coloneqq \left(1 + \left\|\mathbf{M}\right\|^2 \left\|\mathbf{M}^{-\mathrm{T}}\mathbf{k}\right\|^2\right)^{\frac{b}{2}}, \quad \mathbf{k} \in \mathbb{Z}^d. \tag{2.4}$$

When inserting the identity matrix as $\mathbf{M} = \mathbf{Id}_\mathrm{d}$ into the definition of the weight function, it reduces to

$$\sigma_b^{\mathbf{Id}_\mathrm{d}}(\mathbf{k}) = \left(1 + \|\mathbf{k}\|^2\right)^{\frac{b}{2}}.$$

This function is well known from a characterization of the Sobolev spaces $\mathcal{H}^b(\mathbb{T}^d)$ via their Fourier coefficients [95, Definition 1.1].

In Figure 2.1, level set plots of the elliptic weight function $\sigma_b^{\mathbf{M}}$ for $b = 2$ and matrices $\mathbf{M}_1 \coloneqq \left(\begin{smallmatrix} 8 & 0 \\ 0 & 8 \end{smallmatrix}\right)$ and $\mathbf{M}_2 \coloneqq \left(\begin{smallmatrix} 8 & 8 \\ 0 & 8 \end{smallmatrix}\right)$ are shown. The function $\sigma_2^{\mathbf{M}_1}$ has an isotropic behavior, i.e. the level sets are circles. For $\sigma_2^{\mathbf{M}_2}$, the function increases anisotropically, where the function grows much quicker in the direction of $(1,-1)^\mathrm{T}$ than in the direction of $(1,1)^\mathrm{T}$.

The elliptic weight function allows the definition of the anisotropic function spaces. Let $\mathbf{M} \in \mathbb{Z}^{d\times d}$ be regular, $b \in \mathbb{R}$, and let $q \geq 1$. Then the *anisotropic function space*

$\mathcal{A}^b_{\mathbf{M},q}$ is defined as

$$\mathcal{A}^b_{\mathbf{M},q}(\mathbb{T}^d) \coloneqq \left\{ f \in \mathcal{L}^1(\mathbb{T}^d) : \|f\|_{b,\mathbf{M},q} < \infty \right\}$$

with the norm

$$\|f\|_{b,\mathbf{M},q} \coloneqq \left\| \{\sigma_b^{\mathbf{M}}(\mathbf{k}) c_{\mathbf{k}}(f)\}_{\mathbf{k}\in\mathbb{Z}^d} \right\|_q,$$

sporting three indices.

Due to [9, Page 4], the anisotropic function spaces are equivalent to their isotropic counterparts with $\mathbf{M} = \mathbf{Id}_\mathrm{d}$. This can be seen via the inequalities

$$\left(1 + \left\|\mathbf{M}\right\|^2 \left\|\mathbf{M}^{-\mathrm{T}}\mathbf{k}\right\|^2\right)^{\frac{b}{2}} \leq \kappa_{\mathbf{M}}^b \left(1 + \|\mathbf{k}\|^2\right)^{\frac{b}{2}}$$

and

$$\left(1 + \|\mathbf{k}\|^2\right)^{\frac{b}{2}} \leq \left(1 + \left\|\mathbf{M}^{\mathrm{T}}\mathbf{M}^{-\mathrm{T}}\mathbf{k}\right\|^2\right)^{\frac{b}{2}} \leq \left(1 + \left\|\mathbf{M}\right\|^2 \left\|\mathbf{M}^{-\mathrm{T}}\mathbf{k}\right\|^2\right)^{\frac{b}{2}}.$$

These inequalities directly yield

$$\|f\|_{b,\mathbf{M},q} \leq \kappa_{\mathbf{M}}^b \|f\|_{b,\mathbf{Id}_\mathrm{d},q} \tag{2.5}$$

and

$$\|f\|_{b,\mathbf{Id}_\mathrm{d},q} \leq \|f\|_{b,\mathbf{M},q}, \tag{2.6}$$

and thus the spaces $\mathcal{A}^b_{\mathbf{M},q}(\mathbb{T}^d)$ and $\mathcal{A}^b_{\mathbf{Id}_\mathrm{d},q}(\mathbb{T}^d)$ are isomorphic. This definition of the anisotropic function spaces incorporates the Wiener algebra as a special case with $\mathcal{A}(\mathbb{T}^d) = \mathcal{A}^0_{\mathbf{Id}_\mathrm{d},1}$.

Between the Lebesgue space, the isotropic function spaces, and the Sobolev spaces the following embeddings and equivalences are given, see [95, Section 1.1] and [94].

Lemma 2.2. *The following embeddings hold:*

a) $\mathcal{W}^{0,p}(\mathbb{T}^d) = \mathcal{L}^p(\mathbb{T}^d)$ *for all* $1 \leq p \leq \infty$,

b) $\mathcal{H}^b(\mathbb{T}^d) = \mathcal{W}^{b,2}(\mathbb{T}^d) = \mathcal{A}^b_{\mathbf{Id}_\mathrm{d},2}$ *for all* $b \in \mathbb{R}$,

c) $\mathcal{A}^b_{\mathbf{Id}_\mathrm{d},q}(\mathbb{T}^d) \subset \mathcal{A}^{b'}_{\mathbf{Id}_\mathrm{d},q}(\mathbb{T}^d)$ *for* $b \geq b'$ *and* $1 \leq q \leq \infty$,

d) $\mathcal{A}^b_{\mathbf{Id}_\mathrm{d},q}(\mathbb{T}^d) \subset \mathcal{A}^b_{\mathbf{Id}_\mathrm{d},q'}(\mathbb{T}^d)$ *for* $b \in \mathbb{R}$ *and* $q \leq q'$,

e) $\mathcal{W}^{b,q}(\mathbb{T}^d) \subset \mathcal{W}^{b,q'}(\mathbb{T}^d)$ *for* $b \in \mathbb{R}$ *and* $q \geq q'$.

Further information about periodic function spaces can be found for example in [99, Chapter 9] and [3, Section 7.5].

This section has introduced Lebesgue spaces and Sobolev spaces over subsets of $\mathbb{R}^d$ and over the torus $\mathbb{T}^d$ together with their respective norms. On periodic function spaces, the spaces of p-summable sequences are used in conjunction with Fourier series. These series stem from the Schauder basis consisting of complex exponentials. The measurement of the p-th moments of a function to obtain the Lebesgue spaces $\mathcal{L}^p(\mathbb{T}^d)$ stands in contrast to measuring the p-th moments of the Fourier coefficients. Together with anisotropic weights, this leads to the anisotropic function spaces. In case of $p = 2$, these two approaches to define spaces are connected via the Parseval equation.

2.3 Lattices and the discrete Fourier transform

A discretization using the infinite trigonometric Schauder basis introduced in the last section requires the definition of a suitable grid. The classical choice when using Fourier-based methods is a tensor product grid. More general, we introduce regular anisotropic lattices where the vectors that generate the sampling points are not necessarily aligned with the coordinate axes. On such grids a discrete Fourier transform is introduced in [23]. More general, the required algebraic structure to define a discrete Fourier transform is an Abelian group [1].

Anisotropic lattices are used in [10, 53] to develop periodic anisotropic wavelets. The algebraic structure of the lattice parametrization is used for the scaling in the multiresolution analysis. Subsequently, a fast Fourier transform and fast wavelet transform is derived in [4]. The fast Fourier transform algorithm for tensor product grids is adapted to anisotropic lattices using an certain enumeration of the sampling points and frequencies. With this enumeration, the algorithm for tensor product grids can be applied directly without increasing the computational costs.

Of special interest are lattices which can be generated by sampling a single direction, by using the periodicity of the torus. Such lattices are called rank-1-lattices and are studied in detail in [48, 49] and [80]. The authors derive several adaptive schemes to approximate sets of sampling points and frequencies, and give approximation errors for functions of given smoothness. For such lattices, the discrete Fourier transform reduces to a single one-dimensional transform, independent of the dimension of the problem. This simplifies the organization of the data and reduces the costs to compute the transform. A summary and introduction to anisotropic lattices in German can also be found in [5].

This section first introduces the concept of regular lattices and states their properties. It then proceeds to define a discrete Fourier transform on them and concludes by constructing a suitable enumeration of the lattice points, leading to a fast Fourier transform algorithm.

Periodic Lattices

Periodic lattices are parametrized by a regular integer matrix, resulting in a congruence relation which generalizes the notion of periodicity to the anisotropic case. A suitable set of congruence representants then yields a pattern on the torus and, similarly, a generating set of integer frequencies. After introducing these concepts, this section proceeds to state results that identify set inclusions and equalities of such lattices by purely algebraic properties of their parametrizing matrices. Finally, examples for these properties, the resulting lattices, and generating sets are given.

Lattices on the torus are parametrized by a regular integer matrix $\mathbf{M} \in \mathbb{Z}^{d\times d}$, see also the definition of the elliptic weight function (2.4). This matrix defines a congruence relation $\cong$ for vectors $\mathbf{h}, \mathbf{k} \in \mathbb{Z}^d$ via

$$\mathbf{h} \cong \mathbf{k} \mod \mathbf{M} :\Leftrightarrow \text{there exists } \mathbf{z} \in \mathbb{Z}^d \text{ such that } \mathbf{k} = \mathbf{h} + \mathbf{M}\mathbf{z}. \tag{2.7}$$

The resulting *lattice* is then given as

$$\Lambda(\mathbf{M}) \coloneqq \mathbf{M}^{-1}\mathbb{Z}^d = \left\{\mathbf{y} \in \mathbb{R}^d : \mathbf{M}\mathbf{y} \in \mathbb{Z}^d\right\}.$$

The necessary algebraic structure for a discrete Fourier transform is an Abelian group [1]. Consider set of points $\mathcal{P}(\mathbf{M}) \subset \left[-\frac{1}{2}, \frac{1}{2}\right)^d$ constructed by points in the lattice $\Lambda(\mathbf{M})$ modulo the unit cube $\left[-\frac{1}{2}, \frac{1}{2}\right)^d$ by Equation (2.7). We call this set the *pattern* belonging to the pattern matrix $\mathbf{M}$. For an element $\mathbf{y} \in \Lambda(\mathbf{M})$ we denote the mapping onto its representant in $\mathcal{P}(\mathbf{M})$ by $\mathbf{y}\big|_{\mathcal{P}(\mathbf{M})}$. The set $\mathcal{P}(\mathbf{M})$ endowed with the addition of points constitutes such an Abelian group [23] and is therefore suited for the definition of a discrete Fourier transform. The *generating set* is given by $\mathcal{G}(\mathbf{M}) \coloneqq \mathbf{M}\,\mathcal{P}(\mathbf{M})$ and is, together with the addition of points, an Abelian group.

The number of elements in both the pattern and the generating set is given by $|\mathcal{P}(\mathbf{M})| = |\mathcal{G}(\mathbf{M})| = |\det(\mathbf{M})| =: m$, following [13, Lemma II.7]. The special case of a tensor product grid with $m = m_1 m_2 m_3 \cdots m_d$ points is covered by diagonal pattern matrices $\mathbf{M} = \operatorname{diag}(m_1, m_2, \ldots, m_d)$.

Sublattices, i.e. subsets of a lattice $\Lambda(\mathbf{M})$ that are again lattices can be characterized via properties of the pattern matrix [53] as follows.

Lemma 2.3. *Let $\mathbf{M}, \mathbf{N} \in \mathbb{Z}^{d\times d}$ be regular pattern matrices. Then it holds that:*

a) $\Lambda(\mathbf{N}) \subset \Lambda(\mathbf{M})$, $\mathcal{P}(\mathbf{N}) \subset \mathcal{P}(\mathbf{M})$, and $\mathcal{G}(\mathbf{N}) \subset \mathcal{G}(\mathbf{M})$ if and only if there exist a regular matrix $\mathbf{J} \in \mathbb{Z}^{d\times d}$ such that $\mathbf{M} = \mathbf{J}\mathbf{N}$, and

b) $\Lambda(\mathbf{M}) = \Lambda(\mathbf{N})$, $\mathcal{P}(\mathbf{M}) = \mathcal{P}(\mathbf{N})$, and $\mathcal{G}(\mathbf{M}) = \mathcal{G}(\mathbf{N})$ if and only if there exists a matrix $\mathbf{J} \in \mathbb{Z}^{d\times d}$ as in a) that furthermore fulfills $|\det(\mathbf{J})| = 1$.

The inclusion property in Lemma 2.3 a) given by the splitting $\mathbf{M} = \mathbf{J}\mathbf{N}$ also results in a unique splitting of points $\mathbf{x} \in \mathcal{P}(\mathbf{M})$ into components in $\mathcal{P}(\mathbf{N})$ and $\mathcal{P}(\mathbf{J})$ [4, Proof of Theorem 3].

Lemma 2.4. *Let $\mathbf{M}, \mathbf{N}, \mathbf{J} \in \mathbb{Z}^{d\times d}$ be regular matrices with $\mathbf{M} = \mathbf{J}\mathbf{N}$. Then a point $\mathbf{x} \in \mathcal{P}(\mathbf{M})$ can be uniquely decomposed into*

$$\mathbf{x} = \mathbf{y} + \left(\mathbf{N}^{-1}\mathbf{z}\right)\big|_{\mathcal{P}(\mathbf{M})}$$

for $\mathbf{y} \in \mathcal{P}(\mathbf{N})$ and $\mathbf{z} \in \mathcal{P}(\mathbf{J})$.

The discrete Fourier transform connects the pattern $\mathcal{P}(\mathbf{M})$, serving as the sampling points in space, with the generating set $\mathcal{G}(\mathbf{M}^{\mathrm{T}})$ of frequencies in Fourier space. The connection between the two sets can be seen for the complex exponential function in the following lemma.

Lemma 2.5. *Let $\mathbf{M} \in \mathbb{Z}^{d\times d}$ be a regular matrix, let $\mathbf{h} \in \mathcal{G}(\mathbf{M}^{\mathrm{T}})$, let $\mathbf{y} \in \mathcal{P}(\mathbf{M})$, and let $\mathbf{z} \in \mathbb{Z}^d$. Then it holds that*

$$\mathrm{e}^{2\pi\mathrm{i}\mathbf{h}^{\mathrm{T}}\mathbf{y}} = \mathrm{e}^{2\pi\mathrm{i}\left(\mathbf{h}+\mathbf{M}^{\mathrm{T}}\mathbf{z}\right)^{\mathrm{T}}\mathbf{y}}.$$

Proof. As $\mathbf{y} \in \mathcal{P}(\mathbf{M})$, by definition we have $\mathbf{z}^{\mathrm{T}}\mathbf{M}\mathbf{y} \in \mathbb{Z}$ and therefore $\mathrm{e}^{2\pi\mathrm{i}\mathbf{z}^{\mathrm{T}}\mathbf{M}\mathbf{y}} = 1$, see [5, p. 25]. □

Example 2.6. *Figure 2.2 shows the patterns $\mathcal{P}(\mathbf{M})$ and generating sets $\mathcal{G}(\mathbf{M}^{\mathrm{T}})$ for the matrices*

$$\begin{aligned}
\mathbf{M}_1 &\coloneqq \begin{pmatrix} 4 & 4 \\ -4 & 4 \end{pmatrix}, \\
\mathbf{M}_2 &\coloneqq \begin{pmatrix} 1 & -1 \\ 1 & 1 \end{pmatrix} \begin{pmatrix} 4 & 4 \\ -4 & 4 \end{pmatrix} = \begin{pmatrix} 8 & 0 \\ 0 & 8 \end{pmatrix}, \\
\mathbf{M}_3 &\coloneqq \begin{pmatrix} 1 & 1 \\ 0 & 1 \end{pmatrix} \begin{pmatrix} 8 & 0 \\ 0 & 8 \end{pmatrix} = \begin{pmatrix} 8 & 8 \\ 0 & 8 \end{pmatrix}, \\
\mathbf{M}_4 &\coloneqq \begin{pmatrix} 8 & 1 \\ 0 & 8 \end{pmatrix}.
\end{aligned}$$

By Lemma 2.3 a), the inclusion $\mathcal{P}(\mathbf{M}_1) \subset \mathcal{P}(\mathbf{M}_2)$ holds, i.e. the pattern generated by $\mathbf{M}_1$ is a subsampling of the pattern generated by $\mathbf{M}_2$, see the top row of Figure 2.2. Also, the generating sets show the inclusion $\mathcal{G}(\mathbf{M}_1^{\mathrm{T}}) \subset \mathcal{G}(\mathbf{M}_2^{\mathrm{T}})$.

From Lemma 2.3 b) follows further, that $\mathcal{P}(\mathbf{M}_2) = \mathcal{P}(\mathbf{M}_3)$. However, $\mathcal{G}(\mathbf{M}_2^{\mathrm{T}}) \neq \mathcal{G}(\mathbf{M}_3^{\mathrm{T}})$, as can be seen in the middle row of Figure 2.2.

The pattern $\mathcal{P}(\mathbf{M}_4)$ and the generating set $\mathcal{G}(\mathbf{M}_4^{\mathrm{T}})$ are generated by a single sampling direction. The representants of the lattice $\Lambda(\mathbf{M}_4)$ in the unit cube $\left[-\frac{1}{2}, \frac{1}{2}\right)^2$ then yield a sampling set.

The discrete Fourier transform on periodic lattices

Classically, the multivariate discrete Fourier transform is defined on tensor product grids. The patterns introduced in the last section have the structure of a finite group when the group operation is chosen as the addition of points. Such a structure permits the definition of a discrete Fourier transform [86], which is introduced in the following. Due to a decomposition of the pattern into a linearly transformed tensor product of one-dimensional periodic point sets, we can define a pattern basis. This linear transformation hinges on the Smith normal form of the pattern matrix. With this special basis, the fast Fourier transform algorithm known for tensor product grids can be applied directly, see [4], which is detailed in this section. This is followed by the aliasing formula, describing the quality of the approximation on such a pattern.

Definition 2.7. *Let $\mathcal{P}(\mathbf{M})$ be a pattern generated by the regular pattern matrix $\mathbf{M} \in \mathbb{Z}^{d\times d}$. Further, assume that the points in $\mathcal{P}(\mathbf{M})$ and $\mathcal{G}(\mathbf{M}^{\mathrm{T}})$ have an arbitrary but fixed order and let $m = |\det(\mathbf{M})|$. Then the* discrete Fourier transform *$\mathcal{F}(\mathbf{M})$ on $\mathcal{P}(\mathbf{M})$ is defined by*

$$\mathcal{F}(\mathbf{M}) \coloneqq \frac{1}{m}\left(\mathrm{e}^{-2\pi\mathrm{i}\mathbf{h}^{\mathrm{T}}\mathbf{y}}\right)_{\mathbf{h}\in\mathcal{G}(\mathbf{M}^{\mathrm{T}}),\ \mathbf{y}\in\mathcal{P}(\mathbf{M})}$$

with $\mathbf{h} \in \mathcal{G}(\mathbf{M}^{\mathrm{T}})$ indicating the rows and $\mathbf{y} \in \mathcal{P}(\mathbf{M})$ indicating the columns of the matrix $\mathcal{F}(\mathbf{M})$ [23].

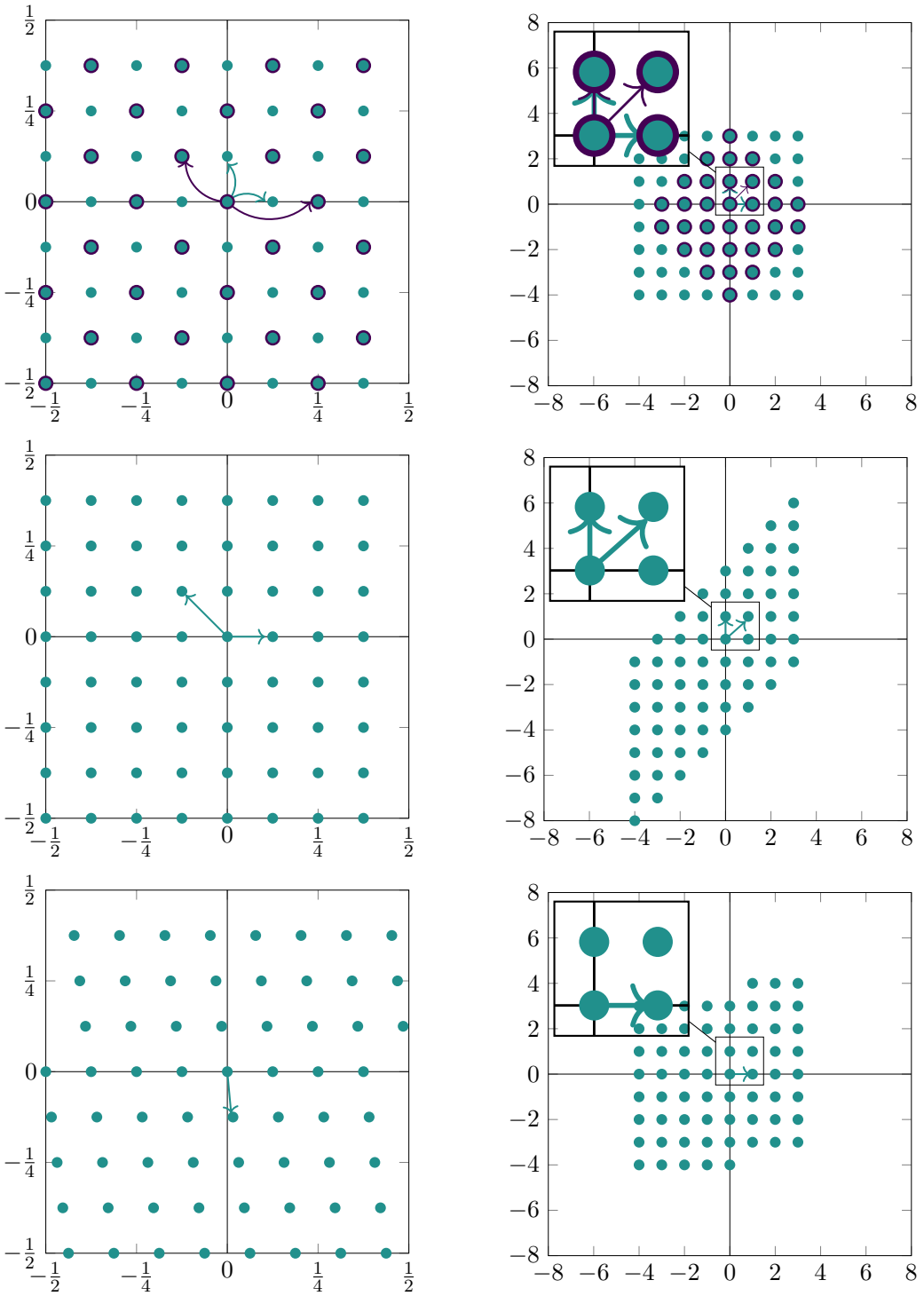

Figure 2.2. Examples for patterns (left column), generating sets (right column) and their respective bases for the matrices $\mathbf{M}_1$ (top row, large dots only, dark arrows), $\mathbf{M}_2$ (top row, small and large dots, light arrows), $\mathbf{M}_3$ (middle row), and $\mathbf{M}_4$ (bottom row).

The discrete Fourier transform of a vector $\mathbf{a} = (a_{\mathbf{y}})_{\mathbf{y}\in\mathcal{P}(\mathbf{M})} \in \mathbb{C}^m$ *is then given as*

$$\hat{\mathbf{a}} = (\hat{a}_{\mathbf{h}})_{\mathbf{h}\in\mathcal{G}(\mathbf{M}^{\mathrm{T}})} \coloneqq \mathcal{F}(\mathbf{M})\mathbf{a} \in \mathbb{C}^m. \tag{2.8}$$

This discrete Fourier transform on anisotropic lattices equals the classic discrete Fourier transform on a tensor product grid in case of $\mathbf{M}$ being a diagonal matrix. In order to derive the fast Fourier transform (FFT) algorithm in this setting, a special ordering of the elements of $\mathcal{P}(\mathbf{M})$ and $\mathcal{G}(\mathbf{M}^{\mathrm{T}})$ is required. This ordering is based on the Smith normal form of $\mathbf{M}$.

Lemma 2.8. *Let* $\mathbf{M} \in \mathbb{Z}^{d\times d}$ *be regular. Then* $\mathbf{M}$ *can be decomposed into*

$$\mathbf{M} = \mathbf{QER}$$

with matrices $\mathbf{Q}, \mathbf{E}, \mathbf{R} \in \mathbb{Z}^{d\times d}$*. If those matrices fulfill* $|\det(\mathbf{R})| = |\det(\mathbf{Q})| = 1$ *and* $\mathbf{E} = \operatorname{diag}(e_1, \ldots, e_d)$ *where* $e_j \in \mathbb{N}$ *and* $e_j | e_{j+1}$ *for* $j = 1, \ldots, d-1$*, i.e.* e_j *divides* e_{j+1}*, then this decomposition is called* Smith normal form (SNF) *of* $\mathbf{M}$*.*

With help of the Smith normal form the *dimension* of a pattern is given by

$$d_{\mathbf{M}} \coloneqq |\{j : e_j > 1\}|,$$

counting the non-trivial directions required to span the pattern $\mathcal{P}(\mathbf{M})$.

The elementary divisors e_j with $j = 1, \ldots, d$ of the Smith normal form motivate the definition of a basis of the pattern $\mathcal{P}(\mathbf{M})$ [4, Section 3]

Definition 2.9. *Let* $\mathbf{M} \in \mathbb{Z}^{d\times d}$ *be a regular pattern matrix with Smith normal form* $\mathbf{M} = \mathbf{QER}$*, let* e_j *be the elementary divisors of* $\mathbf{M}$*, and let* $d_{\mathbf{M}}$ *be the dimension of* $\mathbf{M}$*. A set* $\{\mathbf{y}_1, \ldots, \mathbf{y}_{d_{\mathbf{M}}}\} \subset \mathcal{P}(\mathbf{M})$ *is called* pattern basis *of the pattern* $\mathcal{P}(\mathbf{M})$ *if and only if*

a) for all $j = 1, \ldots, d_{\mathbf{M}}$ *holds that*

$$\min_{a\in\mathbb{N}} \{a : a\mathbf{y_j} \in \mathbb{Z}^d\} = e_{d-d_{\mathbf{M}}+j},$$

b) and if the vectors $\mathbf{y}_1, \ldots, \mathbf{y}_{d_{\mathbf{M}}}$ *are linearly independent.*

If the set $\{\tilde{\mathbf{y}}_1, \ldots, \tilde{\mathbf{y}}_{d_{\mathbf{M}}}\} \subset \mathcal{P}(\mathbf{M}^{\mathrm{T}})$ *is a pattern basis for the pattern* $\mathcal{P}(\mathbf{M}^{\mathrm{T}})$*, then by the definition of the sets,* $\{\mathbf{M}\tilde{\mathbf{y}}_1, \ldots, \mathbf{M}\tilde{\mathbf{y}}_{d_{\mathbf{M}}}\} \subset \mathcal{G}(\mathbf{M}^{\mathrm{T}})$ *is a basis of the generating set* $\mathcal{G}(\mathbf{M}^{\mathrm{T}})$*.*

A lexicographic ordering of the elements of the pattern $\mathcal{P}(\mathbf{M})$ with respect to the coefficients of the vectors $\mathbf{y}_1, \ldots, \mathbf{y}_{d_{\mathbf{M}}}$ yields a way to enumerate the points. This amounts to

$$\mathcal{P}(\mathbf{M}) = \left(\left(\sum_{j=1}^{d_{\mathbf{M}}} a_j \mathbf{y}_j \right) \Big|_{\mathcal{P}(\mathbf{M})} \right)_{(a_1,\ldots,a_{d_{\mathbf{M}}})=\mathbf{0}}^{(a_1,\ldots,a_{d_{\mathbf{M}}})=(e_{d-d_{\mathbf{M}}+1}-1,\ldots,e_d-1)}$$

and bases for the pattern and the generating set are given as follows [4, Section 3]:

Lemma 2.10. *Let* $\mathbf{M} \in \mathbb{Z}^{d\times d}$ *be regular with Smith normal form* $\mathbf{M} = \mathbf{QER}$ *and* $\mathbf{E} = \operatorname{diag}(e_1, \dots, e_d)$. *Let further* $\mathbf{e}_j$ *denote the* j*-th unit vector in* $\mathbb{Z}^d$. *Then basis vectors* $\mathbf{y}_j$ *for the pattern* $\mathcal{P}(\mathbf{M})$ *are given for* $j = 1, \dots, d_{\mathbf{M}}$ *by*

$$\mathbf{y}_j \coloneqq \mathbf{R}^{-1} \frac{1}{e_{d-d_{\mathbf{M}}+j}} \mathbf{e}_{d-d_{\mathbf{M}}+j}.$$

The basis vectors $\tilde{\mathbf{y}}_j$ *for the generating set* $\mathcal{G}(\mathbf{M}^{\mathrm{T}})$ *are*

$$\tilde{\mathbf{y}}_j \coloneqq \mathbf{R}^{\mathrm{T}} \frac{1}{e_{d-d_{\mathbf{M}}+j}} \mathbf{e}_{d-d_{\mathbf{M}}+j}$$

for $j = 1, \dots, d_{\mathbf{M}}$.

These special bases give a ordering of $\mathcal{P}(\mathbf{M})$ and $\mathcal{G}(\mathbf{M}^{\mathrm{T}})$ that allows the use of the (standard) multidimensional fast Fourier transform algorithm on these vectors. The resulting FFT on anisotropic patterns thus retains the complexity of the tensor product case, i.e. $\mathcal{O}(m \log m)$ with the same leading constant [4, Theorem 2].

Patterns with dimension $d_{\mathbf{M}} = 1$, which are also called *rank-1-lattices*, are of special interest. For these, only a single one-dimensional discrete Fourier transform is required to switch between the space domain and the frequency domain. Such lattices are very easy to handle and are studied in detail for example in [48, 49, 80].

The pattern bases and the bases of the generating sets are displayed in Figure 2.2 as arrows. An example for a pattern of rank 1, i.e. a pattern that is generated by only one basis vector, is depicted in the bottom row of Figure 2.2.

Having defined the discrete Fourier transform on vectors, we take a look at the difference between a function in $\mathcal{L}^2(\mathbb{T}^d)$ and its approximation by points on the pattern $\mathcal{P}(\mathbf{M})$. Assume that $f \in \mathcal{L}^2(\mathbb{T}^d) \cap \mathcal{A}(\mathbb{T}^d)$ is sampled on a pattern at the points $\mathbf{y} \in \mathcal{P}(\mathbf{M})$ with $a_{\mathbf{y}} \coloneqq f(2\pi\mathbf{y})$. The *discrete Fourier coefficients* of f are defined as $c_{\mathbf{h}}^{\mathbf{M}}(f) \coloneqq \hat{a}_{\mathbf{h}}$ with $\mathbf{h} \in \mathcal{G}(\mathbf{M}^{\mathrm{T}})$, and $\hat{a}_{\mathbf{h}}$ according to (2.8).

The aliasing formula [5, Lemma 2.1] then states that

$$c_{\mathbf{h}}^{\mathbf{M}}(f) = \sum_{\mathbf{z}\in\mathbb{Z}^d} c_{\mathbf{h}+\mathbf{M}^{\mathrm{T}}\mathbf{z}}(f), \quad \mathbf{h} \in \mathcal{G}(\mathbf{M}^{\mathrm{T}}). \tag{2.9}$$

This means that slowly decaying Fourier coefficients $c_{\mathbf{z}}(f)$ with $\mathbf{z} \in \mathbb{Z}^d$ result in a bad approximation $c_{\mathbf{h}}^{\mathbf{M}}(f) \approx c_{\mathbf{h}}(f)$ for $\mathbf{h} \in \mathcal{G}(\mathbf{M}^{\mathrm{T}})$ if the number of points in the according direction — given by the basis vectors of $\mathcal{G}(\mathbf{M}^{\mathrm{T}})$ and the according elementary divisors e_j of $\mathbf{E}$ — is not sufficiently large. If the number of points is large enough and the spectrum is bounded in that direction, then the difference between $c_{\mathbf{h}}^{\mathbf{M}}(f)$ and $c_{\mathbf{h}}(f)$ is small and f is approximated well by the $a_{\mathbf{h}}$.

The sum on the right-hand side of (2.9) is also called *bracket sum* given for $\mathbf{a} = \{a_{\mathbf{k}}\}_{\mathbf{k}\in\mathbb{Z}^d}$ via

$$[\mathbf{a}]_{\mathbf{k}}^{\mathbf{M}} \coloneqq \sum_{\mathbf{z}\in\mathbb{Z}^d} a_{\mathbf{k}+\mathbf{M}^{\mathrm{T}}\mathbf{z}}, \quad \mathbf{k} \in \mathbb{Z}^d. \tag{2.10}$$

This section has introduced periodic anisotropic lattices as a scaling of the integers by a regular integer matrix. Selecting suitable congruence representants in the unit cube motivates the definition of the pattern and the generating set. The pattern $\mathcal{P}(\mathbf{M})$ constitutes a suitable point set for the definition of a discrete Fourier transform which maps points on the pattern to elements of the generating set $\mathcal{G}(\mathbf{M}^{\mathrm{T}})$. By a suitable enumeration of these point sets, using bases stemming from the Smith normal form, the application of the fast Fourier transform algorithm is possible without losing performance when compared to tensor product grids.

A construction of subsets of the pattern and the generating set is possible via decompositions of the pattern matrix $\mathbf{M}$. With these, the computational effort for the fast Fourier transform can be reduced while adapting the point sets to certain directions, given by the pattern bases. The approximation of a function by the discrete Fourier coefficients is characterized by the aliasing formula. There, a faster decline of the Fourier coefficients — coinciding with a higher smoothness of the function, see also the anisotropic function spaces in the previous section — reduces the approximation error.

2.4 Translation invariant spaces and approximation

Based on the anisotropic patterns introduced above, this section acquaints the reader with the concept of translation invariant spaces, i.e. spaces generated by taking a single function and shifting it to the points on a regular pattern. This endeavor is divided into four steps.

First, the idea of spaces of translates and their properties are presented, including an appropriate interpolation and approximation operator. This is followed by examples for such spaces and plots of the functions generating the space. Third, theoretical results for estimates on the approximation error, depending on properties of the space of translates, are introduced. The speed of convergence of the approximation depends on parameters derived from the spaces of translates. These parameters are exemplified for several ansatz functions.

Translation invariant spaces

The idea behind translation invariant spaces is similar to the idea of finite elements on an equidistant grid. For example, in case of linear finite elements, the hat functions forming a nodal basis can be generated by taking a single hat function and translating it to each grid point, see Figure 2.3. In case of a tensor product grid, such spaces are extensively investigated in [79, 93–95]. A generalization to anisotropic lattices is done in [10, 53], the latter of which serves as the source for this section.

We define translation invariant spaces and characterize their elements by their Fourier coefficients. A special function generating a translation invariant space is the fundamental interpolant, which generates a nodal basis when translated, similar to the hat function in Figure 2.3. Further, orthogonality and orthonormality of such a basis is described via its Fourier coefficients. Finally, we introduce an interpolation and approximation operator on spaces of translates.

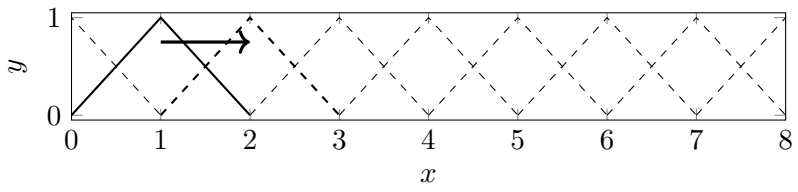

Figure 2.3. Linear finite element ansatz space as a space of translates of a single hat function.

The *translate* of a function $f \in \mathcal{L}^2(\mathbb{T}^d)$ is denoted by $\mathcal{T}(\mathbf{y})f \coloneqq f(\cdot - 2\pi\mathbf{y})$ for $\mathbf{y} \in \mathcal{P}(\mathbf{M})$. In terms of Fourier coefficients this is equivalent to

$$c_{\mathbf{k}}(\mathcal{T}(\mathbf{y})f) = \mathrm{e}^{-2\pi\mathrm{i}\mathbf{k}^{\mathrm{T}}\mathbf{y}} c_{\mathbf{k}}(f), \quad \mathbf{k} \in \mathbb{Z}^d,\ \mathbf{y} \in \mathcal{P}(\mathbf{M}).$$

Spaces invariant under translation are of special interest for the following analysis as they can be characterized by the Fourier coefficients of their functions.

Definition 2.11. *Let $\mathcal{V} \subset \mathcal{L}^2(\mathbb{T}^d)$ be a set, then $\mathcal{V}$ is called a* $\mathbf{M}$-invariant space *if for all functions $f \in \mathcal{V}$ and points $\mathbf{y} \in \mathcal{P}(\mathbf{M})$, also $\mathcal{T}(\mathbf{y})f \in \mathcal{V}$, i.e. the space is closed under translation. Further, define the* $\mathbf{M}$*-invariant space*

$$\mathcal{V}_{\mathbf{M}}^f \coloneqq \operatorname{span}\{\mathcal{T}(\mathbf{y})f : \mathbf{y} \in \mathcal{P}(\mathbf{M})\}$$

generated by the translates of a single function $f \in \mathcal{V}_{\mathbf{M}}^f$.

A function $g \in \mathcal{V}_{\mathbf{M}}^f$ can be decomposed into linear combinations of the translates of f via

$$g = \sum_{\mathbf{y} \in \mathcal{P}(\mathbf{M})} a_{\mathbf{y}}\, \mathcal{T}(\mathbf{y})f.$$

Such a decomposition also holds on the Fourier coefficients of g and makes use of the description of the translation operator $\mathcal{T}(\mathbf{y})$ for $\mathbf{y} \in \mathcal{P}(\mathbf{M})$ in Fourier space [53, Theorem 3.3].

Lemma 2.12. *Let $f \in \mathcal{L}^2(\mathbb{T}^d)$ and $\mathbf{h} \in \mathcal{G}(\mathbf{M}^{\mathrm{T}})$. Consider the unique decomposition of $\mathbf{k} \in \mathbb{Z}^d$ into $\mathbf{k} = \mathbf{h} + \mathbf{M}^{\mathrm{T}}\mathbf{z}$ for $\mathbf{z} \in \mathbb{Z}^d$. Then $g \in \mathcal{V}_{\mathbf{M}}^f$ holds if and only if*

$$c_{\mathbf{k}}(g) = c_{\mathbf{h}+\mathbf{M}^{\mathrm{T}}\mathbf{z}}(g) = \hat{a}_{\mathbf{h}} c_{\mathbf{h}+\mathbf{M}^{\mathrm{T}}\mathbf{z}}(f) \tag{2.11}$$

for all $\mathbf{z} \in \mathbb{Z}^d$ where $\big(\hat{a}_{\mathbf{h}}\big)_{\mathbf{h} \in \mathcal{G}(\mathbf{M}^{\mathrm{T}})} = \mathcal{F}(\mathbf{M})\big(a_{\mathbf{y}}\big)_{\mathbf{y} \in \mathcal{P}(\mathbf{M})}$.

Due to this characterization, the space $\mathcal{V}_{\mathbf{M}}^f$ is finite dimensional. We can do calculations and computations using only the coefficients $a_{\mathbf{y}}$ or their discrete Fourier coefficients $\hat{a}_{\mathbf{h}}$.

A translation invariant space $\mathcal{V}_{\mathbf{M}}^f$ can be easiest characterized by looking at the translates of a fundamental interpolant. These translates act like a nodal basis.

Definition 2.13. *Let $\mathbf{M} \in \mathbb{Z}^{d\times d}$ be regular. A function $\mathrm{I}_{\mathbf{M}} \in \mathcal{V}_{\mathbf{M}}^f$ is called* fundamental interpolant of $\mathcal{V}_{\mathbf{M}}^f$ *if*

$$\mathrm{I}_{\mathbf{M}}(2\pi\mathbf{y}) \coloneqq \delta_{\mathbf{0},\mathbf{y}}^{\mathbf{Id}_\mathrm{d}}, \quad \mathbf{y} \in \mathcal{P}(\mathbf{M})$$

where

$$\delta_{\mathbf{x},\mathbf{y}}^{\mathbf{M}} \coloneqq \begin{cases} 1, & \text{if } \mathbf{y} \equiv \mathbf{x} \bmod \mathbf{M}, \\ 0, & \text{else.} \end{cases}$$

The existence of such a fundamental interpolant is a priori not clear. The following lemma states conditions on the existence of this special function and explains its properties [5, Lemmas 1.23 and 2.2].

Lemma 2.14. *Let $\mathbf{M} \in \mathbb{Z}^{d\times d}$ be regular and let $f \in \mathcal{A}(\mathbb{T}^d)$. Then the following statements hold:*

a) The fundamental interpolant $\mathrm{I}_{\mathbf{M}} \in \mathcal{V}_{\mathbf{M}}^f$ exists if and only if

$$\sum_{\mathbf{z}\in\mathbb{Z}^d} c_{\mathbf{h}+\mathbf{M}^\mathrm{T}\mathbf{z}}(f) \neq 0$$

for all $\mathbf{h} \in \mathcal{G}(\mathbf{M}^\mathrm{T})$. If the fundamental interpolant $\mathrm{I}_{\mathbf{M}} \in \mathcal{V}_{\mathbf{M}}^f$ exists, it is uniquely determined.

b) The set of translates $\{\mathcal{T}(\mathbf{y})f : \mathbf{y} \in \mathcal{P}(\mathbf{M})\}$ is linear independent if and only if

$$\sum_{\mathbf{z}\in\mathbb{Z}^d} |c_{\mathbf{h}+\mathbf{M}^\mathrm{T}\mathbf{z}}(f)|^2 > 0$$

for all $\mathbf{h} \in \mathcal{G}(\mathbf{M}^\mathrm{T})$.

c) The set of translates $\{\mathcal{T}(\mathbf{y})f : \mathbf{y} \in \mathcal{P}(\mathbf{M})\}$ is an orthonormal basis of $\mathcal{V}_{\mathbf{M}}^f$ if and only if

$$\sum_{\mathbf{z}\in\mathbb{Z}^d} |c_{\mathbf{h}+\mathbf{M}^\mathrm{T}\mathbf{z}}(f)|^2 = \frac{1}{m}$$

with $m = |\det(\mathbf{M})|$ for all $\mathbf{h} \in \mathcal{G}(\mathbf{M}^\mathrm{T})$.

d) Let the fundamental interpolant on $\mathcal{V}_{\mathbf{M}}^f$ exist. Given a function $\tilde{g} \in \mathcal{A}(\mathbb{T}^d)$ we can obtain a function $g \in \mathcal{V}_{\mathbf{M}}^f$ fulfilling

$$\tilde{g}(2\pi\mathbf{y}) = g(2\pi\mathbf{y})$$

for all $\mathbf{y} \in \mathcal{P}(\mathbf{M})$ by

$$\hat{a}_{\mathbf{h}} = \frac{\sum_{\mathbf{z}\in\mathbb{Z}^d} c_{\mathbf{h}+\mathbf{M}^\mathrm{T}\mathbf{z}}(\tilde{g})}{\sum_{\mathbf{z}\in\mathbb{Z}^d} c_{\mathbf{h}+\mathbf{M}^\mathrm{T}\mathbf{z}}(f)}, \quad \mathbf{h} \in \mathcal{G}(\mathbf{M}^\mathrm{T}),$$

where the coefficients $\hat{a}_{\mathbf{h}}$ yield g in Fourier coefficients by the characterization (2.11).

Interpolation — and simultaneously best approximation — using the fundamental interpolant $\mathrm{I}_{\mathbf{M}}$ is then defined as follows:

Definition 2.15. *Let $\mathbf{M} \in \mathbb{Z}^{d\times d}$ be regular, let $f \in \mathcal{A}(\mathbb{T}^d)$, and let the fundamental interpolant $\mathrm{I}_{\mathbf{M}}$ on $\mathcal{V}_{\mathbf{M}}^f$ exist. Further, let g be a function that can be evaluated in the pattern points $2\pi\mathbf{y}$ with $\mathbf{y} \in \mathcal{P}(\mathbf{M})$. The* interpolation operator $\mathrm{L}_{\mathbf{M}}$ *on $\mathcal{V}_{\mathbf{M}}^f$ is then given via*

$$\mathrm{L}_{\mathbf{M}}\, g \coloneqq \sum_{\mathbf{y}\in\mathcal{P}(\mathbf{M})} g(2\pi\mathbf{y})\, \mathcal{T}(\mathbf{y})\, \mathrm{I}_{\mathbf{M}}\,.$$

If further $g \in \mathcal{A}(\mathbb{T}^d)$, then a characterization in terms of Fourier coefficients reads

$$c_{\mathbf{k}}(\mathrm{L}_{\mathbf{M}}\, g) = m\big[\{c_{\mathbf{k}'}(g)\}_{\mathbf{k}'\in\mathbb{Z}^d}\big]_{\mathbf{k}}^{\mathbf{M}} c_{\mathbf{k}}(\mathrm{I}_{\mathbf{M}}), \quad \mathbf{k} \in \mathbb{Z}^d$$

for $m = |\det(\mathbf{M})|$ and the Bracket sum as defined in Equation (2.10)*. Therefore, the operator $\mathrm{L}_{\mathbf{M}}$ is also an approximation operator on the space of translates $\mathcal{V}_{\mathbf{M}}^f$.*

Examples of translation invariant spaces

The translation invariant spaces we consider in this thesis can be divided into two classes: functions, which have compact support in space, and functions, that have compact support in frequency domain. This is due to the Breitenberger principle [16], the periodic equivalent of the Heisenberg uncertainty principle [40].

Periodized pattern Box splines belong to the first category and include for example hat functions, but also functions of higher degrees of differentiability. The resulting spaces of translates yield the more intuitive ansatz spaces from the point of classical numerical methods for partial differential equations, like finite elements. They, however, can not be represented by a finite number of Fourier coefficients and thus spectral methods will inherently produce additional approximation errors when computing in Fourier space, e.g. aliasing effects.

Translation invariant spaces with compact support in frequency domain allow for an exact representation by a — possibly large — finite number of Fourier coefficients and thus are suited better for spectral methods. Such functions have global support in space, however, they can be localized well [16, 28]. Among them is the Dirichlet kernel which leads to a translation invariant space that is equivalent to the space of truncated Fourier series and exhibits the Gibbs phenomenon [36, 41]. More general, Box splines in frequency domain allow to dampen the Gibbs phenomenon by smoothing high frequency behavior [15]. Especially de la Vallée Poussin means are an easy representative of this class.

We construct the Box splines in space by periodization:

Definition 2.16. *Let $\tilde{g} : \mathbb{R}^d \to \mathbb{C}$ be a function, then the* periodization $g : \mathbb{T}^d \to \mathbb{C}$ *of $\tilde{g}$ is given by*

$$g(\mathbf{y}) \coloneqq \sum_{\mathbf{z}\in\mathbb{Z}^d} \tilde{g}\Big(\frac{\mathbf{y}}{2\pi} - \mathbf{z}\Big), \quad \mathbf{y} \in \mathbb{T}^d. \tag{2.12}$$

In terms of Fourier coefficients this amounts to taking the continuous Fourier transform of $\tilde{g}$, and evaluating it on a grid [9, Page 41], i.e.

$$c_{\mathbf{k}}(g) = \frac{1}{(2\pi)^d} \int_{\mathbf{y}\in\mathbb{R}^d} \tilde{g}(\mathbf{y})\, \mathrm{e}^{-\mathrm{i}\mathbf{k}^{\mathrm{T}}\mathbf{y}}, \quad \mathbf{k} \in \mathbb{Z}^d.$$

With this, the periodised pattern Box splines are defined as follows:

Definition 2.17. *For $s \geq d$ denote a set of s column vectors that span the entire $\mathbb{R}^d$ by $\mathcal{X} = \{\mathbf{x}_1, \ldots, \mathbf{x}_s\} \in \mathbb{R}^{d\times s}$, abusing notation to interpret the set $\mathcal{X}$ as a matrix with columns $\mathbf{x}_i$. Then the Fourier coefficients [13, p. 11] of the* periodized Box spline *$B_{\mathcal{X}} : \mathbb{T}^d \to \mathbb{R}$ of order $s-1$ are*

$$c_{\mathbf{k}}(B_{\mathcal{X}}) \coloneqq \prod_{\mathbf{x}\in\mathcal{X}} \operatorname{sinc}\bigl(\pi \mathbf{x}^{\mathrm{T}}\mathbf{k}\bigr), \quad \mathbf{k} \in \mathbb{Z}^d, \tag{2.13}$$

where

$$\operatorname{sinc}(t) \coloneqq \frac{\sin(t)}{t}.$$

The periodized pattern Box spline *[9, Section 5] is then obtained by scaling with the regular matrix $\mathbf{M} \in \mathbb{Z}^{d\times d}$:*

$$f_{\mathbf{M},\mathcal{X}}(\mathbf{y}) \coloneqq B_{\mathcal{X}}(\mathbf{M}^{-1}\mathbf{y}), \quad \mathbf{y} \in \mathbb{T}^d. \tag{2.14}$$

The definition of the periodized pattern Box spline (2.14) leads to a periodization as in Equation (2.12) by evaluating the inverse discrete Fourier transformation (2.13).

Example 2.18. *Not all sets of column vectors $\mathcal{X}$ result in linearly independent translates of periodized pattern Box splines [78]. The sets $\mathcal{X} \in \mathbb{R}^{2\times(p+q+r)}$ with vectors*

$$\begin{aligned}
\mathbf{x}_1 = \cdots = \mathbf{x}_p &= (1,0)^{\mathrm{T}},\\
\mathbf{x}_{p+1} = \cdots = \mathbf{x}_{p+q} &= (0,1)^{\mathrm{T}},\\
\mathbf{x}_{p+q+1} = \cdots = \mathbf{x}_{p+q+r} &= (1,1)^{\mathrm{T}},
\end{aligned}$$

where at least two of the values p, q, r are larger than 0 yield a periodized pattern Box spline $f_{\mathbf{M},\mathcal{X}}$ with linear independent translates, see [9] and [12, Section 4].

For the definition of de la Vallée Poussin means we proceed in two steps, following [10].

Definition 2.19. *A function $g : \mathbb{R}^d \to \mathbb{R}$ is called* admissible *if it fulfills*

a) $g(\mathbf{y}) \geq 0$ *for all* $\mathbf{y} \in \mathbb{R}^d$,

b) $g(\mathbf{y}) > 0$ *for all* $\mathbf{y} \in \left[-\frac{1}{2}, \frac{1}{2}\right)^d$, *and*

c) $\displaystyle\sum_{\mathbf{z}\in\mathbb{Z}^d} g(\mathbf{y}+\mathbf{z}) = 1$ *for all* $\mathbf{y} \in \mathbb{R}^d$.

An example for admissible functions are Box splines $B_{\mathcal{X}}$ with

$$\mathcal{X} = \left\{\mathbf{x}_i : \left(\mathbf{x}_i\right)_j \coloneqq \delta_{ij} b_i,\ i = 1, \dots, d\right\} \cup \left\{\mathbf{x}_i : \left(\mathbf{x}_i\right)_j \coloneqq \delta_{ij},\ i = 1, \dots, d\right\} \tag{2.15}$$

with $\mathcal{X} \in \mathbb{R}^{d \times 2d}$ and $b_i \in [0, 1]$ for $i = 1, \dots, d$, see [10, Definition 4.2 for $l = 0$].

Definition 2.20. *Let $\mathbf{M} \in \mathbb{Z}^{d \times d}$ be regular, let $m = |\det(\mathbf{M})|$, and let g be an admissible function. The function $f_{\mathbf{M},g}$, which is defined by its Fourier coefficients via*

$$c_{\mathbf{k}}\left(f_{\mathbf{M},g}\right) \coloneqq \frac{1}{m} g\left(\mathbf{M}^{-\mathrm{T}}\mathbf{k}\right), \quad \mathbf{k} \in \mathbb{Z}^d \tag{2.16}$$

is called generalized de la Vallée Poussin mean.

For generalized de la Vallée Poussin means with g being a periodized Box spline of the form (2.15) we also write $f_{\mathbf{M},\mathbf{b}}$ if it is clear from the context. These functions $f_{\mathbf{M},\mathbf{b}}$ generalize the one-dimensional setting of [82, 92] to the anisotropic multi-dimensional setting. The functions $f_{\mathbf{M},\mathbf{b}}$ are called *de la Vallée Poussin means*.

The *modified Dirichlet kernel*, as a special case of $f_{\mathbf{M},\mathbf{b}}$ with $\mathbf{b} = \mathbf{0} \in \mathbb{R}^d$, has for dimension $d = 1$ the value 1 in the inner of $\mathcal{G}(\mathbf{M}^{\mathrm{T}})$ and $\frac{1}{2}$ at the boundary. The Dirichlet kernel, in contrast, has different behavior at the boundary:

Definition 2.21. *The* Dirichlet kernel $f_{\mathrm{D}_{\mathbf{M}}}$ *is defined via* (2.16) *for the admissible function*

$$g(\mathbf{y}) \coloneqq \begin{cases} 1, & \mathbf{y} \in \left[-\frac{1}{2}, \frac{1}{2}\right)^d, \\ 0, & \textit{otherwise} \end{cases}$$

and (2.16) *for* $\mathbf{y} \in \mathbb{R}^d$.

In Figure 2.4, the Dirichlet kernel $f_{\mathrm{D}_{\mathbf{M}}}$, the de la Vallée Poussin mean $f_{\mathbf{M},g}$ with $g = 0.25$, and the Box spline kernel $f_{\mathbf{M},\mathcal{X}}$ for $\mathcal{X} = (1, 1, 1)$ are depicted on the pattern matrix $\mathbf{M} = (20) \in \mathbb{Z}^{1\times 1}$ together with their Fourier coefficients. In comparison to the Dirichlet kernel, the de la Vallée Poussin mean decays faster in space, however, the values in the central peak are almost identical. These milder oscillations lead to a reduction of the Gibbs phenomenon when using the de la Vallée Poussin means as ansatz functions [15]. The Box spline of second order, i.e. a twice differentiable function, has compact support in space, but infinite support in frequency domain. Still, its Fourier coefficients decay with $\mathcal{O}\left(|k|^3\right)$.

Approximation error

An approximation estimate on the anisotropic space of translates $\mathcal{V}_{\mathbf{M}}^f$ requires additional properties of the fundamental interpolant $\mathrm{I}_{\mathbf{M}} \in \mathcal{V}_{\mathbf{M}}^f$. These properties describe how well trigonometric polynomials are approximated using functions in $\mathcal{V}_{\mathbf{M}}^f$, which in turn can be reduced to the approximation quality of the fundamental interpolant. This section first introduces such conditions, which describe the degree of trigonometric polynomials

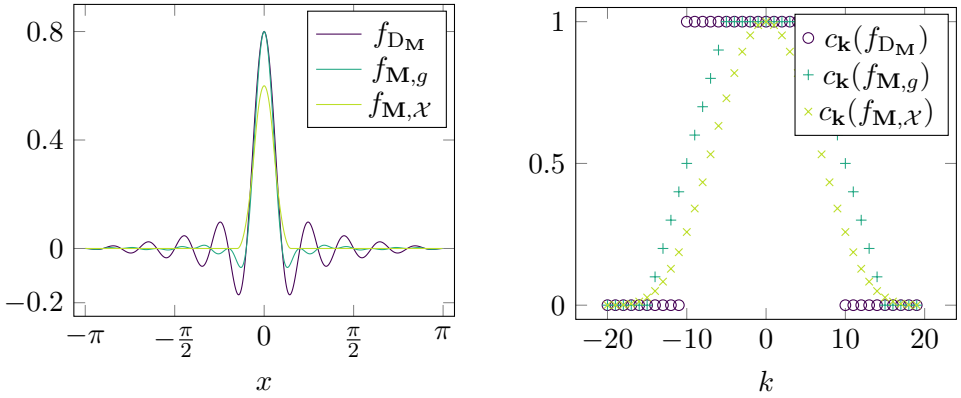

Figure 2.4. The Dirichlet kernel $f_{\mathrm{D}_\mathbf{M}}$, the de la Vallée Poussin mean $f_{\mathbf{M},g}$ with $g = 0.25$, and the Box spline kernel $f_{\mathbf{M},\mathcal{X}}$ with $\mathcal{X} = (1,1,1)$. The pattern matrix is $\mathbf{M} = (20) \in \mathbb{Z}^{1\times 1}$ and the kernels are shown in space (left) and in terms of their Fourier coefficients (right).

that can be reproduced exactly, and the locality of a function in frequency domain. This is followed by an approximation estimate taking into account the smoothness of the function to interpolate and the smoothness of the interpolating function, thus yielding a convergence rate in terms of the pattern matrix $\mathbf{M}$.

Strang and Fix introduced conditions for the order of approximation for polynomials [97]. For trigonometric polynomials in the periodic setting on isotropic grids, such conditions were derived in [79, (1.22)] and generalized to the anisotropic case in [9, Definition 2].

Definition 2.22. *Let $\mathbf{M} \in \mathbb{Z}^{d\times d}$ be regular, let $m = |\det(\mathbf{M})|$, let $a, s \in \mathbb{N} \cup \{0\}$, and let $q \geq 1$. A function $f \in \mathcal{L}^1(\mathbb{T}^d)$ fulfills the* elliptic Strang-Fix conditions *with order s and constant a if and only if there exists a sequence $\mathbf{b} = \{b_\mathbf{z}\}_{\mathbf{z}\in\mathbb{Z}^d} \subset \mathbb{R}$ with $b_\mathbf{z} \geq 0$ for all $\mathbf{z} \in \mathbb{Z}^d$, such that for all $\mathbf{h} \in \mathcal{G}(\mathbf{M}^\mathrm{T})$ and $\mathbf{z} \in \mathbb{Z}^d$ with $\mathbf{z} \neq \mathbf{0}$ the following statements are fulfilled:*

a) $|1 - m c_\mathbf{h}(f)| \leq b_\mathbf{0} \kappa_\mathbf{M}^{-s} \left\|\mathbf{M}^{-\mathrm{T}}\mathbf{h}\right\|^s$,

b) $|m c_{\mathbf{h}+\mathbf{M}^\mathrm{T}\mathbf{z}}(f)| \leq b_\mathbf{h} \kappa_\mathbf{M}^{-s} \left\|\mathbf{M}\right\|^{-a} \left\|\mathbf{M}^{-\mathrm{T}}\mathbf{h}\right\|^s$, *and*

c) $c_{SF} \coloneqq \left\| \left\{ \sigma_a^\mathbf{M}(\mathbf{z}) b_\mathbf{z} \right\}_{\mathbf{z}\in\mathbb{Z}^d} \right\|_q < \infty$, *where $\sigma_a^\mathbf{M}$ is the elliptic weight function* (2.4).

Remark 2.23. *If a function f fulfills the Strang-Fix conditions for a,s, and q, it also fulfills the Strang-Fix conditions for $\tilde{a}$, s, and q, where $0 \leq \tilde{a} \leq a$.*

Proof. This property follows directly from Definition 2.22, where the $\tilde{a} \leq a$ makes the conditions in Definition 2.22 b) and c) weaker. □

The number s in the elliptic Strang-Fix conditions signifies the order of the trigonometric polynomials that can be reproduced exactly by the function f. From the definition of the generating set $\mathbf{h} \in \mathcal{G}(\mathbf{M}^\mathrm{T}) = \mathbf{M}^\mathrm{T}\mathcal{P}(\mathbf{M}^\mathrm{T}) = \mathbb{Z}^d \cap \mathbf{M}^\mathrm{T}\left[-\frac{1}{2},\frac{1}{2}\right)^d$ follows that

$\mathbf{M}^{-\mathrm{T}}\mathbf{h} \in \left[-\frac{1}{2}, \frac{1}{2}\right)^d$. Therefore, the bound with $\|\mathbf{M}^{-\mathrm{T}}\mathbf{h}\|^s$ in Definition 2.22 a) requires a decay of the Fourier coefficients of f with degree s.

Likewise, in Definition 2.22 b) the Fourier coefficients outside of $\mathcal{G}(\mathbf{M}^{\mathrm{T}})$ have to decay even stronger, as the $b_{\mathbf{z}}$ have to converge to 0 in the weighted ℓ^q-norm of Definition 2.22 c). Here, a dependency on the number m of pattern points comes into play.

For example, assume that $\mathbf{M} = \mathrm{diag}(n, \dots, n)$ is a diagonal matrix with $n \in \mathbb{N}$. This results in a matrix condition number $\kappa_{\mathbf{M}} = 1$ and $\|\mathbf{M}\| = n$. Therefore, the condition in Definition 2.22 b) becomes

$$|mc_{\mathbf{h}+\mathbf{M}^{\mathrm{T}}\mathbf{z}}(f)| \leq b_{\mathbf{h}} n^{-a} \|\mathbf{M}^{-\mathrm{T}}\mathbf{h}\|^s,$$

i.e. with an increasing number of pattern points n in each direction, the Fourier coefficients of f have to decay with n^{-a}. This is equivalent to f being at least a-times differentiable.

The elliptic Strang-Fix conditions allow for the formulation of an approximation estimate depending on smoothness properties of the function g to be approximated and properties of the fundamental interpolant [9, Theorem 4]:

Lemma 2.24. *Let $\mathbf{M} \in \mathbb{R}^{d\times d}$ be regular with $m = |\det(\mathbf{M})|$ and $\|\mathbf{M}\| \geq 2$, let $q \geq 1$ and $a \in \mathbb{N}$.Let further $g \in \mathcal{A}^b_{\mathbf{M},q}(\mathbb{T}^d)$ with $b > d\big(1 - q^{-1}\big)$ and let the fundamental interpolant $\mathrm{I}_{\mathbf{M}}$ fulfill the elliptic Strang-Fix conditions for a,s, and q for $b \geq a \geq 0$, and set $r \coloneqq \min\{s, b-a\}$.*

In addition define a constant c_{IP} depending solely on the fundamental interpolant for $q < \infty$ as

$$c_{IP} \coloneqq m \max_{\mathbf{h}\in\mathcal{G}(\mathbf{M}^{\mathrm{T}})} \Big(|c_{\mathbf{h}}(\mathrm{I}_{\mathbf{M}})|^q + \|\mathbf{M}\|^{aq} \sum_{\mathbf{z}\in\mathbb{Z}^d\setminus\{\mathbf{0}\}} \big|\sigma_a^{\mathbf{M}}(\mathbf{z}) c_{\mathbf{h}+\mathbf{M}^{\mathrm{T}}\mathbf{z}}(\mathrm{I}_{\mathbf{M}})\big|^q \Big)^{\frac{1}{q}}$$

and for $q = \infty$ as

$$c_{IP} \coloneqq m \max_{\mathbf{h}\in\mathcal{G}(\mathbf{M}^{\mathrm{T}})} \max\left\{ |c_{\mathbf{h}}(\mathrm{I}_{\mathbf{M}})|, \sup_{\mathbf{z}\in\mathbb{Z}^d\setminus\{\mathbf{0}\}} \|\mathbf{M}\|^a \big|\sigma_a^{\mathbf{M}}(\mathbf{z}) c_{\mathbf{h}+\mathbf{M}^{\mathrm{T}}\mathbf{z}}(\mathrm{I}_{\mathbf{M}})\big| \right\}.$$

Further, define a constant c_{Sm} describing smoothness properties of the function g for $q > 1$ and $p \in \mathbb{R}$ with $\frac{1}{p} + \frac{1}{q} = 1$ as

$$c_{Sm} \coloneqq (1+d)^{\frac{a}{2}} 2^{-b} \left(\sum_{\mathbf{z}\in\mathbb{Z}^d\setminus\{0\}} \big|2\|\mathbf{z}\| - 1\big|^{-pb} \right)^{\frac{1}{p}}$$

and for $q = 1$ as

$$c_{Sm} \coloneqq (1+d)^{\frac{a}{2}} 2^{-b} \sup_{\mathbf{z}\in\mathbb{Z}^d\setminus\{0\}} \big|2\|\mathbf{z}\| - 1\big|^{-b}.$$

Let

$$c \coloneqq \begin{cases} c_{SF} + 2^{b-a} + c_{IP}c_{Sm}, & \text{if } r = s, \\ (1+d)^{s+a-b} c_{SF} + 2^{b-a} + c_{IP}c_{Sm}, & \text{if } r = b-a. \end{cases}$$

be defined, then it holds true that

$$\|g - \mathrm{L}_{\mathbf{M}}\, g\|_{a,\mathbf{M},q} \leq c \|\mathbf{M}\|^{-r} \|g\|_{b,\mathbf{M},q}.$$

With the equivalence of the anisotropic and the isotropic function spaces and, for $q = 2$, the Sobolev spaces, we further get an estimate in $\mathcal{H}^a(\mathbb{T}^d)$.

Corollary 2.25. *Let the assumptions of Lemma 2.24 hold and let $q = 2$. Then the estimate*

$$\|g - \mathrm{L}_{\mathbf{M}}\, g\|_{a,2} \leq c\kappa_{\mathbf{M}}^{b} \|\mathbf{M}\|^{-r} \|g\|_{b,2}$$

holds true with the constants from above.

Proof. The statement follows directly from Lemma 2.24 and the norm estimates (2.5) and (2.6). □

Lemma 2.26. *The constants c_{SF}, c_{IP}, and c_{Sm} can be bounded from above, independent of $\mathbf{M}$, assuming that the condition number $\kappa_{\mathbf{M}}$ can be uniformly bounded from above for regular $\mathbf{M} \in \mathbb{Z}^{d\times d}$.*

Proof. The constant c_{SF} form the Strang-Fix conditions depends, with regards to $\mathbf{M}$, on the elliptic weight function $\sigma_a^{\mathbf{M}}(\mathbf{k})$ for $\mathbf{k} \in \mathbb{Z}^d$. With the norm estimate (2.5), the constant is then bounded, using the boundedness of $\kappa_{\mathbf{M}}$.

For the tensor product case, i.e. for $\tilde{\mathbf{M}} = \mathrm{diag}(n, n, \ldots, n) \in \mathbb{Z}^{d\times d}$ for $n \in \mathbb{Z}$, a bound on c_{IP} is proven in [94, Remark after Theorem 4]. There, a bound is established with

$$c_{\mathrm{IP}} \leq \pi^s d^{\frac{s}{2}} \left(c_{\mathrm{SF}}^q - b_{\mathbf{0}}^q + \left(b_{\mathbf{0}} + \pi^{-s} d^{-\frac{s}{2}} \right)^q \right)^{\frac{1}{q}}$$

for $1 \leq q < \infty$ and

$$c_{\mathrm{IP}} \leq \pi^s d^{\frac{s}{2}} \max\left\{ c_{\mathrm{SF}}, b_{\mathbf{0}} + \pi^{-s} d^{-\frac{s}{2}} \right\}$$

for $q = \infty$. Here, s is the order, q the Lebesgue index, and $b_{\mathbf{0}}$ the constant from the Strang-Fix conditions, and d is the dimension.

To get to general integer matrices $\mathbf{M} \in \mathbb{Z}^{d\times d}$, consider the largest eigenvalue $n_{\max}$ of $\mathbf{M}$. Then the estimates can be applied to the isotropic case with the matrix $\tilde{\mathbf{M}} \coloneqq n_{\max}\, \mathbf{Id}_{\mathrm{d}}$ and yield an upper bound on c_{IP}.

The constant c_{Sm} is independent of $\mathbf{M}$ and therefore the proof is finished. □

Examples for approximation orders

We have seen above, that the order of convergence of the approximation depends not only on the smoothness of the approximated function g, but also on smoothness properties of the fundamental interpolant $\mathrm{I}_{\mathbf{M}}$. Here, we compute the parameters of the Strang-Fix conditions for the Dirichlet kernel, de la Vallée Poussin means and the ones belonging to 3-directional 2-dimensional periodized pattern Box spline.

The Dirichlet kernel $f_{\mathrm{D}_{\mathbf{M}}}$ given in Definition 2.21 results in a zero left-hand side in the conditions in Definition 2.22 a) and b) of the elliptic Strang-Fix conditions. Therefore, the parameters s and a in the elliptic Strang-Fix conditions can be chosen arbitrarily large.

The de la Vallée Poussin means with kernel $f = f_{\mathbf{M},\mathbf{b}}$ have compact support, because their Fourier coefficients are given by sampling Box splines on $\mathbb{Z}^d$, see Definition 2.20 and thereafter. Hence, there is always a q-summable sequence $b_{\mathbf{z}}$ such that $|mc_{\mathbf{h}+\mathbf{M}^{\mathrm{T}}\mathbf{z}}|$ is bounded for all $\mathbf{z} \in \mathbb{Z}^d$ and $\mathbf{h} \in \mathcal{G}(\mathbf{M}^{\mathrm{T}})$. Definition 2.22 a) is easily fulfilled, as the kernels $f_{\mathbf{M},\mathbf{b}}$ are bounded from below on $\mathcal{G}(\mathbf{M}^{\mathrm{T}})$. Thus, the de la Vallée Poussin means also fulfill the elliptic Strang-Fix conditions with arbitrarily high coefficicients s and a and for all q.

For the periodic pattern Box spline with kernel $f_{\mathbf{M},\mathcal{X}}$ defined in Definition 2.17 we consider here the case of dimension $d = 2$ and the 3-directional Box splines described in Example 2.18. Then, the Box splines fulfill the elliptic Strang-Fix conditions with the following constants [9, Theorem 5]:

Lemma 2.27. *Let $\mathbf{M} \in \mathbb{Z}^{2\times 2}$ be regular and let $B_{\mathcal{X}}$ be a periodized pattern box spline defined by the set $\mathcal{X} \in \mathbb{R}^{2\times(p_1+p_2+p_3)}$ with $\mathcal{X} \coloneqq \{\mathbf{x}_1, \ldots, \mathbf{x}_{p_1+p_2+p_3}\}$. Let further*

$$\begin{aligned}\mathbf{x}_1 = \cdots = \mathbf{x}_{p_1} &= (1,0)^{\mathrm{T}},\\ \mathbf{x}_{p_1+1} = \cdots = \mathbf{x}_{p_1+p_2} &= (0,1)^{\mathrm{T}},\\ \mathbf{x}_{p_1+p_2+1} = \cdots = \mathbf{x}_{p_1+p_2+p_3} &= (1,1)^{\mathrm{T}},\end{aligned}$$

let $\tilde{s} \coloneqq \min\{p_1+p_2, p_1+p_3, p_2+p_3\}$, let $a \geq 0$ with $\tilde{s} - a > 2$, and let $q \geq 2$.

Then the fundamental interpolant $\mathrm{I}_{\mathbf{M}} \in \mathcal{V}^f_{\mathbf{M}}$ with $f = f_{\mathbf{M},\mathcal{X}}$ fulfills the elliptic Strang-Fix conditions with order $s = \tilde{s} - a$ and constants a and q.

This section introduced translation invariant spaces. These spaces are constructed by taking a single function in $\mathcal{L}^2(\mathbb{T}^d)$ and translating it to the points of a pattern. The functions in such a space can also be characterized by their Fourier coefficients. Of special interest is the Dirichlet kernel $f_{\mathrm{D}_{\mathbf{M}}}$ as a generator, as the resulting function space coincides with the space of truncated trigonometric polynomials belonging to a pattern $\mathcal{P}(\mathbf{M})$. A generalization of this space is given by the de la Vallée Poussin means $f_{\mathbf{M},\mathbf{a}}$ which result in a reduced Gibbs phenomenon. Moreover, functions which have infinite support in frequency domain can be used with this ansatz. In this thesis, Box splines in space are used as an example for such functions.

A special function in the space of translates is the fundamental interpolant $\mathrm{I}_{\mathbf{M}}$ which generates a nodal basis by translation. Such a fundamental interpolant can then be used to define an interpolation and approximation operator. Assuming the Strang-Fix conditions — measuring the degree of exactly reproduced trigonometric polynomials — are met, a convergence rate for the approximation is be given.

2.5 Periodic homogenization

In applications one often deals with the simulation of structures that have complicated microstructures. The computation of the elastic behavior of a composite material, i.e. a geometry consisting of more than one material, with small-scale variations involves a

large number of degrees of freedom. A remedy is provided by periodic homogenization, which computes the homogeneous elastic properties of a composite.

This section is divided into two parts. The first one derives the equation of linear elasticity in homogenization as a limit process of a scale separation. Further, it introduces stiffness distributions as fields of coefficients for the elliptic partial differential equation. We analyze the resulting equation further in the second part. This includes deriving two equivalent formulations based on a projection operator onto the space of test functions.

Periodic homogenization as a limit process

The aim of homogenization is to replace a composite of different materials by a homogeneous one which exhibits the same — restricted here to linear material laws — elastic behavior. It is necessary, that the geometry of the composite can be divided into two parts, a macroscopic and a microscopic one. The macroscopic part is assumed to change slowly over the domain and, in contrast, the microscopic part describes the quickly changing local material properties. The latter is further assumed to be periodic, thus making computations on a single reference volume element sufficient to determine the overall elastic stiffness — also called effective stiffness — of the microscopic scale. Mathematically, this separation is achieved by making an outer expansion of the solution in terms of the parameter describing the scale separation. If this parameter is sufficiently small — which we assume here — the homogenization process is successful and mathematically sound. If higher order terms of the outer expansion are required for computations, e.g. for certain nonlinear material laws on the macroscopic scale, a derivation is found in [14, 98].

This section first defines stiffness distributions with the conditions to ensure the existence and uniqueness of a solution as required by the theorem of Lax-Milgram. Then follows a description of the homogenization process and convergence results for it.

The elastic behavior of the materials is described by a stiffness distibution $\mathcal{C} \in \mathrm{SSym}_d\big(\mathcal{L}^\infty(\mathcal{R})\big)$ for an open set $\mathcal{R} \subset \mathbb{R}^d$. In the context of homogenization, this leads to a piecewise constant function describing the geometry and the material properties.

Definition 2.28. *Let $\mathcal{R} \subset \mathbb{R}^d$ be an open set. A function $\mathcal{C} \in \mathrm{SSym}_d\big(\mathcal{L}^\infty(\mathcal{R})\big)$ is called* stiffness distribution *if it is*

a) bounded, *i.e. there exists $c_b > 0$ such that*

$$\|\mathcal{C}\gamma\|_2 \leq c_b \|\gamma\|_2$$

for all $\gamma \in \mathrm{Sym}_d\big(\mathcal{L}^2(\mathcal{R})\big)$, and

b) elliptic, *i.e. there exists $c_e > 0$ such that*

$$\langle \mathcal{C} : \gamma, \gamma \rangle_2 \geq c_e \|\gamma\|_2^2$$

for all $\gamma \in \mathrm{Sym}_d\big(\mathcal{L}^2(\mathcal{R})\big)$.

We call a fourth-order tensor $\mathcal{C}^0 \in \mathrm{SSym}_d(\mathbb{R})$ *a* stiffness tensor *if it fulfills the above conditions when considered as a constant function.*

As a special case an isotropic stiffness tensor is parametrized by two parameters, the first and second Lamé parameters $\lambda, \mu \in \mathbb{R}$ with $\mu \geq 0$, respectively. Such a stiffness tensor then has the form $\mathcal{C}_{ijkl} = \lambda\delta_{ij}\delta_{kl} + \mu(\delta_{ik}\delta_{jl} + \delta_{il}\delta_{jk}) \in \mathrm{SSym}_d(\mathbb{R})$ for $d = 3$ and $i, j, k, l = 1, \ldots, 3$.

When applying a load to the geometry described by the stiffness distribution $\mathcal{C}$, the material deforms. This deformation is given by the displacement $\tilde{\mathbf{u}} \in \mathcal{H}^1(\mathcal{R})^d$ with respect to the unloaded configuration. Due to the deformation, the strain $\varepsilon \in \mathcal{E}(\mathcal{R})$ and the stress $\sigma \in \mathrm{Sym}_d\big(\mathcal{L}^2(\mathcal{R})\big)$ increase in the material.

We assume that the displacements $\tilde{\mathbf{u}}$ are small, i.e. that the load applied to the material is small. Thus, the strain and displacement are connected via

$$\varepsilon = \nabla_{\mathrm{Sym}}\, \mathbf{u},$$

where ∇_{Sym} is the symmetric gradient operator from (2.2). Hooke's law yields the formula

$$\sigma = \mathcal{C} : \varepsilon$$

for the stress σ.

With these components, the equation of linear elasticity then states:
find a displacement $\tilde{\mathbf{u}} \in \mathcal{H}^1(\mathcal{R})^d$ such that

$$\begin{cases} \operatorname{div} \mathcal{C} : \nabla_{\mathrm{Sym}}\, \tilde{\mathbf{u}} = 0 & \text{in } \mathcal{R}, \\ \tilde{\mathbf{u}} = 0 & \text{on } \partial\mathcal{R}, \end{cases}$$

in weak sense.

The main assumption of homogenization is that the stiffness distribution can be decomposed into a macroscopic and a microscopic part, where the microscopic structure is assumed to be periodic. This division into scales presumes that the characteristic length scales of the microscopic and macroscopic structures are separated well with a factor $a \ll 1$. This allows to — artificially — write the stiffness distribution $\mathcal{C}$ as $\mathcal{C}^a(\mathbf{x}, \mathbf{y})$ with $\mathbf{x} = a^{-1}\mathbf{y}$. The vector $\mathbf{y} \in \mathcal{R}$ denotes the macroscopic change and the periodic microscopic variable is $\mathbf{x} \in \mathbb{T}^d$.

We split the displacement into two scales and expand it as a power series in a, i.e.

$$\mathbf{u}^a(\mathbf{x}, \mathbf{y}) = \sum_{i=0}^{\infty} a^i \mathbf{u}_i(\mathbf{x}, \mathbf{y})$$

with vector fields $\mathbf{u}_i \in \mathcal{H}^1(\mathbb{T}^d \times \mathcal{R})^d$. This means that the equation

$$\operatorname{div} \mathcal{C}^a : \nabla_{\mathrm{Sym}}\, \mathbf{u}^a = 0 \quad \text{on } \mathbb{T}^d \times \mathbb{R} \tag{2.17}$$

has to be fulfilled in weak sense. The macroscopic behavior with a homogeneous stiffness is then attained for $a \to 0$.

The transition from the global problem to the macroscopic problem with homogenized coefficients is described in the following lemma [25, Theorem 10.11]:

Lemma 2.29. *Let* $\mathbf{u}^a \in \mathcal{H}^1(\mathbb{T}^d \times \mathcal{R})^d$ *fulfill* (2.17) *with homogeneous Dirichlet boundary conditions. Let further* $\mathbf{u}^0 \in \mathcal{H}^1(\mathcal{R})^d$*, depending only on the macroscopic variable* $\mathbf{y}$*, fulfill the equation*

$$\operatorname{div} \mathcal{C}^{\text{eff}} : \nabla_{\text{Sym}} \mathbf{u}^0 = 0 \quad \text{on } \mathcal{R}$$

in weak sense with homogeneous boundary conditions and constant stiffness $\mathcal{C}^{\text{eff}} \in \text{SSym}_d(\mathbb{R})$*. Then for* $a \to 0$

a) $\mathbf{u}^a \to \mathbf{u}^0$ *weakly in* $\mathcal{H}^1(\mathbb{T}^d \times \mathcal{R})^d$*, and*

b) $\mathcal{C}^a : \nabla_{\text{Sym}} \mathbf{u}^a \to \mathcal{C}^{\text{eff}} : \nabla_{\text{Sym}} \mathbf{u}^0$ *weakly in* $\text{Sym}_d\big(\mathcal{L}^2(\mathbb{T}^d \times \mathcal{R})\big)$*.*

Further, the homogenized stiffness tensor $\mathcal{C}^{\text{eff}}$ *is given for any* $\varepsilon^0 \in \text{Sym}_d(\mathbb{R})$ *by*

$$\mathcal{C}^{\text{eff}} : \varepsilon^0 \coloneqq \int_{\mathbb{T}^d} \mathcal{C}(\mathbf{x}) : \nabla_{\text{Sym}} \mathbf{u}(\mathbf{x}) \, \mathrm{d}\mathbf{x}$$

where $\mathcal{C} \in \text{SSym}_d\big(\mathcal{L}^\infty(\mathbb{T}^d)\big)$ *is the periodic part of the stiffness distribution, and* $\mathbf{u}(\mathbf{x})$ *is the solution of the partial differential equation:*
find $\mathbf{u} \in \mathcal{H}^1(\mathbb{T}^d)^d$ *such that*

$$\operatorname{div} \mathcal{C} : \big(\varepsilon^0 + \nabla_{\text{Sym}} \mathbf{u}\big) = 0 \quad \text{in } \mathbb{T}^d \tag{2.18}$$

in the weak sense.

In the context of homogenization, the d-torus is also called *representative volume element*. The macroscopic strain ε^0 can be interpreted as pulling at this representative volume element in certain directions.

The homogenized — or effective — stiffness tensor $\mathcal{C}^{\text{eff}}$ then describes the macroscopic elastic behavior of the microstructure characterized by the materials in the representative volume element.

We rearrange the equation solving the homogenization problem (2.18) to read: find $\mathbf{u} \in \mathcal{H}^1(\mathbb{T}^d)^d$ such that

$$\langle \mathcal{C} : \nabla_{\text{Sym}} \mathbf{u}, \nabla_{\text{Sym}} \tilde{\gamma} \rangle_2 = -\langle \mathcal{C} : \varepsilon^0, \nabla_{\text{Sym}} \tilde{\gamma} \rangle_2 \tag{2.19}$$

holds true for all $\tilde{\gamma} \in \mathcal{H}^1(\mathbb{T}^d)^d$. In this thesis we do not solve (2.19) in terms of the displacements $\mathbf{u}$ but solve for the strain ε directly. This necessitates the use of the space of symmetric gradient fields with zero mean $\mathcal{E}(\mathbb{T}^d)$ introduced in (2.3).

Definition 2.30. *Let* $\mathcal{C} \in \text{SSym}_d\big(\mathcal{L}^\infty(\mathbb{T}^d)\big)$ *be a stiffness distribution and let* $\varepsilon^0 \in \text{Sym}_d(\mathbb{R})$*. Then the* equation of linear elasticity in periodic homogenization *reads: find* $\varepsilon \in \mathcal{E}(\mathbb{T}^d)$ *such that*

$$\langle \mathcal{C} : \varepsilon, \gamma \rangle_2 = -\langle \mathcal{C} : \varepsilon^0, \gamma \rangle_2 \tag{LE}$$

for all $\gamma \in \mathcal{E}(\mathbb{T}^d)$*.*

Further information about mathematical homogenization can be found for example in [25].

Alternative formulations of the homogenization equation

The equation of linear elasticity in periodic homogenization shown in Definition 2.30 is the basis for the numerical approach of [73, 74], this thesis builds on using the formulation in [105]. They do not solve the equation directly, but rearrange it into an equation with the strain ε as a fixed-point.

We start this section by defining a projection operator — the Green operator — that maps functions from $\mathrm{Sym}_d\big(\mathcal{L}^2(\mathbb{T}^d)\big)$ onto the space $\mathcal{E}(\mathbb{T}^d)$ and list its crucial properties. An application of this operator then replaces the test functions in (LE) by more simple ones, dropping the requirement to be gradient fields. This leads to an equivalent formulation, here called variational equation. The equation considered by Moulinec and Suquet is then obtained by rearranging the terms and leads to the Lippmann-Schwinger equation, which also appeares in the quantum theory of scattering [62].

The space $\mathcal{E}(\mathbb{T}^d)$ is numerically difficult to handle and [105] derives a projection operator that maps the Lebesgue space $\mathrm{Sym}_d\big(\mathcal{L}^2(\mathbb{T}^d)\big)$ onto the space of gradient fields $\mathcal{E}(\mathbb{T}^d)$. This projection operator $\Gamma^0\mathcal{C}^0$ originates from the Green operator of an equation of linear elasticity with constant coefficients $\mathcal{C}^0 \in \mathrm{SSym}_d(\mathbb{R})$, see [51, 110]. This stiffness tensor $\mathcal{C}^0$ is also called *reference stiffness*. The idea to use this Green operator originates from [73, 74] and the operator acts as the second order derivative of a preconditioner.

Consider the constant reference stiffness tensor $\mathcal{C}^0 \in \mathrm{SSym}_d(\mathbb{R})$ and the weak partial differential equation

$$\operatorname{div} \mathcal{C}^0 : \nabla_{\mathrm{Sym}} \mathbf{u} = f$$

for the displacement $\mathbf{u}$ with some right-hand side $f \in \mathcal{L}^2(\mathbb{T}^d)$. Transforming this partial differential equation to Fourier coefficients yields

$$\overline{\nabla_{\mathrm{Sym}_\mathbf{k}}}^{\mathrm{T}} : \mathcal{C}^0 : \nabla_{\mathrm{Sym}_\mathbf{k}} c_\mathbf{k}(\mathbf{u}) = c_\mathbf{k}(f)$$

for all $\mathbf{k} \in \mathbb{Z}^d$. The stiffness tensor $\mathcal{C}^0$ is by definition positive definite and therefore the equation can be solved for $c_\mathbf{k}(\mathbf{u})$ and we obtain

$$c_\mathbf{k}(\mathbf{u}) = \big(\overline{\nabla_{\mathrm{Sym}_\mathbf{k}}}^{\mathrm{T}} : \mathcal{C}^0 : \nabla_{\mathrm{Sym}_\mathbf{k}}\big)^{-1} c_\mathbf{k}(f), \quad \mathbf{k} \in \mathbb{Z}^d.$$

We replace the right-hand side by $f = \operatorname{div} \sigma$ for a stress field $\sigma \in \mathrm{Sym}_d\big(\mathcal{L}^2(\mathbb{T}^d)\big)$, i.e.

$$c_\mathbf{k}(f) = \overline{\nabla_{\mathrm{Sym}_\mathbf{k}}}^{\mathrm{T}} c_\mathbf{k}(\sigma), \quad \mathbf{k} \in \mathbb{Z}^d.$$

Further, to result in a strain ε, we apply the symmetric gradient operator from the left. This motivates the definition of the Green operator.

Definition 2.31. *Let $\mathcal{C}^0 \in \mathrm{SSym}_d(\mathbb{R})$ be a stiffness tensor and let $\sigma \in \mathrm{Sym}_d\big(\mathcal{L}^2(\mathbb{T}^d)\big)$. The* Green operator $\Gamma^0 : \mathrm{Sym}_d\big(\mathcal{L}^2(\mathbb{T}^d)\big) \to \mathcal{E}(\mathbb{T}^d)$ *acts as a Fourier multiplier via*

$$\Gamma^0 : \sigma \coloneqq \sum_{\mathbf{k} \in \mathbb{Z}^d} \hat{\Gamma}^0_\mathbf{k} : c_\mathbf{k}(\sigma)\, \mathrm{e}^{\mathrm{i}\mathbf{k}^{\mathrm{T}}\cdot}. \tag{2.20}$$

The Fourier coefficients of the Green operator are given by

$$\hat{\Gamma}^0_\mathbf{k} : c_\mathbf{k}(\sigma) \coloneqq \nabla_{\mathrm{Sym}_\mathbf{k}} \Big(\overline{\nabla_{\mathrm{Sym}_\mathbf{k}}}^{\mathrm{T}} : \mathcal{C}^0 : \nabla_{\mathrm{Sym}_\mathbf{k}}\Big)^{-1} \overline{\nabla_{\mathrm{Sym}_\mathbf{k}}}^{\mathrm{T}} c_\mathbf{k}(\sigma), \quad \mathbf{k} \in \mathbb{Z}^d. \tag{2.21}$$

With the Green operator we define a projection operator $\Gamma^0\mathcal{C}^0$ that maps the $\mathrm{Sym}_d\big(\mathcal{L}^2(\mathbb{T}^d)\big)$ onto $\mathcal{E}(\mathbb{T}^d)$. The main properties of this projection operator are given by the following lemma [105, Lemma 2]:

Lemma 2.32. *Let $\mathcal{C}^0 \in \mathrm{SSym}_d(\mathbb{R})$ be a stiffness tensor with c_b and c_e the constants for boundedness and ellipticity from Definition 2.28. Then it holds true that:*

a) $\Gamma^0\mathcal{C}^0$ is a bounded operator with $\|\Gamma^0\mathcal{C}^0 : \sigma\|_2 \leq \frac{c_b}{c_e}\|\sigma\|_2$ for all $\sigma \in \mathrm{Sym}_d\big(\mathcal{L}^2(\mathbb{T}^d)\big)$.

b) The adjoint operator to $\Gamma^0\mathcal{C}^0$ is given by $\langle \Gamma^0\mathcal{C}^0 : \sigma, \nu\rangle_2 = \langle \sigma, \mathcal{C}^0\Gamma^0 : \nu\rangle_2$ for all $\sigma, \nu \in \mathrm{Sym}_d\big(\mathcal{L}^2(\mathbb{T}^d)\big)$.

c) $\Gamma^0\mathcal{C}^0$ is a projection onto $\mathcal{E}(\mathbb{T}^d)$.

d) $\Gamma^0\mathcal{C}^0 : \sigma = 0$ for all $\sigma \in \mathrm{Sym}_d\big(\mathcal{L}^2(\mathbb{T}^d)\big)$ that are constant almost everywhere.

An important requisite for the above properties of the Green operator Γ^0 is the invariance of its Fourier coefficients under complex conjugation.

Lemma 2.33. *It holds*

$$\hat{\Gamma}^0_{\mathbf{k}} = \overline{\hat{\Gamma}^0_{\mathbf{k}}},$$

i.e. , the Fourier coefficients of Γ^0 are real-valued tensors.

Proof. This property follows directly from the definition of $\hat{\Gamma}^0_{\mathbf{k}}$, $\mathbf{k} \in \mathbb{Z}^d$ and the symmetry of the reference stiffness $\mathcal{C}^0$. □

With help of the projection operator $\Gamma^0\mathcal{C}^0$ the equation of linear elasticity in periodic homogenization (LE) can be rewritten. Instead of testing with functions $\gamma \in \mathcal{E}(\mathbb{T}^d)$ the projection allows to test with functions in the simpler space $\mathrm{Sym}_d\big(\mathcal{L}^2(\mathbb{T}^d)\big)$, projecting them onto $\mathcal{E}(\mathbb{T}^d)$ [105, Proposition 3].

Lemma 2.34. *The strain $\varepsilon \in \mathcal{E}(\mathbb{T}^d)$ is a solution of*

$$\langle \mathcal{C} : \varepsilon, \gamma\rangle_2 = -\langle \mathcal{C} : \varepsilon^0, \gamma\rangle_2$$

for all $\gamma \in \mathcal{E}(\mathbb{T}^d)$ if and only if ε is a solution of the variational equation

$$\langle \mathcal{C}^0\Gamma^0\mathcal{C} : \varepsilon, \nu\rangle_2 = -\langle \mathcal{C}^0\Gamma^0\mathcal{C} : \varepsilon^0, \nu\rangle_2 \tag{VE}$$

for all $\nu \in \mathrm{Sym}_d\big(\mathcal{L}^2(\mathbb{T}^d)\big)$.

Proof. The proof is a direct application of Lemma 2.32 c) and b). □

The publication [74] does not deal use the above equation for the discretization. They instead derive a partial differential equation with strain ε as a fixed-point using calculation on the Fourier coefficients of strain ε and displacement $\mathbf{u}$. All those formulations are equaivalent [105, Proposition 3]. The (short) proof of the following lemma is of special interest because the equivalence between the variational equation and the so-called Lippmann-Schwinger equation of Moulinec and Suquet depends crucially on Lemma 2.32 d).

Lemma 2.35. *The strain $\varepsilon \in \mathcal{E}(\mathbb{T}^d)$ is a solution of*

$$\langle \mathcal{C}^0\Gamma^0\mathcal{C} : \varepsilon, \nu\rangle_2 = -\langle \mathcal{C}^0\Gamma^0\mathcal{C} : \varepsilon^0, \nu\rangle_2$$

for all $\nu \in \mathrm{Sym}_d\big(\mathcal{L}^2(\mathbb{T}^d)\big)$ if and only if ε is a solution of the Lippmann-Schwinger equation

$$\langle \varepsilon + \Gamma^0\big(\mathcal{C} - \mathcal{C}^0\big) : \big(\varepsilon + \varepsilon^0\big), \gamma\rangle_2 = 0 \tag{LS}$$

for all $\gamma \in \mathrm{Sym}_d\big(\mathcal{L}^2(\mathbb{T}^d)\big)$.

Proof. Consider the equation

$$(\varepsilon^0 + \varepsilon) - \Gamma^0\mathcal{C}^0 : (\varepsilon^0 + \varepsilon) = (\varepsilon^0 + \varepsilon) - \Gamma^0\mathcal{C}^0 : \varepsilon$$

which holds true because of Lemma 2.32 d). Further, as $\varepsilon \in \mathcal{E}(\mathbb{T}^d)$ and $\Gamma^0\mathcal{C}^0$ is a projection onto $\mathcal{E}(\mathbb{T}^d)$ via Lemma 2.32 c) this yields

$$(\varepsilon^0 + \varepsilon) - \Gamma^0\mathcal{C}^0 : (\varepsilon^0 + \varepsilon) = \varepsilon^0. \tag{2.22}$$

A multiplication of (VE) from the left with $\big(\mathcal{C}^0\big)^{-1}$ results in

$$\langle \Gamma^0\mathcal{C} : \big(\varepsilon^0 + \varepsilon\big), \nu\rangle_2 = 0$$

and inserting (2.22) yields the Lippmann-Schwinger equation

$$\langle \varepsilon + \Gamma^0\big(\mathcal{C} - \mathcal{C}^0\big) : \big(\varepsilon + \varepsilon^0\big), \nu\rangle_2 = 0$$

for all $\nu \in \mathrm{Sym}_d(\mathcal{L}^2(\mathbb{T}^d))$, concluding the proof. □

This thesis deals with the equation of linear elasticity in homogenization. This equation is derived from a limit process, where a macroscopic structure is assumed to contain a much smaller periodic substructure. The resulting solution of the macroscopic problem is decomposed into large changes and changes happening on the microscale. In the limit, the elastic behavior of the microstructure is replaced by a single stiffness tensor, that has the same elastic behavior — considering only the first term of the expansion.

This equation, an elliptic partial differential equation studied in detail in literature, can then be rearranged to a fixed-point equation in terms of the strain ε. This is done by using the projection property of the Green operator $\Gamma^0\mathcal{C}^0$ that maps onto the solution space of the equation. The Green operator can be understood as a preconditioner derived from a constant coefficient equation, differentiated twice. This reformulation then leads to the Lippmann-Schwinger equation, the starting point of the field of FFT-based homogenization created by Moulinec and Suquet 20 years ago.

2.6 Solution theory for partial differential equations

The analysis of the equation of linear elasticity in periodic homogenization requires mainly the use of the Lemma of Lax-Milgram, providing an existence and uniqueness result. For that, the mildest assumption on the coefficients of the partial differential equation — namely the stiffness distribution $\mathcal{C}$ — is a boundedness almost everywhere. Naturally, the question arises, how a higher regularity of the coefficients carries over to the solution and a respective result is stated in this section. Further, preparing the convergence analysis of discretizations of the equations, we state the first Strang lemma, giving a result on the error between a continuous and a discrete solution to certain variational problems.

The existence and uniqueness of solutions of partial differential equations and their discretizations is inevitably tied to the Theorem of Lax-Milgram [29, Section 6.2, Theorem 1]. There, a bounded and elliptic bilinear form on a Hilbert space is required to proof the unique solvability of a variational problem.

Theorem 2.36. *Let $\mathcal{V}$ be a Hilbert space and let $B : \mathcal{V} \times \mathcal{V} \to \mathbb{R}$ be a bilinear form. Let B be bounded, i.e. there exist a constant $c_b > 0$ such that for all $\gamma, \varphi \in \mathcal{V}$ holds*

$$|B(\gamma, \varphi)| \leq c_b \|\gamma\|_2 \|\varphi\|_2,$$

and let B be elliptic, i.e. there exists a constant $c_e > 0$ such that for all $\gamma \in \mathcal{V}$ holds

$$c_e \|\gamma\|_2^2 \leq B(\gamma, \gamma).$$

Further, let $F \in \mathcal{V}'$ be an element of the dual space of $\mathcal{V}$. Then there exists a unique element $\varepsilon \in \mathcal{V}$ such that

$$B(\varepsilon, \gamma) = \langle F, \gamma \rangle_2,$$

where $\langle F, \gamma \rangle_2$ is provided by the Riesz representation theorem, see [29, Section D.2, Theorem 2].

The definition carries over to the stiffness distribution $\mathcal{C}$ [3, Section 8.3].

Remark 2.37. *Define a bilinear form $B : \mathrm{Sym}_d\big(\mathcal{L}^2(\mathbb{T}^d)\big) \times \mathrm{Sym}_d\big(\mathcal{L}^2(\mathbb{T}^d)\big) \to \mathbb{R}$ with*

$$B(\varepsilon, \gamma) \coloneqq \langle \mathcal{C} : \varepsilon, \gamma \rangle_2, \quad \varepsilon, \gamma \in \mathrm{Sym}_d\big(\mathcal{L}^2(\mathbb{T}^d)\big).$$

Then the definitions of boundedness and ellipticity from Definition 2.28 are equivalent to those required in Theorem 2.36.

Applied to the equation of linear elasticity in periodic homogenization (LE), this yields the following result.

Theorem 2.38. *The equation of linear elasticity in homogenization searching for a strain $\varepsilon \in \mathcal{E}(\mathbb{T}^d)$ such that*

$$\langle \mathcal{C} : \varepsilon, \gamma \rangle_2 = -\langle \mathcal{C} : \varepsilon^0, \gamma \rangle_2$$

for all $\gamma \in \mathcal{E}(\mathbb{T}^d)$ has a solution that is unique.

Proof. The space of curl-free functions $\mathcal{E}(\mathbb{T}^d)$ is a Hilbert space. By Definition 2.28 and Remark 2.37 the bilinear form is elliptic and bounded, and the linear form is bounded. Therefore, Theorem 2.36 is applicable and the proof finished. □

The coefficients $\mathcal{C}$ of the equation of linear elasticity (LE) are at least assumed to be in $\mathrm{SSym}_d\big(\mathcal{L}^\infty(\mathbb{T}^d)\big)$ and are thus in general not even continuous. The effect of higher regularity in the stiffness distribution $\mathcal{C}$ onto the regularity of the strain ε is explained by the following theorem [29, Section 6.3.1, Theorem 2]:

Lemma 2.39. *Let $\mathcal{C} \in \mathrm{SSym}_d\big(\mathcal{W}^{b,\infty}(\mathbb{T}^d)\big)$ for $b \in \mathbb{N}$ and let $\varepsilon \in \mathcal{E}(\mathbb{T}^d)$ be a solution of the continuous equation of linear elasticity in periodic homogenization* (LE) *with macroscopic strain ε^0. Then it holds that*

$$\varepsilon \in \mathrm{Sym}_d\big(\mathcal{H}^b(\mathbb{T}^d)\big)$$

with

$$\|\varepsilon\|_{b,2} \leq c\|\mathcal{C}\|_{b,\infty}\|\varepsilon^0\|_2.$$

The constant $c \in \mathbb{R}$ depends only on ε^0.

An important result when analyzing the convergence of discretizations of partial differential equations is the first Strang lemma. Provided a Hilbert space $\mathcal{V}$, the continuous equation searches for a solution $\varepsilon \in \mathcal{V}$ such that

$$B(\varepsilon, \gamma) = F(\gamma)$$

holds true for all $\gamma \in \mathcal{V}$. The bilinear form B is assumed to be elliptic and bounded and F is a linear operator.

For the discretization, the infinite-dimensional function space $\mathcal{V}$ is replaced by a finite-dimensional space $\mathcal{V}_\mathbf{M} \subset \mathcal{V}$. The bilinear form B and the linear form F are replaced by approximations $B_\mathbf{M}$ and $F_\mathbf{M}$, respectively, called a "variational crime" [96]. This yields a family of variational problems to find solutions $\varepsilon_\mathbf{M} \in \mathcal{V}_\mathbf{M}$ such that

$$B_\mathbf{M}(\varepsilon_\mathbf{M}, \gamma_\mathbf{M}) = F_\mathbf{M}(\gamma_\mathbf{M})$$

holds for all $\gamma_\mathbf{M} \in \mathcal{V}_\mathbf{M}$. The first Strang lemma [24, p. 192, Theorem 26.1] then gives an error estimate:

Lemma 2.40. *For a Hilbert space $\mathcal{V}$ consider the variational problem: find $\varepsilon \in \mathcal{V}$ such that*

$$B(\varepsilon, \gamma) = F(\gamma)$$

for all $\gamma \in \mathcal{V}$, where $B : \mathcal{V} \times \mathcal{V} \to \mathbb{R}$ is bounded with constant c_b and an elliptic bilinear form, and $F : \mathcal{V} \to \mathbb{R}$ is a bounded linear form.

Further, let $\mathcal{V}_\mathbf{M} \subset \mathcal{V}$ be a finite-dimensional subspace and let

$$B_\mathbf{M}(\varepsilon_\mathbf{M}, \gamma_\mathbf{M}) = F_\mathbf{M}(\gamma_\mathbf{M})$$

be a family of equations indexed by $\mathbf{M}$*, solved by* $\varepsilon_{\mathbf{M}} \in \mathcal{V}_{\mathbf{M}}$ *for all* $\gamma_{\mathbf{M}} \in \mathcal{V}_{\mathbf{M}}$*. Further, assume that the biliner forms* $B_{\mathbf{M}} : \mathcal{V}_{\mathbf{M}} \times \mathcal{V}_{\mathbf{M}} \to \mathbb{R}$ *are bounded and uniformly elliptic with a common constant* $c_e > 0$ *from Definition 2.28 b), independent of* $\mathcal{V}_{\mathbf{M}}$*. Further, let* $F_{\mathbf{M}} : \mathcal{V}_{\mathbf{M}} \to \mathbb{R}$ *be a linear form.*

Then the estimate

$$\begin{aligned}\|\varepsilon - \varepsilon_{\mathbf{M}}\| \leq & \Big(1 + \frac{c_b}{c_e}\Big) \inf_{\varphi_{\mathbf{M}} \in \mathcal{V}_{\mathbf{M}}} \|\varepsilon - \varphi_{\mathbf{M}}\| \\ & + \frac{1}{c_e} \inf_{\varphi_{\mathbf{M}} \in \mathcal{V}_{\mathbf{M}}} \sup_{\eta_{\mathbf{M}} \in \mathcal{V}_{\mathbf{M}}} \frac{|B(\varphi_{\mathbf{M}}, \eta_{\mathbf{M}}) - B_{\mathbf{M}}(\varphi_{\mathbf{M}}, \eta_{\mathbf{M}})|}{\|\eta_{\mathbf{M}}\|} \\ & + \frac{1}{c_e} \sup_{\eta_{\mathbf{M}} \in \mathcal{V}_{\mathbf{M}}} \frac{|F(\eta_{\mathbf{M}}) - F_{\mathbf{M}}(\eta_{\mathbf{M}})|}{\|\eta_{\mathbf{M}}\|}\end{aligned}$$

holds. The norm $\|\cdot\|$ *is the induced norm in the Hilbert space* $\mathcal{V}$*.*

3 Periodic homogenization on spaces of translates

The discretization of the Lippmann-Schwinger equation (LS) in [74] uses a Fourier collocation scheme and results in an algorithm with the strain ε as a fixed point. In et al. [105] the authors solve the variational equation (VE) by a Galerkin projection onto the space of truncated Fourier series, i.e. Fourier polynomials, and obtain the same discretization and solutions.

In this chapter we derive discretized equations for both (LS) and (VE) with translation invariant spaces as ansatz spaces. First, we introduce and analyze the periodized Green operator on translation invariant spaces. With this new operator we discretize both partial differential equations and, similar to [105], characterize the connection between the two solutions. Afterwards, we explain the convergence of the discretization scheme and the resulting numerical algorithms.

The content of Sections 3.1, 3.2, and 3.3 are based on [8].

3.1 The periodized Green operator

When discretizing the Lippmann-Schwinger equation and the variational equation, [74] and [105] arrive at a discretized Green operator which stems from the Green operator Γ^0 in Definition 2.31 by truncating its Fourier series. In [18, 21] an energy-based formulation using constant finite elements is discretized. This approach leads to an operator that derives from a convolution of the Green operator Γ^0 with the basis function, i.e. a constant finite element, which is then periodized in frequency domain. In this section we generalize the Green operator to anisotropic spaces of translates and prove the properties of the operator.

A Galerkin projection of the partial differential equations (LS) and (VE) requires the definition of a discretized version of the Green operator Γ^0 from Equation (2.20). The Green operator Γ^{p} we propose here results from a periodization of Γ^0. It uses the function f that generates the finite dimensional ansatz space $\mathcal{V}_{\mathbf{M}}^f$ of translates. This approach is a generalization of the Green operators of [74] and [18], as both of them can be found as special cases for a suitable choice of the space $\mathcal{V}_{\mathbf{M}}^f$.

This section proceeds by first defining the new Green operator and then stating these special cases.

Let $\mathbf{M} \in \mathbb{Z}^{d\times d}$ denote a regular pattern matrix and let $\mathcal{V}_{\mathbf{M}}^f$ be the according translation invariant space spanned by the translates $\mathcal{T}(\mathbf{y})f$, $\mathbf{y} \in \mathcal{P}(\mathbf{M})$ of a function $f \in \mathcal{A}(\mathbb{T}^d)$. We assume that a fundamental interpolant $\mathrm{I}_{\mathbf{M}} \in \mathcal{V}_{\mathbf{M}}^f$ exists according to Lemma 2.14 a), which also implies the linear independence of the translates $\mathcal{T}(\mathbf{y})f$, see Lemma 2.14 b).

The coefficients $\hat{a}_{\mathbf{h}}$, $\mathbf{h} \in \mathcal{G}(\mathbf{M}^{\mathrm{T}})$ belonging to $\mathrm{I}_{\mathbf{M}}$ from Lemma 2.12 are

$$c_{\mathbf{h}+\mathbf{M}^{\mathrm{T}}\mathbf{z}}(\mathrm{I}_{\mathbf{M}}) = \hat{a}_{\mathbf{h}} c_{\mathbf{h}+\mathbf{M}^{\mathrm{T}}\mathbf{z}}(f), \quad \mathbf{h} \in \mathcal{G}(\mathbf{M}^{\mathrm{T}}),\ \mathbf{z} \in \mathbb{Z}^d. \tag{3.1}$$

We assume from now on that functions $\gamma, \nu \in \mathrm{Sym}_d\big(\mathcal{V}_{\mathbf{M}}^f\big)$ have the decompositions

$$\gamma = \sum_{\mathbf{y}\in\mathcal{P}(\mathbf{M})} \mathbf{G}_{\mathbf{y}}\, \mathcal{T}(\mathbf{y})f \tag{3.2}$$

and

$$\nu = \sum_{\mathbf{y}\in\mathcal{P}(\mathbf{M})} \mathbf{V}_{\mathbf{y}}\, \mathcal{T}(\mathbf{y})f, \tag{3.3}$$

respectively. The discrete Fourier transform of $\big(\mathbf{G}_{\mathbf{y}}\big)_{\mathbf{y}\in\mathcal{P}(\mathbf{M})}$ is denoted by $\big(\hat{\mathbf{G}}_{\mathbf{h}}\big)_{\mathbf{h}\in\mathcal{G}(\mathbf{M}^{\mathrm{T}})} = \mathcal{F}(\mathbf{M})\big(\mathbf{G}_{\mathbf{y}}\big)_{\mathbf{y}\in\mathcal{P}(\mathbf{M})}$ and for ν similarly $\big(\hat{\mathbf{V}}_{\mathbf{h}}\big)_{\mathbf{h}\in\mathcal{G}(\mathbf{M}^{\mathrm{T}})} = \mathcal{F}(\mathbf{M})\big(\mathbf{V}_{\mathbf{y}}\big)_{\mathbf{y}\in\mathcal{P}(\mathbf{M})}$.

The discretized version of the space of curlfree fields $\mathcal{E}(\mathbb{T}^d)$ is given by

$$\mathcal{E}_{\mathbf{M}}^f(\mathbb{T}^d) \coloneqq \mathcal{E}(\mathbb{T}^d) \cap \mathrm{Sym}_d\big(\mathcal{V}_{\mathbf{M}}^f\big). \tag{3.4}$$

With these definitions at hand, we can now define the periodic Green operator, first introduced in [8, Definition 3.6].

Definition 3.1. *We call the Fourier multiplier* $\Gamma^{\mathrm{p}} : \mathrm{Sym}_d(\mathcal{V}_{\mathbf{M}}^f) \to \mathrm{Sym}_d(\mathcal{V}_{\mathbf{M}}^f)$ *the* periodized Green operator on $\mathcal{V}_{\mathbf{M}}^f$ *and define its action on a field* $\gamma \in \mathrm{Sym}_d(\mathcal{V}_{\mathbf{M}}^f)$ *by*

$$\Gamma^{\mathrm{p}} : \gamma \coloneqq \sum_{\mathbf{y} \in \mathcal{P}(\mathbf{M})} \Gamma^{\mathrm{p}}_{\mathbf{y}} : \mathbf{G}_{\mathbf{y}}\, \mathcal{T}(\mathbf{y}) f. \tag{3.5}$$

In terms of Fourier coefficients this is equal to

$$\Gamma^{\mathrm{p}} : \gamma \coloneqq \sum_{\mathbf{h} \in \mathcal{G}(\mathbf{M}^{\mathrm{T}})} \hat{\Gamma}^{\mathrm{p}}_{\mathbf{h}} : \hat{\mathbf{G}}_{\mathbf{h}} c^{\mathbf{M}}_{\mathbf{h}}(f) e^{2\pi \mathrm{i} \mathbf{h}^{\mathrm{T}} \cdot}$$

with

$$\hat{\Gamma}^{\mathrm{p}}_{\mathbf{h}} : \hat{\mathbf{G}}_{\mathbf{h}} \coloneqq m\Big[\{ \hat{\Gamma}^0_{\mathbf{k}} |c_{\mathbf{k}}(f)|^2 \}_{\mathbf{k} \in \mathbb{Z}^d} \Big]^{\mathbf{M}}_{\mathbf{h}} : \hat{\mathbf{G}}_{\mathbf{h}}, \quad \mathbf{h} \in \mathcal{G}(\mathbf{M}^{\mathrm{T}}). \tag{3.6}$$

The operator stemming from the truncated Fourier series approach [74, 105] is included in this definition via the Dirichlet kernel $f = \mathrm{D}_{\mathbf{M}}$ for diagonal matrices $\mathbf{M}$. This space of translates results in

$$\hat{\Gamma}^{\mathrm{p}}_{\mathbf{h}} : \hat{\mathbf{G}}_{\mathbf{h}} = \hat{\Gamma}^0_{\mathbf{h}} : \hat{\mathbf{G}}_{\mathbf{h}}.$$

In [18, 21] the authors introduce a Green operator stemming from a energy-based formulation using elementwise constant finite elements, which are also part of this framework for translation invariant spaces. These special cases are summarized in the following theorem.

Theorem 3.2. *a) Let* $\mathcal{V}_{\mathbf{M}}^f = \mathcal{V}_{\mathbf{M}}^{f_{\mathrm{D}_{\mathbf{M}}}}$ *be generated by the translates of the Dirichlet kernel, then the periodized Green operator* Γ^{p} *coincides with the Green operator* Γ^0 *on anisotropic lattices of [6].*

Let further $\mathbf{M}$ *be a diagonal matrix, then* Γ^{p} *coincides with the operator* Γ^0 *from the truncated Fourier series approach from e.g. [105] and [74].*

b) Let $\mathcal{V}_{\mathbf{M}}^f = \mathcal{V}_{\mathbf{M}}^{B_{\mathcal{X}}}$ *for dimension* $d = 2$ *be generated by the translates of the periodized Box spline* $B_{\mathcal{X}}$ *with* $\mathcal{X} = \Big\{ \mathbf{x}_j : \big(\mathbf{x}_j\big)_i = \delta_{ij}, \quad i, j = 1, 2 \Big\}$. *Then the Green operator* Γ^{p} *coincides with the operator from [18, 21].*

Proof. a) Inserting the definition of the Dirichlet kernel $f_{\mathrm{D}_{\mathbf{M}}}$ into the definition of $\hat{\Gamma}^{\mathrm{p}}$ in (3.6) reduces the bracket sum to one single term $\hat{\Gamma}^0_{\mathbf{k}}$ and thus the proof is completed.

b) With the formula for the Fourier coefficients of the periodized Box spline (2.13) inserted into (3.6) one directly obtains the operator from [18, (14)]. □

For functions f which have compact support in the frequency domain, the bracket sum in (3.6) can be evaluated exactly, because only finitely many terms are non-zero. If this is not the case, computations require a suitable approximation of the infinite sum.

If the ansatz function f is of high smoothness, which directly translates into a faster decay of the Fourier coefficients $c_{\mathbf{k}}(f)$, the approximation of the bracket sum converges

faster. Therefore, approximations of Γ^{p} using a finite number of terms in the sum in (3.6) get more accurate for smoother functions f.

The properties of the Green operator Γ^0 and a resulting projection operator $\Gamma^0\mathcal{C}^0$ are analyzed in [105, Lemma 2] for the continuous case and in [105, Lemma 10] for the discrete case. These properties are shown via calculations on the Fourier coefficients and lead both in the continuous case, see Lemma 2.32, and the discrete case to similar results.

For the periodized Green operator Γ^{p}, the properties are collected in the following and split into three separate theorems. First, we show the well-definedness of the operator $\Gamma^{\mathrm{p}}\mathcal{C}^0$ and characterize the image space and boundedness, independent of the function f. The second theorem collects further results which hold universally independent of the choice of $\mathcal{V}_{\mathbf{M}}^f$. These are the ellipticity of $\Gamma^{\mathrm{p}}\mathcal{C}^0$, a formula for its adjoint operator, and that the Fourier coefficients are real-valued.

The similarity between the continuous operator $\Gamma^0\mathcal{C}^0$ and the discretized operator $\Gamma^{\mathrm{p}}\mathcal{C}^0$ is no longer the case for the properties stated in the third theorem. There, the underlying space of translates plays a crucial role. This means that $\Gamma^{\mathrm{p}}\mathcal{C}^0$ is a projection operator and maps constants to zero if and only if $\mathcal{V}_{\mathbf{M}}^f = \mathcal{V}_{\mathbf{M}}^{f_{\mathrm{D}_{\mathbf{M}}}}$ is generated by the Dirichlet kernel.

Theorem 3.3. *Let $\mathcal{C}^0 \in \mathrm{SSym}_d(\mathbb{R})$ be a stiffness tensor and let the translates of f be orthonormal, then $\Gamma^{\mathrm{p}}\mathcal{C}^0$ is a well-defined bounded operator $\mathrm{Sym}_d\big(\mathcal{V}_{\mathbf{M}}^f\big) \to \mathcal{E}_{\mathbf{M}}^f(\mathbb{T}^d)$ with the following properties.*

a) The operator $\Gamma^{\mathrm{p}}\mathcal{C}^0$ maps onto $\mathrm{Sym}_d\big(\mathcal{V}_{\mathbf{M}}^f\big)$.

b) The operator $\Gamma^{\mathrm{p}}\mathcal{C}^0$ maps onto $\mathcal{E}(\mathbb{T}^d)$.

c) The operator $\Gamma^{\mathrm{p}}\mathcal{C}^0$ is bounded with

$$\|\Gamma^{\mathrm{p}}\mathcal{C}^0 : \gamma\|_2 \leq \frac{c_{b,0}}{c_{e,0}}\|\gamma\|_2$$

for all $\gamma \in \mathrm{Sym}_d\big(\mathcal{V}_{\mathbf{M}}^f\big)$. The constants $c_{b,0} > 0$ and $c_{e,0} > 0$ are the constants of boundedness and ellipticity for $\mathcal{C}^0$, respectively, from Definition 2.28.

Proof. a) For all $\mathbf{y} \in \mathcal{P}(\mathbf{M})$ we have for $\gamma \in \mathrm{Sym}_d\big(\mathcal{V}_{\mathbf{M}}^f\big)$ with (3.2) and (3.6) that

$$\begin{aligned}\big(\Gamma^{\mathrm{p}}\mathcal{C}^0 : \gamma\big)(\mathbf{y}) &= \sum_{\mathbf{h}\in\mathcal{G}(\mathbf{M}^{\mathrm{T}})} \hat{\Gamma}^{\mathrm{p}}_{\mathbf{h}}\mathcal{C}^0 : \hat{\mathbf{G}}_{\mathbf{h}} c^{\mathbf{M}}_{\mathbf{h}}(f) e^{2\pi\mathrm{i}\mathbf{h}^{\mathrm{T}}\mathbf{y}} \\ &= \sum_{\mathbf{h}\in\mathcal{G}(\mathbf{M}^{\mathrm{T}})} m\Big[\big\{\hat{\Gamma}^0_{\mathbf{k}}|c_{\mathbf{k}}(f)|^2\big\}_{\mathbf{k}\in\mathbb{Z}^d}\Big]^{\mathbf{M}}_{\mathbf{h}}\mathcal{C}^0 : \hat{\mathbf{G}}_{\mathbf{h}} c^{\mathbf{M}}_{\mathbf{h}}(f) e^{2\pi\mathrm{i}\mathbf{h}^{\mathrm{T}}\mathbf{y}}.\end{aligned}$$

We introduce new Fourier coefficients

$$\tilde{\mathbf{G}}_{\mathbf{h}} \coloneqq m\Big[\big\{\hat{\Gamma}^0_{\mathbf{k}}|c_{\mathbf{k}}(f)|^2\big\}_{\mathbf{k}\in\mathbb{Z}^d}\Big]^{\mathbf{M}}_{\mathbf{h}}\mathcal{C}^0 : \hat{\mathbf{G}}_{\mathbf{h}}, \quad \mathbf{h} \in \mathcal{G}(\mathbf{M}^{\mathrm{T}})$$

and thus obtain

$$\big(\Gamma^{\mathrm{p}}\mathcal{C}^0 : \gamma\big)(\mathbf{y}) = \sum_{\mathbf{h}\in\mathcal{G}(\mathbf{M}^{\mathrm{T}})} \tilde{\mathbf{G}}_{\mathbf{h}} c^{\mathbf{M}}_{\mathbf{h}}(f) e^{2\pi\mathrm{i}\mathbf{h}^{\mathrm{T}}\mathbf{y}}.$$

With Lemma 2.12 then $\Gamma^{\mathrm{p}}\mathcal{C}^0 : \gamma \in \mathrm{Sym}_d\big(\mathcal{V}_{\mathbf{M}}^f\big)$ and the first part of the proof is completed.

b) Let $\gamma \in \mathrm{Sym}_d\big(\mathcal{V}_{\mathbf{M}}^f\big)$ and $\mathbf{y} \in \mathcal{P}(\mathbf{M})$, then by Definition 3.1 and (3.2) it holds that

$$\big(\Gamma^{\mathrm{p}}\mathcal{C}^0 : \gamma\big)(\mathbf{y}) = \sum_{\mathbf{h}\in\mathcal{G}(\mathbf{M}^{\mathrm{T}})} \sum_{\mathbf{z}\in\mathbb{Z}^d} m\hat{\Gamma}^0_{\mathbf{h}+\mathbf{M}^{\mathrm{T}}\mathbf{z}} |c_{\mathbf{h}+\mathbf{M}^{\mathrm{T}}\mathbf{z}}(f)|^2 \mathcal{C}^0 : \hat{\mathbf{G}}_{\mathbf{h}} c^{\mathbf{M}}_{\mathbf{h}}(f)\, \mathrm{e}^{2\pi \mathrm{i}\mathbf{h}^{\mathrm{T}}\mathbf{y}}.$$

Define Fourier coefficients

$$\hat{\mathbf{F}}_{\mathbf{h}+\mathbf{M}^{\mathrm{T}}\mathbf{z}} \coloneqq m|c_{\mathbf{h}+\mathbf{M}^{\mathrm{T}}\mathbf{z}}(f)|^2 \mathcal{C}^0 : \hat{\mathbf{G}}_{\mathbf{h}} c^{\mathbf{M}}_{\mathbf{h}}(f)$$

and thus with Lemma 2.5 and the unique splitting $\mathbf{k} = \mathbf{h} + \mathbf{M}^{\mathrm{T}}\mathbf{z}$ for $\mathbf{k}, \mathbf{z} \in \mathbb{Z}^d$, and $\mathbf{h} \in \mathcal{G}(\mathbf{M}^{\mathrm{T}})$ this results in

$$\begin{aligned}
\big(\Gamma^{\mathrm{p}}\mathcal{C}^0 : \gamma\big)(\mathbf{y}) &= \sum_{\mathbf{h}\in\mathcal{G}(\mathbf{M}^{\mathrm{T}})} \sum_{\mathbf{z}\in\mathbb{Z}^d} \hat{\Gamma}^0_{\mathbf{h}+\mathbf{M}^{\mathrm{T}}\mathbf{z}} \hat{\mathbf{F}}_{\mathbf{h}+\mathbf{M}^{\mathrm{T}}\mathbf{z}}\, \mathrm{e}^{2\pi \mathrm{i}\mathbf{h}^{\mathrm{T}}\mathbf{y}} \\
&= \sum_{\mathbf{h}\in\mathcal{G}(\mathbf{M}^{\mathrm{T}})} \sum_{\mathbf{z}\in\mathbb{Z}^d} \hat{\Gamma}^0_{\mathbf{h}+\mathbf{M}^{\mathrm{T}}\mathbf{z}} \hat{\mathbf{F}}_{\mathbf{h}+\mathbf{M}^{\mathrm{T}}\mathbf{z}}\, \mathrm{e}^{2\pi \mathrm{i}(\mathbf{h}+\mathbf{M}^{\mathrm{T}}\mathbf{z})^{\mathrm{T}}\mathbf{y}} \\
&= \sum_{\mathbf{k}\in\mathbb{Z}^d} \hat{\Gamma}^0_{\mathbf{k}} \hat{\mathbf{F}}_{\mathbf{k}}\, \mathrm{e}^{2\pi \mathrm{i}\mathbf{k}^{\mathrm{T}}\mathbf{y}}.
\end{aligned}$$

With the projection property of Γ^0 from Lemma 2.32 c) the resulting function is in $\mathcal{E}(\mathbb{T}^d)$ and the claim is proven.

c) For the boundedness assume that the reference stiffness $\mathcal{C}^0$ is bounded and elliptic as in Definition 2.28 with constants c_{b} and c_{e}, respectively. Then for $\gamma \in \mathrm{Sym}_d\big(\mathcal{V}_{\mathbf{M}}^f\big)$ the Parseval equation (2.1) with the unique splitting $\mathbf{k} = \mathbf{h} + \mathbf{M}^{\mathrm{T}}\mathbf{z}$ for $\mathbf{h} \in \mathcal{G}(\mathbf{M}^{\mathrm{T}})$ and $\mathbf{k}, \mathbf{z} \in \mathbb{Z}^d$ gives

$$\begin{aligned}
\big\|\Gamma^{\mathrm{p}}\mathcal{C}^0 : \gamma\big\|_2^2 &= \sum_{\mathbf{h}\in\mathcal{G}(\mathbf{M}^{\mathrm{T}})} \sum_{\mathbf{z}\in\mathbb{Z}^d} \Big\|\hat{\Gamma}^{\mathrm{p}}_{\mathbf{h}}\mathcal{C}^0 : \hat{\mathbf{G}}_{\mathbf{h}} c_{\mathbf{h}+\mathbf{M}^{\mathrm{T}}\mathbf{z}}(f)\Big\|_2^2 \\
&= \sum_{\mathbf{h}\in\mathcal{G}(\mathbf{M}^{\mathrm{T}})} \sum_{\mathbf{z}\in\mathbb{Z}^d} \Big\| m\Big[\big\{\hat{\Gamma}^0_{\mathbf{k}}|c_{\mathbf{k}}(f)|^2\big\}_{\mathbf{k}\in\mathbb{Z}^d}\Big]^{\mathbf{M}}_{\mathbf{h}} \mathcal{C}^0 : \hat{\mathbf{G}}_{\mathbf{h}} c_{\mathbf{h}+\mathbf{M}^{\mathrm{T}}\mathbf{z}}(f)\Big\|_2^2.
\end{aligned}$$

Writing the bracket sum in the unabbreviated form (2.10) and an application of the theorem of Cauchy-Schwarz gives the upper bound

$$\big\|\Gamma^{\mathrm{p}}\mathcal{C}^0 : \gamma\big\|_2^2 \leq \sum_{\mathbf{h}\in\mathcal{G}(\mathbf{M}^{\mathrm{T}})} \sum_{\mathbf{z}\in\mathbb{Z}^d} m^2 \sum_{\mathbf{z}'\in\mathbb{Z}^d} \big\|\hat{\Gamma}^0_{\mathbf{h}+\mathbf{M}^{\mathrm{T}}\mathbf{z}'}\mathcal{C}^0 : \hat{\mathbf{G}}_{\mathbf{h}} c_{\mathbf{h}+\mathbf{M}^{\mathrm{T}}\mathbf{z}}(f)\big\|_2 |c_{\mathbf{h}+\mathbf{M}^{\mathrm{T}}\mathbf{z}'}(f)|^4.$$

With (2.21) we obtain $\big\|\hat{\Gamma}^0_{\mathbf{k}}\big\| \leq \frac{1}{c_{\mathrm{e},0}}$ and this leads to

$$\big\|\Gamma^{\mathrm{p}}\mathcal{C}^0 : \gamma\big\|_2^2 \leq \sum_{\mathbf{h}\in\mathcal{G}(\mathbf{M}^{\mathrm{T}})} \sum_{\mathbf{z}\in\mathbb{Z}^d} m^2 \frac{c_{\mathrm{b},0}^2}{c_{\mathrm{e},0}^2} \big\|\hat{\mathbf{G}}_{\mathbf{h}} c_{\mathbf{h}+\mathbf{M}^{\mathrm{T}}\mathbf{z}}(f)\big\|^2 \sum_{\mathbf{z}'\in\mathbb{Z}^d} |c_{\mathbf{h}+\mathbf{M}^{\mathrm{T}}\mathbf{z}'}(f)|^4.$$

Jensens's inequality together with Lemma 2.14 c) results in

$$\begin{aligned}\left\|\Gamma^{\mathrm{p}}\mathcal{C}^0:\gamma\right\|_2^2 &\leq \sum_{\mathbf{h}\in\mathcal{G}(\mathbf{M}^{\mathrm{T}})}\sum_{\mathbf{z}\in\mathbb{Z}^d} m^2\frac{c_{\mathrm{b},0}^2}{c_{\mathrm{e},0}^2}\left\|\hat{\mathbf{G}}_{\mathbf{h}}c_{\mathbf{h}+\mathbf{M}^{\mathrm{T}}\mathbf{z}}(f)\right\|^2\Bigg(\sum_{\mathbf{z}'\in\mathbb{Z}^d}|c_{\mathbf{h}+\mathbf{M}^{\mathrm{T}}\mathbf{z}'}(f)|^2\Bigg)^2\\ &= \sum_{\mathbf{h}\in\mathcal{G}(\mathbf{M}^{\mathrm{T}})}\sum_{\mathbf{z}\in\mathbb{Z}^d} m^2\frac{c_{\mathrm{b},0}^2}{c_{\mathrm{e},0}^2}\left\|\hat{\mathbf{G}}_{\mathbf{h}}c_{\mathbf{h}+\mathbf{M}^{\mathrm{T}}\mathbf{z}}(f)\right\|^2 m^{-2}.\end{aligned}$$

Another application of the Parseval equation gives the estimate

$$\left\|\Gamma^{\mathrm{p}}\mathcal{C}^0:\gamma\right\|_2^2 \leq \sum_{\mathbf{h}\in\mathcal{G}(\mathbf{M}^{\mathrm{T}})}\sum_{\mathbf{z}\in\mathbb{Z}^d}\frac{c_{\mathrm{b},0}^2}{c_{\mathrm{e},0}^2}\left\|\hat{\mathbf{G}}_{\mathbf{h}}c_{\mathbf{h}+\mathbf{M}^{\mathrm{T}}\mathbf{z}}(f)\right\|^2 = \frac{c_{\mathrm{b},0}^2}{c_{\mathrm{e},0}^2}\|\gamma\|_2^2$$

and the proof is finished. □

After showing that the operator $\Gamma^0\mathcal{C}^0$ is a well-defined operator, we now proceed to the other properties that are valid for all spaces of translates $\mathcal{V}_{\mathbf{M}}^f$.

Theorem 3.4. *Let $\mathcal{C}^0 \in \mathrm{SSym}_d(\mathbb{R})$ be a stiffness tensor and let the translates of f be orthonormal. Then the following statements hold.*

a) Let $c_{b,0}$ and $c_{e,0}$ be the constants of boundedness and ellipticity for $\mathcal{C}^0$ from Definition 2.28. Then the operator $\Gamma^{\mathrm{p}}\mathcal{C}^0$ is elliptic with

$$\left\langle\Gamma^{\mathrm{p}}\mathcal{C}^0:\gamma,\gamma\right\rangle_2 \geq \frac{c_{e,0}}{c_{b,0}}\|\gamma\|_2^2$$

for all $\gamma\in\mathrm{Sym}_d(\mathcal{V}_{\mathbf{M}}^f)$.

b) The operator $\Gamma^{\mathrm{p}}\mathcal{C}^0$ has the $\mathcal{L}^2$-adjoint $\mathcal{C}^0\Gamma^{\mathrm{p}}$.

c) Let $\gamma\in\mathrm{Sym}_d(\mathcal{V}_{\mathbf{M}}^f)$, then it holds that

$$\overline{\hat{\Gamma}_{\mathbf{h}}^{\mathrm{p}}}:\mathbf{G}_{\mathbf{h}} = \hat{\Gamma}_{\mathbf{h}}^{\mathrm{p}}:\mathbf{G}_{\mathbf{h}},\quad \mathbf{h}\in\mathcal{G}(\mathbf{M}^{\mathrm{T}}),$$

i.e. the Fourier coefficients of Γ^{p} are real-valued tensors.

Proof. a) By the Definition 3.1 of Γ^{p}, the decomposition (3.2), and the Parseval equation (2.1) it holds that

$$\begin{aligned}\left\langle\Gamma^{\mathrm{p}}\mathcal{C}^0:\gamma,\gamma\right\rangle_2 &= \left\langle\sum_{\mathbf{h}\in\mathcal{G}(\mathbf{M}^{\mathrm{T}})}\hat{\Gamma}_{\mathbf{h}}^{\mathrm{p}}\mathcal{C}^0:\hat{\mathbf{G}}_{\mathbf{h}}c_{\mathbf{h}}^{\mathbf{M}}(f)\,\mathrm{e}^{2\pi\mathrm{i}\mathbf{h}^{\mathrm{T}}\cdot},\sum_{\mathbf{h}\in\mathcal{G}(\mathbf{M}^{\mathrm{T}})}\hat{\mathbf{G}}_{\mathbf{h}}c_{\mathbf{h}}^{\mathbf{M}}(f)\,\mathrm{e}^{2\pi\mathrm{i}\mathbf{h}^{\mathrm{T}}\cdot}\right\rangle_2\\ &= \sum_{\mathbf{h}\in\mathcal{G}(\mathbf{M}^{\mathrm{T}})}\left\langle\hat{\Gamma}_{\mathbf{h}}^{\mathrm{p}}\mathcal{C}^0:\hat{\mathbf{G}}_{\mathbf{h}}c_{\mathbf{h}}^{\mathbf{M}}(f),\hat{\mathbf{G}}_{\mathbf{h}}c_{\mathbf{h}}^{\mathbf{M}}(f)\right\rangle_2\\ &= \sum_{\mathbf{h}\in\mathcal{G}(\mathbf{M}^{\mathrm{T}})}\sum_{\mathbf{z}\in\mathbb{Z}^d}\left\langle m\hat{\Gamma}_{\mathbf{h}+\mathbf{M}^{\mathrm{T}}\mathbf{z}}^0|c_{\mathbf{h}+\mathbf{M}^{\mathrm{T}}\mathbf{z}}(f)|^2\mathcal{C}^0:\hat{\mathbf{G}}_{\mathbf{h}}c_{\mathbf{h}}^{\mathbf{M}}(f),\hat{\mathbf{G}}_{\mathbf{h}}c_{\mathbf{h}}^{\mathbf{M}}(f)\right\rangle_2.\end{aligned}$$

Rewriting and applying the estimate

$$\|\hat{\Gamma}^0_{\mathbf{k}}\mathcal{C}^0\|_2 \geq \frac{c_{\mathrm{e},0}}{c_{\mathrm{c},0}},$$

see also the proof of Theorem 3.3 c), yields

$$\begin{aligned}\langle \Gamma^{\mathrm{p}}\mathcal{C}^0 : \gamma, \gamma\rangle_2 &= \sum_{\mathbf{h}\in\mathcal{G}(\mathbf{M}^{\mathrm{T}})}\sum_{\mathbf{z}\in\mathbb{Z}^d} m|c_{\mathbf{h}+\mathbf{M}^{\mathrm{T}}\mathbf{z}}(f)|^2\langle \hat{\Gamma}^0_{\mathbf{h}+\mathbf{M}^{\mathrm{T}}\mathbf{z}}\mathcal{C}^0 : \hat{\mathbf{G}}_{\mathbf{h}}c^{\mathbf{M}}_{\mathbf{h}}(f), \hat{\mathbf{G}}_{\mathbf{h}}c^{\mathbf{M}}_{\mathbf{h}}(f)\rangle_2 \\ &\geq \frac{c_{\mathrm{e},0}}{c_{\mathrm{b},0}}\sum_{\mathbf{h}\in\mathcal{G}(\mathbf{M}^{\mathrm{T}})}\sum_{\mathbf{z}\in\mathbb{Z}^d} m|c_{\mathbf{h}+\mathbf{M}^{\mathrm{T}}\mathbf{z}}(f)|^2\langle \hat{\mathbf{G}}_{\mathbf{h}}c^{\mathbf{M}}_{\mathbf{h}}(f), \hat{\mathbf{G}}_{\mathbf{h}}c^{\mathbf{M}}_{\mathbf{h}}(f)\rangle_2.\end{aligned}$$

The translates of f were assumed to be orthonormal and thus by Lemma 2.14 c) we have $\sum_{\mathbf{z}\in\mathbb{Z}^d}|c_{\mathbf{h}+\mathbf{M}^{\mathrm{T}}\mathbf{z}}(f)|^2 = m^{-1}$ for all $\mathbf{h}\in\mathcal{G}(\mathbf{M}^{\mathrm{T}})$. Together with the Parseval equation this results in

$$\langle \Gamma^{\mathrm{p}}\mathcal{C}^0 : \gamma, \gamma\rangle_2 \geq \frac{c_{\mathrm{e},0}}{c_{\mathrm{b},0}}\sum_{\mathbf{h}\in\mathcal{G}(\mathbf{M}^{\mathrm{T}})}\langle \hat{\mathbf{G}}_{\mathbf{h}}c^{\mathbf{M}}_{\mathbf{h}}(f), \hat{\mathbf{G}}_{\mathbf{h}}c^{\mathbf{M}}_{\mathbf{h}}(f)\rangle_2 = \frac{c_{\mathrm{e},0}}{c_{\mathrm{b},0}}\|\gamma\|_2^2$$

and the proof is complete.

b) For the adjointness of $\Gamma^{\mathrm{p}}\mathcal{C}^0$ and $\mathcal{C}^0\Gamma^{\mathrm{p}}$ the equation

$$\langle \Gamma^{\mathrm{p}}\mathcal{C}^0 : \gamma, \nu\rangle_2 = \langle \gamma, \mathcal{C}^0\Gamma^{\mathrm{p}} : \nu\rangle_2$$

has to hold for all $\gamma, \nu \in \mathrm{Sym}_d(\mathcal{V}^f_{\mathbf{M}})$. The Parseval equation transforms the left-hand side to Fourier coefficients yielding with (3.3) that

$$\langle \Gamma^{\mathrm{p}}\mathcal{C}^0 : \gamma, \nu\rangle_2 = \sum_{\mathbf{h}\in\mathcal{G}(\mathbf{M}^{\mathrm{T}})}\langle \hat{\Gamma}^{\mathrm{p}}_{\mathbf{h}}\mathcal{C}^0 : \hat{\mathbf{G}}_{\mathbf{h}}c^{\mathbf{M}}_{\mathbf{h}}(f), \hat{\mathbf{V}}_{\mathbf{h}}c^{\mathbf{M}}_{\mathbf{h}}(f)\rangle_2$$

which is equivalent to

$$\langle \Gamma^{\mathrm{p}}\mathcal{C}^0 : \gamma, \nu\rangle_2 = \sum_{\mathbf{h}\in\mathcal{G}(\mathbf{M}^{\mathrm{T}})}\big(\hat{\Gamma}^{\mathrm{p}}_{\mathbf{h}}\mathcal{C}^0 : \hat{\mathbf{G}}_{\mathbf{h}}c^{\mathbf{M}}_{\mathbf{h}}(f)\big)^{\mathrm{T}}\overline{\hat{\mathbf{V}}_{\mathbf{h}}c^{\mathbf{M}}_{\mathbf{h}}(f)}.$$

Rewriting gives

$$\langle \Gamma^{\mathrm{p}}\mathcal{C}^0 : \gamma, \nu\rangle_2 = \sum_{\mathbf{h}\in\mathcal{G}(\mathbf{M}^{\mathrm{T}})} c^{\mathbf{M}}_{\mathbf{h}}(f)\hat{\mathbf{G}}^{\mathrm{T}}_{\mathbf{h}} : \big(\mathcal{C}^0\big)^{\mathrm{T}}\big(\hat{\Gamma}^{\mathrm{p}}_{\mathbf{h}}\big)^{\mathrm{T}} : \overline{\hat{\mathbf{V}}_{\mathbf{h}}c^{\mathbf{M}}_{\mathbf{h}}(f)}.$$

The reference stiffness $\mathcal{C}^0$ and the Green operator Γ^{p} are symmetric and an application of Theorem 3.4 c) results in

$$\langle \Gamma^{\mathrm{p}}\mathcal{C}^0 : \gamma, \nu\rangle_2 = \sum_{\mathbf{h}\in\mathcal{G}(\mathbf{M}^{\mathrm{T}})} c^{\mathbf{M}}_{\mathbf{h}}(f)\hat{\mathbf{G}}^{\mathrm{T}}_{\mathbf{h}} : \overline{\mathcal{C}^0\hat{\Gamma}^{\mathrm{p}}_{\mathbf{h}} : \hat{\mathbf{V}}_{\mathbf{h}}c^{\mathbf{M}}_{\mathbf{h}}(f)}.$$

A further application of the Parseval equation then leads to

$$\langle \Gamma^{\mathrm{p}}\mathcal{C}^0 : \gamma, \nu\rangle_2 = \langle \gamma, \mathcal{C}^0\Gamma^{\mathrm{p}} : \nu\rangle_2$$

and the proof is finished.

c) We insert the Definition of $\hat{\Gamma}^{\mathrm{p}}_{\mathbf{h}}$ and obtain

$$\overline{\hat{\Gamma}^{\mathrm{p}}_{\mathbf{h}}} : \mathbf{G}_{\mathbf{h}} = \overline{m \sum_{\mathbf{z} \in \mathcal{G}(\mathbf{M}^{\mathrm{T}})} \hat{\Gamma}^{0}_{\mathbf{h}+\mathbf{M}^{\mathrm{T}}\mathbf{z}} |c_{\mathbf{h}+\mathbf{M}^{\mathrm{T}}\mathbf{z}}(f)|^2} : \mathbf{G}_{\mathbf{h}}$$

Pulling the complex conjugate into the sum and Proposition 2.33 together with $|c_{\mathbf{h}+\mathbf{M}^{\mathrm{T}}\mathbf{z}}(f)|^2 \in \mathbb{R}$ for all $\mathbf{h} \in \mathcal{G}(\mathbf{M}^{\mathrm{T}})$ and $\mathbf{z} \in \mathbb{Z}^d$ yields

$$\begin{aligned}\overline{\hat{\Gamma}^{\mathrm{p}}_{\mathbf{h}}} : \mathbf{G}_{\mathbf{h}} &= m \sum_{\mathbf{z} \in \mathcal{G}(\mathbf{M}^{\mathrm{T}})} \overline{\hat{\Gamma}^{0}_{\mathbf{h}+\mathbf{M}^{\mathrm{T}}\mathbf{z}} |c_{\mathbf{h}+\mathbf{M}^{\mathrm{T}}\mathbf{z}}(f)|^2} : \mathbf{G}_{\mathbf{h}} \\ &= m \sum_{\mathbf{z} \in \mathcal{G}(\mathbf{M}^{\mathrm{T}})} \hat{\Gamma}^{0}_{\mathbf{h}+\mathbf{M}^{\mathrm{T}}\mathbf{z}} |c_{\mathbf{h}+\mathbf{M}^{\mathrm{T}}\mathbf{z}}(f)|^2 : \mathbf{G}_{\mathbf{h}} = \hat{\Gamma}^{\mathrm{p}}_{\mathbf{h}} : \mathbf{G}_{\mathbf{h}}\end{aligned}$$

and the proof is done. □

The space generated by translates of the Dirichlet kernel $f_{\mathrm{D}_{\mathbf{M}}}$ plays a special role, as shown in the following theorem. This is in accordance with the properties shown in [105, Lemma 10].

Theorem 3.5. *Let $\mathcal{C}^0 \in \mathrm{SSym}_d(\mathbb{R})$ be a stiffness tensor. Then the following holds:*

a) The operator $\Gamma^{\mathrm{p}}\mathcal{C}^0$ is a projection operator if and only if $\mathcal{V}^f_{\mathbf{M}} = \mathcal{V}^{f_{\mathrm{D}_{\mathbf{M}}}}_{\mathbf{M}}$, i.e. if and only if either f or one of its orthonormalized translates is the Dirichlet kernel $f_{\mathrm{D}_{\mathbf{M}}}$.

b) Let $\sigma \in \mathrm{Sym}_d\big(\mathcal{V}^f_{\mathbf{M}}\big)$ interpolate a constant and non-zero function. Then $\Gamma^{\mathrm{p}}\mathcal{C}^0 : \sigma = \mathbf{0}$ if and only if $\mathcal{V}^f_{\mathbf{M}} = \mathcal{V}^{f_{\mathrm{D}_{\mathbf{M}}}}_{\mathbf{M}}$.

Proof. a) For $\Gamma^{\mathrm{p}}\mathcal{C}^0$ to be a projection operator, the equation

$$\Gamma^{\mathrm{p}}\mathcal{C}^0\Gamma^{\mathrm{p}}\mathcal{C}^0 : \gamma = \Gamma^{\mathrm{p}}\mathcal{C}^0 : \gamma$$

has to hold for all $\gamma \in \mathrm{Sym}_d\big(\mathcal{V}^f_{\mathbf{M}}\big)$. The left-hand side of this equation reads in terms of Fourier coefficients

$$\sum_{\mathbf{h} \in \mathcal{G}(\mathbf{M}^{\mathrm{T}})} \hat{\Gamma}^{\mathrm{p}}_{\mathbf{h}} \mathcal{C}^0 \hat{\Gamma}^{\mathrm{p}}_{\mathbf{h}} \mathcal{C}^0 \hat{\mathbf{G}}_{\mathbf{h}} c^{\mathbf{M}}_{\mathbf{h}}(f) e^{2\pi \mathrm{i} \mathbf{h}^{\mathrm{T}} \mathbf{y}}$$

for $\mathbf{y} \in \mathcal{P}(\mathbf{M})$. Insert the definition of the periodized Green operator (3.6) to get

$$\sum_{\mathbf{h} \in \mathcal{G}(\mathbf{M}^{\mathrm{T}})} \sum_{\mathbf{z}, \mathbf{z}' \in \mathbb{Z}^d} m^2 |c_{\mathbf{h}+\mathbf{M}^{\mathrm{T}}\mathbf{z}}(f)|^2 |c_{\mathbf{h}+\mathbf{M}^{\mathrm{T}}\mathbf{z}'}(f)|^2 \hat{\Gamma}^{0}_{\mathbf{h}+\mathbf{M}^{\mathrm{T}}\mathbf{z}} \mathcal{C}^0 \hat{\Gamma}^{0}_{\mathbf{h}+\mathbf{M}^{\mathrm{T}}\mathbf{z}'} \mathcal{C}^0 \hat{\mathbf{G}}_{\mathbf{h}} c^{\mathbf{M}}_{\mathbf{h}}(f) e^{2\pi \mathrm{i} \mathbf{h}^{\mathrm{T}} \mathbf{y}}. \tag{3.7}$$

From Lemma 2.32 c) we know that $\Gamma^0\mathcal{C}^0$ is a projection operator, i.e. that for $\mathbf{k} \in \mathbb{Z}^d$ it holds that $\hat{\Gamma}^0_{\mathbf{k}} \mathcal{C}^0 \hat{\Gamma}^0_{\mathbf{k}} \mathcal{C}^0 = \hat{\Gamma}^0_{\mathbf{k}} \mathcal{C}^0$. This does not hold true for the mixed terms in (3.7), i.e. summands with $\mathbf{z} \neq \mathbf{z}'$. These vanish if and only if $c_{\mathbf{h}+\mathbf{M}^{\mathrm{T}}\mathbf{z}}(f) = 0$ for $\mathbf{z} \neq \mathbf{0}$, i.e. for $f \in \mathcal{V}^{f_{\mathrm{D}_{\mathbf{M}}}}_{\mathbf{M}}$, cf. Theorem 3.2 a). This concludes the proof.

b) In case of $\mathcal{V}_{\mathbf{M}}^{f} = \mathcal{V}_{\mathbf{M}}^{f_{\mathrm{D}_\mathbf{M}}}$ constant functions are characterized by the Fourier coefficient $c_{\mathbf{0}}(\sigma)$ and thus

$$\Gamma^0\mathcal{C}^0 : \sigma(\mathbf{y}) = \sum_{\mathbf{h}\in\mathcal{G}(\mathbf{M}^{\mathrm{T}})} \hat{\Gamma}^0_{\mathbf{h}}\mathcal{C}^0 : c_{\mathbf{0}}(\sigma)\, \mathrm{e}^{2\pi\mathrm{i}\mathbf{h}^{\mathrm{T}}\mathbf{y}} = \hat{\Gamma}^0_{\mathbf{0}}\mathcal{C}^0 : c_{\mathbf{0}}(\sigma)$$

holds for all $\mathbf{y} \in \mathcal{P}(\mathbf{M})$. This evaluates to $\mathbf{0}$ by the definition of $\hat{\Gamma}^0_{\mathbf{h}}$ in (2.21), i.e. because of $\big(\hat{\Gamma}^0_{\mathbf{0}}\big)_{ijkl} = 0$ for $i, j, k, l = 1, \ldots, d$.

In general, however, $\big(\hat{\Gamma}^{\mathrm{p}}_{\mathbf{0}}\big)_{ijkl} \neq 0$ for $i, j, k, l = 1, \ldots, d$ due to the non-trivial summation in the bracket sum of (3.6). Further, after interpolating the constant function γ in $\mathcal{V}_{\mathbf{M}}^{f} \neq \mathcal{V}_{\mathbf{M}}^{f_{\mathrm{D}_\mathbf{M}}}$ with coefficients $\mathbf{G}_{\mathbf{y}}$ with $\mathbf{y} \in \mathcal{P}(\mathbf{M})$, the value of the function is no longer characterized solely by the value of the zeroth Fourier coefficient $\hat{\mathbf{G}}_{\mathbf{0}}$. □

Summarizing, the periodized Green operator Γ^{p} has the same properties as the operator Γ^0 in case of the Dirichlet kernel $f_{\mathrm{D}_\mathbf{M}}$. For general spaces of translates $\mathcal{V}_{\mathbf{M}}^{f}$, the operator is well-defined, bounded, elliptic, and the adjoint operator is known. The proofs use the same techniques as [105], the technical steps involving the bracket sum in Γ^{p}, however, are more involved. For $\mathcal{V}_{\mathbf{M}}^{f} \neq \mathcal{V}_{\mathbf{M}}^{f_{\mathrm{D}_\mathbf{M}}}$, the operator $\Gamma^{\mathrm{p}}\mathcal{C}^0$ is not a projection and does not map constants to zero.

3.2 Discretization on spaces of translates

With the definition of the periodized Green operator Γ^{p} and its properties detailed in the previous section at hand, we proceed with the discretization of the variational equation (VE) and the Lippmann-Schwinger equation (LS) on spaces of translates $\mathcal{V}_{\mathbf{M}}^{f}$.

These discretizations are equivalent to the ones obtained in [74] and [105] in case of the Dirichlet kernel $f_{\mathrm{D}_\mathbf{M}}$ and equivalent to the one derived in [18] in case of constant Box splines, see also Theorem 3.2. This section is split into the discretization of the Lippmann-Schwinger equation and the variational equation, detailing the steps for the former and explaining the crucial differences in the derivation of the latter.

The discretized Lippmann-Schwinger equation

In addition to the functions γ and ν defined in Equations (3.2) and (3.3), respectively, let the discrete strain $\varepsilon_{\mathbf{M}} \in \mathcal{E}_{\mathbf{M}}^{f}(\mathbb{T}^d)$ be a function on the discretized space of gradient fields. In terms of coefficients of translates of the function f, we write

$$\varepsilon_{\mathbf{M}} \coloneqq \mathrm{L}_{\mathbf{M}}\,\varepsilon = \sum_{\mathbf{y}\in\mathcal{P}(\mathbf{M})} \mathbf{E}_{\mathbf{y}}\,\mathcal{T}(\mathbf{y})\,\mathrm{I}_{\mathbf{M}} \tag{3.8}$$

from here on. We understand $\varepsilon_{\mathbf{M}}$ as the approximation of the strain ε in $\mathcal{V}_{\mathbf{M}}^{f}$, in accordance with the definition of the space $\mathcal{E}_{\mathbf{M}}^{f}(\mathbb{T}^d)$ in Equation (3.4). The discrete Fourier transform of the coefficient vector is denoted by $\big(\hat{\mathbf{E}}_{\mathbf{h}}\big)_{\mathbf{h}\in\mathcal{G}(\mathbf{M}^{\mathrm{T}})} = \mathcal{F}(\mathbf{M})\big(\mathbf{E}_{\mathbf{y}}\big)_{\mathbf{y}\in\mathcal{P}(\mathbf{M})}$.

Theorem 3.6. *Let the translates of f be orthonormal, let $\mathcal{C} \in \mathrm{SSym}_d\big(\mathcal{A}(\mathbb{T}^d)\big)$, and let $\varepsilon_{\mathbf{M}} \in \mathcal{E}^f_{\mathbf{M}}(\mathbb{T}^d)$. Then $\varepsilon_{\mathbf{M}}$ fulfills the weak form*

$$\big\langle \varepsilon_{\mathbf{M}} + \Gamma^0 \,\mathrm{L}_{\mathbf{M}}\big(\mathcal{C} - \mathcal{C}^0\big) : \big(\varepsilon_{\mathbf{M}} + \varepsilon^0\big), \gamma \big\rangle_2 = 0 \tag{3.9}$$

for all $\gamma \in \mathrm{Sym}_d\big(\mathcal{V}^f_{\mathbf{M}}\big)$ if and only if

$$\sum_{\mathbf{y} \in \mathcal{P}(\mathbf{M})} \Big(\mathbf{E}_{\mathbf{y}} + \Gamma^{\mathrm{p}}_{\mathbf{y}} \big(\mathcal{C}(\mathbf{y}) - \mathcal{C}^0\big) : \big(\mathbf{E}_{\mathbf{y}} + \varepsilon^0\big) \Big) \big(\mathcal{T}(\mathbf{y})\,\mathrm{I}_{\mathbf{M}}\big)(\mathbf{x}) = \mathbf{0} \tag{3.10}$$

for all $\mathbf{x} \in \mathcal{P}(\mathbf{M})$.

Proof. For the proof of this theorem we proceed in two steps. First, we derive an equivalent formulation of the Lippmann-Schwinger equation in terms of Fourier coefficients. There, it will also become apparent where the form of the Green operator Γ^{p} results from. The second step makes the transition to coefficients of the translates, thus reducing the problem to solving for the finite set of degrees of freedom $\mathbf{E}_{\mathbf{y}}$ with $\mathbf{y} \in \mathcal{P}(\mathbf{M})$.

Step 1: First, we show that the equation

$$\begin{aligned} \big\langle \varepsilon_{\mathbf{M}} + \Gamma^0 \,\mathrm{L}_{\mathbf{M}} \Big(\big(\mathcal{C} - \mathcal{C}^0\big) : \big(\varepsilon_{\mathbf{M}} + \varepsilon^0\big) \Big), \gamma \big\rangle_2 = \\ \frac{1}{m} \sum_{\mathbf{h} \in \mathcal{G}(\mathbf{M}^{\mathrm{T}})} \big\langle \hat{\mathbf{E}}_{\mathbf{h}} \hat{a}_{\mathbf{h}}, \hat{\mathbf{G}}_{\mathbf{h}} \big\rangle_2 + \big\langle \hat{a}_{\mathbf{h}} \hat{\Gamma}^{\mathrm{p}}_{\mathbf{h}} : \hat{\mathbf{B}}_{\mathbf{h}}, \hat{\mathbf{G}}_{\mathbf{h}} \big\rangle_2 \end{aligned} \tag{3.11}$$

holds, where the $\hat{a}_{\mathbf{h}}$ stem from Equation (3.1), and we define

$$\mathrm{L}_{\mathbf{M}} \Big(\big(\mathcal{C} - \mathcal{C}^0\big) : \big(\varepsilon + \varepsilon^0\big) \Big) =: \sum_{\mathbf{y} \in \mathcal{P}(\mathbf{M})} \mathbf{B}_{\mathbf{y}}\, \mathcal{T}(\mathbf{y})\, \mathrm{I}_{\mathbf{M}} \tag{3.12}$$

together with $\big(\hat{\mathbf{B}}_{\mathbf{h}}\big)_{\mathbf{h} \in \mathcal{G}(\mathbf{M}^{\mathrm{T}})} = \mathcal{F}(\mathbf{M}) \big(\mathbf{B}_{\mathbf{y}}\big)_{\mathbf{y} \in \mathcal{P}(\mathbf{M})}$.

The coefficients $\mathbf{B}_{\mathbf{y}}$ in Equation (3.12) are well-defined, because with $\varepsilon_{\mathbf{M}} \in \mathcal{E}_{\mathbf{M}}(\mathbb{T}^d) \subset \mathrm{Sym}_d\big(\mathcal{V}^f_{\mathbf{M}}\big) \subset \mathrm{Sym}_d\big(\mathcal{A}(\mathbb{T}^d)\big)$ and $\mathcal{C} \in \mathrm{SSym}_d\big(\mathcal{A}(\mathbb{T}^d)\big)$ it follows that $\big(\mathcal{C} - \mathcal{C}^0\big) : (\varepsilon_{\mathbf{M}} + \varepsilon^0) \in \mathrm{Sym}_d\big(\mathcal{A}(\mathbb{T}^d)\big)$ and thus an interpolation with $\mathrm{L}_{\mathbf{M}}$ on $\mathrm{Sym}_d\big(\mathcal{V}^f_{\mathbf{M}}\big)$ is possible.

We apply the Parseval equation (2.1) to the left-hand side of Equation (3.11) and get

$$\sum_{\mathbf{k} \in \mathbb{Z}^d} \left\langle c_{\mathbf{k}}(\varepsilon_{\mathbf{M}}) + \hat{\Gamma}^0_{\mathbf{k}} c_{\mathbf{k}}\, \mathrm{L}_{\mathbf{M}} \Big(\big(\mathcal{C} - \mathcal{C}^0\big) : \big(\varepsilon_{\mathbf{M}} + \varepsilon^0\big) \Big), c_{\mathbf{k}}(\gamma) \right\rangle_2 . \tag{3.13}$$

Next, we apply the splitting $\mathbf{k} = \mathbf{h} + \mathbf{M}^{\mathrm{T}}\mathbf{z}$ with $\mathbf{k}, \mathbf{z} \in \mathbb{Z}^d$ and $\mathbf{h} \in \mathcal{G}(\mathbf{M}^{\mathrm{T}})$ to express the Fourier coefficients in terms of coefficients of translates. Lemma 2.12

together with the coefficients of the fundamental interpolant (3.1) results in the expressions

$$\begin{aligned} c_{\mathbf{k}}\Big(\mathrm{L}_{\mathbf{M}}\Big((\mathcal{C}-\mathcal{C}^0):(\varepsilon_{\mathbf{M}}+\varepsilon^0)\Big)\Big) &= \hat{\mathbf{B}}_{\mathbf{h}}\hat{a}_{\mathbf{h}}c_{\mathbf{h}+\mathbf{M}^{\mathrm{T}}\mathbf{z}}(f),\\ c_{\mathbf{k}}(\gamma) &= \hat{\mathbf{G}}_{\mathbf{h}}c_{\mathbf{h}+\mathbf{M}^{\mathrm{T}}\mathbf{z}}(f),\\ c_{\mathbf{k}}(\varepsilon_{\mathbf{M}}) &= \hat{\mathbf{E}}_{\mathbf{h}}\hat{a}_{\mathbf{h}}c_{\mathbf{h}+\mathbf{M}^{\mathrm{T}}\mathbf{z}}(f). \end{aligned}$$

Inserting these equations into the expression (3.13) above yields

$$\sum_{\mathbf{h}\in\mathcal{G}(\mathbf{M}^{\mathrm{T}})}\sum_{\mathbf{z}\in\mathbb{Z}^d}\Big\langle\hat{\mathbf{E}}_{\mathbf{h}}\hat{a}_{\mathbf{h}}c_{\mathbf{h}+\mathbf{M}^{\mathrm{T}}\mathbf{z}}(f),\hat{\mathbf{G}}_{\mathbf{h}}c_{\mathbf{h}+\mathbf{M}^{\mathrm{T}}\mathbf{z}}(f)\Big\rangle_2 + \Big\langle\hat{\Gamma}^0_{\mathbf{h}+\mathbf{M}^{\mathrm{T}}\mathbf{z}}:\hat{\mathbf{B}}_{\mathbf{h}}\hat{a}_{\mathbf{h}}c_{\mathbf{h}+\mathbf{M}^{\mathrm{T}}\mathbf{z}}(f),\hat{\mathbf{G}}_{\mathbf{h}}c_{\mathbf{h}+\mathbf{M}^{\mathrm{T}}\mathbf{z}}(f)\Big\rangle_2.$$

Bracket sums simplify this expression by collecting all terms depending on $\mathbf{z}\in\mathbb{Z}^d$ to the result of

$$\sum_{\mathbf{h}\in\mathcal{G}(\mathbf{M}^{\mathrm{T}})}\left\langle\hat{\mathbf{E}}_{\mathbf{h}}\hat{a}_{\mathbf{h}}\Big[\big\{|c_{\mathbf{k}}(f)|^2\big\}_{\mathbf{k}\in\mathbb{Z}^d}\Big]^{\mathbf{M}}_{\mathbf{h}},\hat{\mathbf{G}}_{\mathbf{h}}\right\rangle_2+\left\langle\hat{a}_{\mathbf{h}}\Big[\big\{\hat{\Gamma}^0_{\mathbf{k}}|c_{\mathbf{k}}(f)|^2\big\}_{\mathbf{k}\in\mathbb{Z}^d}\Big]^{\mathbf{M}}_{\mathbf{h}}:\hat{\mathbf{B}}_{\mathbf{h}},\hat{\mathbf{G}}_{\mathbf{h}}\right\rangle_2.$$

By assumption, the translates of f are orthonormal and thus by Lemma 2.14 c) they fulfill

$$\Big[\big\{|c_{\mathbf{k}}(f)|^2\big\}_{\mathbf{k}\in\mathbb{Z}^d}\Big]^{\mathbf{M}}_{\mathbf{h}}=\frac{1}{m}.$$

We insert the definition of the periodized Green operator, which gives immediately the desired result

$$\frac{1}{m}\sum_{\mathbf{h}\in\mathcal{G}(\mathbf{M}^{\mathrm{T}})}\Big\langle\hat{\mathbf{E}}_{\mathbf{h}}\hat{a}_{\mathbf{h}},\hat{\mathbf{G}}_{\mathbf{h}}\Big\rangle_2+\Big\langle\hat{a}_{\mathbf{h}}\hat{\Gamma}^{\mathrm{p}}_{\mathbf{h}}:\hat{\mathbf{B}}_{\mathbf{h}},\hat{\mathbf{G}}_{\mathbf{h}}\Big\rangle_2.$$

Step 2: Next, we translate the Lippmann-Schwinger equation to an equation on the coefficients of the translates of the fundamental interpolant $\mathrm{I}_{\mathbf{M}}$. This results in a purely algebraic problem, i.e. an equation in the coefficients $\mathbf{E}_{\mathbf{y}}$ with $\mathbf{y}\in\mathcal{P}(\mathbf{M})$ of $\varepsilon_{\mathbf{M}}$.

By Step 1, we have that

$$\Big\langle\varepsilon_{\mathbf{M}}+\Gamma^0\,\mathrm{L}_{\mathbf{M}}\Big((\mathcal{C}-\mathcal{C}^0):(\varepsilon_{\mathbf{M}}+\varepsilon^0)\Big),\gamma\Big\rangle_2=0$$

for all $\gamma\in\mathrm{Sym}_d\big(\mathcal{V}^f_{\mathbf{M}}\big)$ is equivalent to

$$\frac{1}{m}\sum_{\mathbf{h}\in\mathcal{G}(\mathbf{M}^{\mathrm{T}})}\Big\langle\hat{\mathbf{E}}_{\mathbf{h}}\hat{a}_{\mathbf{h}},\hat{\mathbf{G}}_{\mathbf{h}}\Big\rangle_2+\Big\langle\hat{a}_{\mathbf{h}}\hat{\Gamma}^{\mathrm{p}}_{\mathbf{h}}:\hat{\mathbf{B}}_{\mathbf{h}},\hat{\mathbf{G}}_{\mathbf{h}}\Big\rangle_2=0 \tag{3.14}$$

for all $\hat{\mathbf{G}}_{\mathbf{h}}\in\mathrm{Sym}_d\big(\mathbb{R}\big)$ and all $\mathbf{h}\in\mathcal{G}(\mathbf{M}^{\mathrm{T}})$.

It is sufficient to look at Equation (3.14) componentwise. We replace $\hat{\mathbf{G}}_{\mathbf{h}}$ by

$$\hat{\mathbf{G}}_{\mathbf{h},\mathbf{y},i,j} \coloneqq \mathbf{Q}_{ij}\big(\mathbf{q}_i\mathbf{q}_j^{\mathrm{T}} + \mathbf{q}_j\mathbf{q}_i^{\mathrm{T}}\big)\,\mathrm{e}^{-2\pi\mathrm{i}\mathbf{h}^{\mathrm{T}}\mathbf{y}}$$

for all $\mathbf{h} \in \mathcal{G}(\mathbf{M}^{\mathrm{T}})$ and $\mathbf{y} \in \mathcal{P}(\mathbf{M})$ and $i, j = 1, \dots, d$. The vector $\mathbf{q}_i \in \mathbb{R}^d$ denotes the i-th unit vector and $\mathbf{Q}_{ij} \coloneqq 1 - \frac{1}{2}\delta_{ij}$ normalizes the resulting matrix. This parametrization is the trigonometric basis of $\mathrm{Sym}_d\big(\mathcal{V}_{\mathbf{M}}^f\big)$ on the pattern $\mathcal{P}(\mathbf{M})$.

Hence, the equation

$$\frac{1}{m}\sum_{\mathbf{h}\in\mathcal{G}(\mathbf{M}^{\mathrm{T}})} \hat{\mathbf{E}}_{\mathbf{h}}\hat{a}_{\mathbf{h}}e^{2\pi\mathrm{i}\mathbf{h}^{\mathrm{T}}\mathbf{y}} + \hat{a}_{\mathbf{h}}\hat{\Gamma}^{\mathrm{p}}_{\mathbf{h}} : \hat{B}_{\mathbf{h}}\,\mathrm{e}^{2\pi\mathrm{i}\mathbf{h}^{\mathrm{T}}\mathbf{y}} = \mathbf{0},$$

for all $\mathbf{y} \in \mathcal{P}(\mathbf{M})$, is equivalent to Equation (3.14), bearing in mind the necessary complex conjugate.

This, however, is an inverse discrete Fourier transform on the pattern $\mathcal{P}(\mathbf{M})$, see Definition 2.7, and setting $\hat{\tilde{\mathbf{B}}}_{\mathbf{h}} \coloneqq \hat{\Gamma}^{\mathrm{p}}_{\mathbf{h}}\hat{\mathbf{B}}_{\mathbf{h}}$ yields

$$\frac{1}{m}\sum_{\mathbf{h}\in\mathcal{G}(\mathbf{M}^{\mathrm{T}})} \Big(\hat{\mathbf{E}}_{\mathbf{h}}\hat{a}_{\mathbf{h}} + \hat{a}_{\mathbf{h}}\hat{\Gamma}^{\mathrm{p}}_{\mathbf{h}} : \hat{B}_{\mathbf{h}}\Big)\,\mathrm{e}^{2\pi\mathrm{i}\mathbf{h}^{\mathrm{T}}\mathbf{y}} = \frac{1}{m}\sum_{\mathbf{h}\in\mathcal{G}(\mathbf{M}^{\mathrm{T}})} \Big(\hat{\mathbf{E}}_{\mathbf{h}} + \hat{\tilde{\mathbf{B}}}_{\mathbf{h}}\Big)\hat{a}_{\mathbf{h}}\,\mathrm{e}^{2\pi\mathrm{i}\mathbf{h}^{\mathrm{T}}\mathbf{y}} = \mathbf{0}.$$

The coefficients $\big(\tilde{\mathbf{B}}_{\mathbf{y}}\big)_{\mathbf{y}\in\mathcal{P}(\mathbf{M})} \coloneqq \overline{\mathcal{F}}(\mathbf{M})^{\mathrm{T}}\big(\hat{\tilde{\mathbf{B}}}_{\mathbf{h}}\big)_{\mathbf{h}\in\mathcal{G}(\mathbf{M}^{\mathrm{T}})}$ can be interpreted as coefficients of translates of the fundamental interpolant with Lemma 2.14 c) and d), i.e. it holds that

$$\frac{1}{m}\sum_{\mathbf{h}\in\mathcal{G}(\mathbf{M}^{\mathrm{T}})} \Big(\hat{\mathbf{E}}_{\mathbf{h}} + \hat{\tilde{\mathbf{B}}}_{\mathbf{h}}\Big)\hat{a}_{\mathbf{h}}\,\mathrm{e}^{2\pi\mathrm{i}\mathbf{h}^{\mathrm{T}}\mathbf{y}} = \sum_{\mathbf{y}\in\mathcal{P}(\mathbf{M})} \big(\mathbf{E}_{\mathbf{y}} + \tilde{\mathbf{B}}_{\mathbf{y}}\big)\big(\mathcal{T}(\mathbf{y})\,\mathrm{I}_{\mathbf{M}}\big)(\mathbf{x}) = \mathbf{0}$$

for all $\mathbf{x} \in \mathbb{T}^d$. By Definition 3.1, the operator Γ^{p} acts as a Fourier multiplier with Fourier coefficients (3.6). This transforms the above equation to

$$\sum_{\mathbf{y}\in\mathcal{P}(\mathbf{M})} \Big(\mathbf{E}_{\mathbf{y}} + \Gamma^{\mathrm{p}}_{\mathbf{y}} : \mathbf{B}_{\mathbf{y}}\Big)\big(\mathcal{T}(\mathbf{y})\,\mathrm{I}_{\mathbf{M}}\big)(\mathbf{x}) = \mathbf{0}.$$

The coefficients $\mathbf{B}_{\mathbf{y}}$ were chosen such that they coincide with the function values of $\big(\mathcal{C}(\mathbf{y}) - \mathcal{C}^0\big) : \big(\varepsilon_{\mathbf{M}}(\mathbf{y}) + \varepsilon^0\big)$ at points $\mathbf{y} \in \mathcal{P}(\mathbf{M})$, see Equation (3.12), by the interpolation property of $\mathrm{I}_{\mathbf{M}}$ in Definition 2.13. Likewise, $\varepsilon_{\mathbf{M}}$ coincides on the points $\mathbf{y} \in \mathcal{P}(\mathbf{M})$ with the coefficients $\mathbf{E}_{\mathbf{y}}$. Inserting these relations, we obtain

$$\sum_{\mathbf{y}\in\mathcal{P}(\mathbf{M})} \Big(\mathbf{E}_{\mathbf{y}} + \Gamma^{\mathrm{p}}_{\mathbf{y}}\big(\mathcal{C}(\mathbf{y}) - \mathcal{C}^0\big) : \big(\mathbf{E}_{\mathbf{y}} + \varepsilon^0\big)\Big)\big(\mathcal{T}(\mathbf{y})\,\mathrm{I}_{\mathbf{M}}\big)(\mathbf{x}) = \mathbf{0}$$

for all $\mathbf{x} \in \mathcal{P}(\mathbf{M})$, which yields the desired result. □

The discretized variational equation

The discretization approach on spaces of translates in Theorem 3.6 can also be applied on the variational equation (VE) and is given as follows:

Theorem 3.7. *Let the translates of f be orthonormal, let $\mathcal{C} \in \mathrm{SSym}_d\big(\mathcal{A}(\mathbb{T}^d)\big)$, and let $\varepsilon_{\mathbf{M}} \in \mathcal{E}^f_{\mathbf{M}}(\mathbb{T}^d)$. Then $\varepsilon_{\mathbf{M}}$ fulfills the weak form*

$$\Big\langle \mathcal{C}^0\Gamma^0\,\mathrm{L}_{\mathbf{M}}\Big(\mathcal{C}:\big(\varepsilon_{\mathbf{M}}+\varepsilon^0\big)\Big), \gamma \Big\rangle_2 = 0 \tag{3.15}$$

for all $\gamma \in \mathrm{Sym}_d\big(\mathcal{V}^f_{\mathbf{M}}\big)$ if and only if

$$\sum_{\mathbf{y}\in\mathcal{P}(\mathbf{M})} \mathcal{C}^0\Gamma^{\mathrm{p}}_{\mathbf{y}}\mathcal{C}(\mathbf{y}):\big(\mathbf{E}_{\mathbf{y}}+\varepsilon^0\big)\big(\mathcal{T}(\mathbf{y})\,\mathrm{I}_{\mathbf{M}}\big)(\mathbf{x}) = \mathbf{0} \tag{3.16}$$

for all $\mathbf{x} \in \mathcal{P}(\mathbf{M})$.

Proof. The proof of this theorem proceeds in the same way as the proof of Theorem 3.6 and is thus only sketched. First, it is shown that

$$\Big\langle \mathcal{C}^0\Gamma^0\,\mathrm{L}_{\mathbf{M}}\Big(\mathcal{C}:\big(\varepsilon_{\mathbf{M}}+\varepsilon^0\big)\Big), \gamma \Big\rangle_2 = \frac{1}{m}\sum_{\mathbf{h}\in\mathcal{G}(\mathbf{M}^{\mathrm{T}})} \Big\langle \mathcal{C}^0\hat{\Gamma}^{\mathrm{p}}_{\mathbf{h}} : \hat{\mathbf{B}}_{\mathbf{h}}, \hat{\mathbf{G}}_{\mathbf{h}} \Big\rangle_2,$$

where

$$\mathrm{L}_{\mathbf{M}}\Big(\mathcal{C}:\big(\varepsilon+\varepsilon^0\big)\Big) = \sum_{\mathbf{y}\in\mathcal{P}(\mathbf{M})} \mathbf{B}_{\mathbf{y}}\,\mathcal{T}(\mathbf{y})\,\mathrm{I}_{\mathbf{M}}$$

and $\big(\hat{\mathbf{B}}_{\mathbf{h}}\big)_{\mathbf{h}\in\mathcal{G}(\mathbf{M}^{\mathrm{T}})} = \mathcal{F}(\mathbf{M})\big(\mathbf{B}_{\mathbf{y}}\big)_{\mathbf{y}\in\mathcal{P}(\mathbf{M})}$. From there on, the proof goes analogously to the proof of Theorem 3.6, mutatis mutandis. □

When replacing the strain $\varepsilon \in \mathcal{E}(\mathbb{T}^d)$ by its interpolant on the space of translates $\varepsilon_{\mathbf{M}} \in \mathcal{E}^f_{\mathbf{M}}(\mathbb{T}^d)$, the Lippmann-Schwinger equation and the variational equation can be discretized on $\mathcal{V}^f_{\mathbf{M}}$. The infinite dimensional problems and their discretizations have the same structure, where the Green operator Γ^0 is replaced by the periodized Green operator Γ^{p}. Then, we can state the equations in terms of the coefficients $\mathbf{E}_{\mathbf{y}}$ of the strain $\varepsilon_{\mathbf{M}}$. These coefficients represent the value of $\varepsilon_{\mathbf{M}}$ at the points $\mathbf{y} \in \mathcal{P}(\mathbf{M})$, i.e. they are the factors for the linear combination of the translates $\mathcal{T}(\mathbf{y})\,\mathrm{I}_{\mathbf{M}}$ of the fundamental interpolant.

3.3 Characterization of solutions

The solutions of the Lippmann-Schwinger equation (LS) and the variational equation (VE) coincide in the continuous case, see Theorem 2.35. After discretization with truncated trigonometric polynomials, i.e. on $\mathcal{V}^f_{\mathbf{M}}$ with the Dirichlet kernel $f = f_{\mathrm{D}_{\mathbf{M}}}$, and assuming a tensor product grid, the solutions of the two equations coincide as well [105, Proposition 3].

The following theorem identifies the Dirichlet kernel as a special case in this regard, i.e. it produces the only translation invariant space where the solutions of the two partial differential equations are equal. This result is then followed by an overview of the connections between the solutions of the Lippmann-Schwinger equation and the variational formulation, for both the continuous case and various discretizations, i.e. choices of $\mathcal{V}_{\mathbf{M}}^{f}$.

We extend the results in [105] to anisotropic patterns using the Dirichlet kernel. We then generalize the connection between the solutions of the Lippmann-Schwinger equation and the variational formulation of spaces of translates.

Theorem 3.8. *Let the translates of f be orthonormal and let $\mathcal{C} \in \mathrm{SSym}_d\big(\mathcal{A}(\mathbb{T}^d)\big)$ be a stiffness distribution. Let $\mathbf{E}_{\mathbf{y}}$ with $\mathbf{y} \in \mathcal{P}(\mathbf{M})$ solve the Lippmann-Schwinger equation* (3.10) *and let further $\tilde{\mathbf{E}}_{\mathbf{y}}$ solve the variational equation* (3.16) *on the space $\mathcal{V}_{\mathbf{M}}^{f}$.*

Then $\mathbf{E}_{\mathbf{y}} = \tilde{\mathbf{E}}_{\mathbf{y}}$ for all $\mathbf{y} \in \mathcal{P}(\mathbf{M})$ if and only if $\mathcal{V}_{\mathbf{M}}^{f} = \mathcal{V}_{\mathbf{M}}^{f_{\mathrm{D}_{\mathbf{M}}}}$.

Proof. Let first $\mathcal{V}_{\mathbf{M}}^{f} = \mathcal{V}_{\mathbf{M}}^{f_{\mathrm{D}_{\mathbf{M}}}}$, then the Lippmann-Schwinger equation (3.10) can be rewritten as

$$\begin{aligned}
0 &= \sum_{\mathbf{y}\in\mathcal{P}(\mathbf{M})} \Big(\mathbf{E}_{\mathbf{y}} + \Gamma^{\mathrm{p}}_{\mathbf{y}}\big(\mathcal{C}(\mathbf{y}) - \mathcal{C}^0\big) : \big(\mathbf{E}_{\mathbf{y}} + \varepsilon^0\big)\Big)\big(\mathcal{T}(\mathbf{y})\,\mathrm{I}_{\mathbf{M}}\big)(\mathbf{x}) \\
&= \sum_{\mathbf{y}\in\mathcal{P}(\mathbf{M})} \mathbf{E}_{\mathbf{y}}\big(\mathcal{T}(\mathbf{y})\,\mathrm{I}_{\mathbf{M}}\big)(\mathbf{x}) + \sum_{\mathbf{y}\in\mathcal{P}(\mathbf{M})} \Gamma^{\mathrm{p}}_{\mathbf{y}}\mathcal{C}(\mathbf{y}) : \big(\mathbf{E}_{\mathbf{y}} + \varepsilon^0\big)\big(\mathcal{T}(\mathbf{y})\,\mathrm{I}_{\mathbf{M}}\big)(\mathbf{x}) \\
&\quad - \sum_{\mathbf{y}\in\mathcal{P}(\mathbf{M})} \Gamma^{\mathrm{p}}_{\mathbf{y}}\mathcal{C}^0 : \mathbf{E}_{\mathbf{y}}\big(\mathcal{T}(\mathbf{y})\,\mathrm{I}_{\mathbf{M}}\big)(\mathbf{x}) - \sum_{\mathbf{y}\in\mathcal{P}(\mathbf{M})} \Gamma^{\mathrm{p}}_{\mathbf{y}}\mathcal{C}^0 : \varepsilon^0\big(\mathcal{T}(\mathbf{y})\,\mathrm{I}_{\mathbf{M}}\big)(\mathbf{x})
\end{aligned}$$

for $\mathbf{x} \in \mathbb{T}^d$. With Equations (3.8) and (3.5) this is the same as

$$0 = \varepsilon_{\mathbf{M}}(\mathbf{x}) + \Big(\Gamma^{\mathrm{p}}\mathcal{C} : \big(\varepsilon_{\mathbf{M}} + \varepsilon^0\big)\Big)(\mathbf{x}) - \Big(\Gamma^{\mathrm{p}}\mathcal{C}^0 : \varepsilon_{\mathbf{M}}\Big)(\mathbf{x}) - \Big(\Gamma^{\mathrm{p}}\mathcal{C}^0 : \varepsilon^0\Big)(\mathbf{x}). \tag{3.17}$$

We are in the case of the Dirichlet kernel, so due to Theorem 3.5 the operator $\Gamma^{\mathrm{p}}\mathcal{C}^0$ is a projection operator and maps constants to zero and thus $\Gamma^{\mathrm{p}}\mathcal{C}^0\varepsilon_{\mathbf{M}} = \varepsilon_{\mathbf{M}}$ and $\Gamma^{\mathrm{p}}\mathcal{C}^0\varepsilon^0 = \mathbf{0}$. Therefore, the above equation reduces to

$$0 = \Big(\Gamma^{\mathrm{p}}\mathcal{C} : \big(\varepsilon_{\mathbf{M}} - \varepsilon^0\big)\Big)(\mathbf{x}) \tag{3.18}$$

which, after multiplication with $\mathcal{C}^0$ from the left, is the variational equation (3.16), using the representation of $\varepsilon_{\mathbf{M}}$ in coefficients $\mathbf{E}_{\mathbf{y}}$ with $\mathbf{y} \in \mathcal{P}(\mathbf{M})$. Now, assume that $\mathcal{V}_{\mathbf{M}}^{f} \neq \mathcal{V}_{\mathbf{M}}^{f_{\mathrm{D}_{\mathbf{M}}}}$, i.e. that we are not in the case of the Dirichlet kernel. Then, applying again Theorem 3.5, the operator $\Gamma^{\mathrm{p}}\mathcal{C}^0$ is not a projection and does not map constants to zero. Therefore, the last term in (3.17) does not vanish and the equation is not reduced to (3.18). This results in different solutions for the Lippmann-Schwinger equation and the variational equation. Hence, the proof is finished. □

The connections between various discretizations are summarized in Figure 3.1. The equivalence between the variational equation (VE) and the Lippmann-Schwinger equation (LS) in the continuous case and in case of truncated trigonometric polynomials on

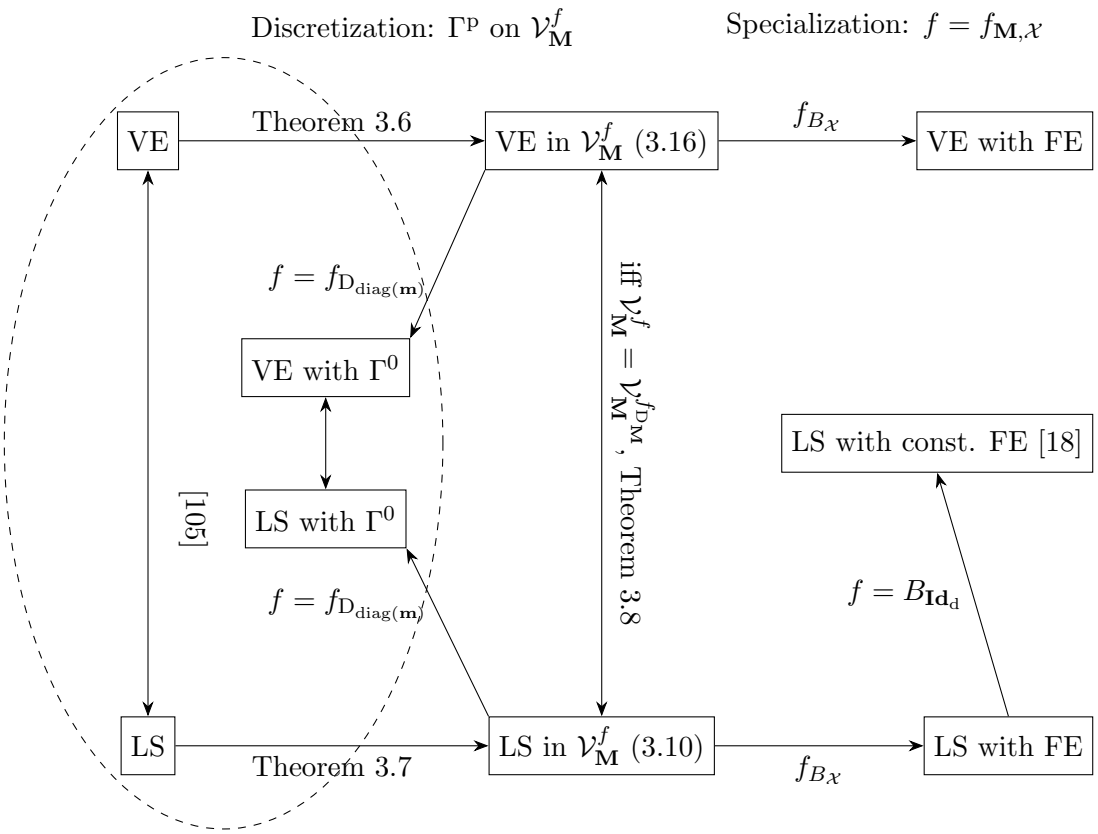

Figure 3.1. A diagram of connections between the Lippmann-Schwinger equation (LS) and the variational equation (VE) for different discretizations. The term diag(**m**) with $\mathbf{m} \in \mathbb{N}^d$ denotes a diagonal matrix and thus $f_{\mathrm{D}_{\mathrm{diag}(\mathbf{m})}}$ is the Dirichlet kernel on a tensor product grid.

tensor product grids, i.e. for diagonal pattern matrices $\mathbf{M}$, called (VE with Γ^0), and (LS with Γ^0), respectively, is established in [105]. The discretizations detailed in Section 3.2 lead in the special case of $\mathcal{V}_{\mathbf{M}}^{f} = \mathcal{V}_{\mathbf{M}}^{f_{\mathrm{D}_{\mathbf{M}}}}$ generated by the Dirichlet kernel back to the discretization in [105]. This case is also the only one where the solutions of the two equations coincide.

When choosing periodized pattern Box splines of order 0, i.e. piecewise constant functions, as generators for the translation invariant space one arrives at the discretization of [18] denoted by (LS with const. FE). This approach is based on a energy formulation of the partial differential equation and it uses constant finite elements as ansatz space. This is a special case of (LS with FE), which uses general Box-splines. These ansatz functions can be considered as finite elements with reduced integration. The resulting operator Γ^{p} here coincides with the Green operator in [18].

3.4 Convergence of the discretization

Convergence proofs for discretizations of the equation of elasticity in periodic homogenization exist in the case of truncated trigonometric polynomials. There, two kinds of results have to be distinguished. First, a convergence proof requiring only Riemann integrability and convexity of the stiffness distribution $\mathcal{C}$ is established in [89]. These assumptions on the coefficients, however, do not allow to compute a convergence rate. Second, convergence proofs assuming higher regularity of the stiffness distribution are shown in [102, Paper 5] and [105]. There, the regularity of the coefficients yields a smooth solution, which in turn gives rise to a higher convergence rate.

This section introduces a convergence proof and a convergence rate in case of smooth coefficients. The order of convergence not only depends on the smoothness of the continuous solution, but also on the regularity of the function f generating the ansatz space $\mathcal{V}_{\mathbf{M}}^{f}$.

The setting in [105] is on a tensor product grid and the convergence analysis corresponds to the results for translation invariant spaces in [95] in case of the Dirichlet kernel. We generalize these results to anisotropic patterns in the sense of [23]. Further, we generalize the Dirichlet kernel to spaces of translates and use the convergence analysis on anisotropic patterns [5, 9].

This section is divided into two parts. First, we reformulate the Lippmann-Schwinger equation in terms of a variational equation with bilinear and linear form to fit the first Strang lemma in Lemma 2.40. The same is done for the discretized equation. We show in the following section that these discrete bilinear and linear forms are be bounded and elliptic. This is followed by the convergence proof, making use of various upper and lower bounds on the operators and the approximation results from Lemma 2.24.

Boundedness and ellipticity results

The convergence theorem requires three ingredients: the first transfers the smoothness in the stiffness distribution $\mathcal{C}$ to the strain ε solving the equation, see Lemma 2.39. The second result is the first Strang lemma that provides estimates on the difference between the analytical solution and numerical discretizations, see Lemma 2.40. These are combined with the approximation estimates for spaces of translates in Lemma 2.24. The convergence proof then follows the idea in [102, Paper 5, Section 3.4] and generalizes it to anisotropic spaces of translates.

To prepare the proof, we first show that the discretized Lippmann-Schwinger equation (3.9) can be rewritten in terms of a bilinear form and a linear form such that they fulfill the conditions on boundedness and uniform ellipticity required by the first Strang lemma in Lemma 2.40.

The discretized Lippmann-Schwinger equation

$$\left\langle \varepsilon_{\mathbf{M}} + \Gamma^0 \, \mathrm{L}_{\mathbf{M}}\Big(\big(\mathcal{C} - \mathcal{C}^0\big) : \big(\varepsilon_{\mathbf{M}} + \varepsilon^0\big) \Big), \gamma_{\mathbf{M}} \right\rangle_2 = 0$$

is equivalent to an equation of the form

$$B_{\mathbf{M}}(\varepsilon_{\mathbf{M}}, \gamma_{\mathbf{M}}) = F_{\mathbf{M}}(\gamma_{\mathbf{M}})$$

for all $\gamma_{\mathbf{M}} \in \mathrm{Sym}_d(\mathcal{V}_{\mathbf{M}}^f)$. The bilinear form $B_{\mathbf{M}}$ and the linear form $F_{\mathbf{M}}$ are given via

$$B_{\mathbf{M}}(\varepsilon_{\mathbf{M}}, \gamma_{\mathbf{M}}) \coloneqq \left\langle \varepsilon_{\mathbf{M}} + \Gamma^0 \, \mathrm{L}_{\mathbf{M}}\Big(\big(\mathcal{C} - \mathcal{C}^0\big) : \varepsilon_{\mathbf{M}} \Big), \gamma_{\mathbf{M}} \right\rangle_2, \tag{3.19}$$

$$F_{\mathbf{M}}(\gamma_{\mathbf{M}}) \coloneqq \left\langle \Gamma^0 \, \mathrm{L}_{\mathbf{M}}\Big(\big(\mathcal{C} - \mathcal{C}^0\big) : \varepsilon^0 \Big), \gamma_{\mathbf{M}} \right\rangle_2 \tag{3.20}$$

for $\varepsilon_{\mathbf{M}} \in \mathcal{E}_{\mathbf{M}}^f(\mathbb{T}^d)$ and $\gamma_{\mathbf{M}} \in \mathrm{Sym}_d(\mathcal{V}_{\mathbf{M}}^f)$, respectively. They can be bounded from above and below as follows:

Lemma 3.9. *Let $f = \mathrm{I}_{\mathbf{M}}$ be the fundamental interpolant generating the space $\mathcal{V}_{\mathbf{M}}^f$ and let the translates $\mathcal{T}(\mathbf{y})\,\mathrm{I}_{\mathbf{M}}$ for $\mathbf{y} \in \mathcal{P}(\mathbf{M})$ be orthonormal, and let $\mathcal{C} \in \mathrm{SSym}_d\big(\mathcal{A}(\mathbb{T}^d)\big)$. Let further $c_{b,\mathcal{C}} > 0$ and $c_{e,\mathcal{C}} > 0$ be the constants of boundedness and ellipticity for $\mathcal{C}$, and the constants $c_{b,\mathcal{C}^0}$ and $c_{e,\mathcal{C}^0}$ be likewise defined for $\mathcal{C}^0$, see Definition 2.28.*

Further, assume that $c_{e,\mathcal{C}} \leq c_{e,\mathcal{C}^0}$ and $c_{b,\mathcal{C}^0} \leq c_{e,\mathcal{C}}$. Then the following statements hold:

a) The bilinear form (3.19) *is bounded with*

$$\big|B_{\mathbf{M}}(\varepsilon_{\mathbf{M}}, \gamma_{\mathbf{M}})\big| \leq \left(1 + \frac{c_{b,\mathcal{C}^0}}{c_{e,\mathcal{C}^0}^2}(c_{b,\mathcal{C}} - c_{b,\mathcal{C}^0})\right) \|\varepsilon_{\mathbf{M}}\|_2 \|\gamma_{\mathbf{M}}\|_2$$

for all $\varepsilon_{\mathbf{M}} \in \mathcal{E}_{\mathbf{M}}^f(\mathbb{T}^d)$ and $\gamma_{\mathbf{M}} \in \mathrm{Sym}_d(\mathcal{V}_{\mathbf{M}}^f)$.

b) The bilinear form (3.19) *is uniformly elliptic with*

$$B_{\mathbf{M}}(\gamma_{\mathbf{M}}, \gamma_{\mathbf{M}}) \geq \left(1 + \frac{c_{e,\mathcal{C}^0}}{c_{b,\mathcal{C}^0}^2}(c_{e,\mathcal{C}} - c_{e,\mathcal{C}^0})\right) \|\gamma_{\mathbf{M}}\|_2^2$$

for all $\gamma_{\mathbf{M}} \in \mathrm{Sym}_d(\mathcal{V}_{\mathbf{M}}^f)$.

c) The linear form (3.20) *is bounded with*

$$\big|F_{\mathbf{M}}(\gamma_{\mathbf{M}})\big| \leq \left(1 + \frac{c_{b,\mathcal{C}^0}}{c_{e,\mathcal{C}^0}^2}(c_{b,\mathcal{C}} - c_{b,\mathcal{C}^0})\right) \|\varepsilon^0\|_2 \|\gamma_{\mathbf{M}}\|_2$$

for all $\gamma_{\mathbf{M}} \in \mathrm{Sym}_d(\mathcal{V}_{\mathbf{M}}^f)$.

Proof. Consider the bilinear form

$$B_{\mathbf{M}}(\varepsilon_{\mathbf{M}}, \gamma_{\mathbf{M}}) \coloneqq \left\langle \varepsilon_{\mathbf{M}} + \Gamma^0 \, \mathrm{L}_{\mathbf{M}}\Big(\big(\mathcal{C} - \mathcal{C}^0\big) : \varepsilon_{\mathbf{M}} \Big), \gamma_{\mathbf{M}} \right\rangle_2$$

for $\varepsilon_{\mathbf{M}}, \gamma_{\mathbf{M}} \in \mathrm{Sym}_d(\mathcal{V}_{\mathbf{M}}^f)$ which is, using Theorem 3.6, equivalent to

$$B_{\mathbf{M}}(\varepsilon_{\mathbf{M}}, \gamma_{\mathbf{M}}) = \left\langle \sum_{\mathbf{y}\in\mathcal{P}(\mathbf{M})} \left(\mathbf{E}_{\mathbf{y}} + \Gamma^{\mathrm{p}}_{\mathbf{y}}\big(\mathcal{C}(\mathbf{y}) - \mathcal{C}^0\big) : \mathbf{E}_{\mathbf{y}}\right) \mathcal{T}(\mathbf{y})\, \mathrm{I}_{\mathbf{M}}, \sum_{\mathbf{y}\in\mathcal{P}(\mathbf{M})} \mathbf{G}_{\mathbf{y}}\, \mathcal{T}(\mathbf{y})\, \mathrm{I}_{\mathbf{M}} \right\rangle_2,$$

where

$$\varepsilon_{\mathbf{M}} = \sum_{\mathbf{y}\in\mathcal{P}(\mathbf{M})} \mathbf{E}_{\mathbf{y}}\, \mathcal{T}(\mathbf{y})\, \mathrm{I}_{\mathbf{M}},$$
$$\gamma = \sum_{\mathbf{y}\in\mathcal{P}(\mathbf{M})} \mathbf{G}_{\mathbf{y}}\, \mathcal{T}(\mathbf{y})\, \mathrm{I}_{\mathbf{M}}.$$

The translates of the fundamental interpolant $\mathrm{I}_{\mathbf{M}}$ are orthonormal by assumption, which reduces the above expression to

$$\begin{aligned} B_{\mathbf{M}}(\varepsilon_{\mathbf{M}}, \gamma_{\mathbf{M}}) &= \sum_{\mathbf{y}\in\mathcal{P}(\mathbf{M})} \left\langle \mathbf{E}_{\mathbf{y}} + \Gamma^{\mathrm{p}}_{\mathbf{y}}\big(\mathcal{C}(\mathbf{y}) - \mathcal{C}^0\big) : \mathbf{E}_{\mathbf{y}}, \mathbf{G}_{\mathbf{y}} \right\rangle_2 \\ &= \sum_{\mathbf{y}\in\mathcal{P}(\mathbf{M})} \langle \mathbf{E}_{\mathbf{y}}, \mathbf{G}_{\mathbf{y}} \rangle_2 + \left\langle \Gamma^{\mathrm{p}}_{\mathbf{y}} \mathcal{C}^0 \big(\mathcal{C}^0\big)^{-1} \big(\mathcal{C}(\mathbf{y}) - \mathcal{C}^0\big) : \mathbf{E}_{\mathbf{y}}, \mathbf{G}_{\mathbf{y}} \right\rangle_2. \end{aligned} \tag{3.21}$$

From Theorem 3.3 c), Theorem 3.4 a), the boundedness and ellipticity assumption on $\mathcal{C}$, and — via its smallest and largest eigenvalue — on $\mathcal{C}^0$, we have

$$\begin{aligned} \big\|\mathcal{C} : \gamma_{\mathbf{M}}\big\|_2 &\leq c_{\mathrm{b},\mathcal{C}} \|\gamma_{\mathbf{M}}\|_2, \\ \big\|\mathcal{C}^0 : \gamma_{\mathbf{M}}\big\|_2 &\leq c_{\mathrm{b},\mathcal{C}^0} \|\gamma_{\mathbf{M}}\|_2, \\ \big\|\Gamma^{\mathrm{p}}\mathcal{C}^0 : \gamma_{\mathbf{M}}\big\|_2 &\leq \frac{c_{\mathrm{b},\mathcal{C}^0}}{c_{\mathrm{e},\mathcal{C}^0}} \|\gamma_{\mathbf{M}}\|_2, \end{aligned}$$

and

$$\begin{aligned} \big\langle \mathcal{C} : \gamma_{\mathbf{M}}, \gamma_{\mathbf{M}} \big\rangle &\geq c_{\mathrm{e},\mathcal{C}} \|\gamma_{\mathbf{M}}\|_2^2, \\ \big\langle \mathcal{C}^0 : \gamma_{\mathbf{M}}, \gamma_{\mathbf{M}} \big\rangle &\geq c_{\mathrm{e},\mathcal{C}^0} \|\gamma_{\mathbf{M}}\|_2^2, \\ \big\langle \Gamma^{\mathrm{p}}\mathcal{C}^0 : \gamma_{\mathbf{M}}, \gamma_{\mathbf{M}} \big\rangle &\geq \frac{c_{\mathrm{e},\mathcal{C}^0}}{c_{\mathrm{b},\mathcal{C}^0}} \|\gamma_{\mathbf{M}}\|_2^2. \end{aligned}$$

a) We apply the above estimates to the expression (3.21) and get with the Cauchy-Schwarz inequality and

$$\Big\|\big(\mathcal{C}^0\big)^{-1} : \gamma_{\mathbf{M}}\Big\|_2 \leq \frac{1}{c_{\mathrm{e},\mathcal{C}^0}} \|\gamma_{\mathbf{M}}\|_2$$

the estimate

$$\big|B_{\mathbf{M}}(\varepsilon_{\mathbf{M}}, \gamma_{\mathbf{M}})\big| \leq \left(1 + \frac{c_{\mathrm{b},\mathcal{C}^0}}{c_{\mathrm{e},\mathcal{C}^0}} \frac{1}{c_{\mathrm{e},\mathcal{C}^0}} (c_{\mathrm{b},\mathcal{C}} - c_{\mathrm{b},\mathcal{C}^0})\right) \|\varepsilon_{\mathbf{M}}\|_2 \|\gamma_{\mathbf{M}}\|_2.$$

If the inequality if fulfilled, the bounding constant has to be positive. This is guaranteed by the assumption $c_{\mathrm{b},\mathcal{C}^0} \leq c_{\mathrm{b},\mathcal{C}}$.

b) Further, it holds with

$$\left\langle \left(\mathcal{C}^0\right)^{-1} : \gamma_{\mathbf{M}}, \gamma_{\mathbf{M}} \right\rangle_2 \geq \frac{1}{c_{\mathrm{b},\mathcal{C}^0}} \|\gamma_{\mathbf{M}}\|_2^2$$

that

$$B_{\mathbf{M}}(\gamma_{\mathbf{M}}, \gamma_{\mathbf{M}}) \geq \left(1 + \frac{c_{\mathrm{e},\mathcal{C}^0}}{c_{\mathrm{b},\mathcal{C}^0}} \frac{1}{c_{\mathrm{b},\mathcal{C}^0}} (c_{\mathrm{e},\mathcal{C}} - c_{\mathrm{e},\mathcal{C}^0})\right) \|\gamma_{\mathbf{M}}\|_2^2.$$

If the inequality if fulfilled, the constant of ellipticity has to be positive. The assumption $c_{\mathrm{e},\mathcal{C}} \leq c_{\mathrm{e},\mathcal{C}^0}$ assures this. Further, the constant is independent of $\mathbf{M}$ and thus $B_{\mathbf{M}}$ is uniformly elliptic.

c) With the same arguments as above, the linear form

$$F_{\mathbf{M}}(\gamma_{\mathbf{M}}) = \left\langle \Gamma^0 \, \mathrm{L}_{\mathbf{M}}\Big(\left(\mathcal{C} - \mathcal{C}^0\right) : \varepsilon^0 \Big), \gamma_{\mathbf{M}} \right\rangle_2$$

is equivalent to

$$F_{\mathbf{M}}(\gamma_{\mathbf{M}}) = \sum_{\mathbf{y} \in \mathcal{P}(\mathbf{M})} \left\langle \Gamma^{\mathrm{p}}_{\mathbf{y}} \mathcal{C}^0 \left(\mathcal{C}^0\right)^{-1} \left(\mathcal{C}(\mathbf{y}) - \mathcal{C}^0\right) : \varepsilon^0, \mathbf{G}_{\mathbf{y}} \right\rangle_2.$$

Therefore, $F_{\mathbf{M}}$ is bounded with

$$F_{\mathbf{M}}(\gamma_{\mathbf{M}}) \leq \left(1 + \frac{c_{\mathrm{b},\mathcal{C}^0}}{c_{\mathrm{e},\mathcal{C}^0}} \frac{1}{c_{\mathrm{e},\mathcal{C}^0}} (c_{\mathrm{b},\mathcal{C}} - c_{\mathrm{b},\mathcal{C}^0})\right) \|\varepsilon^0\|_2 \|\gamma_{\mathbf{M}}\|_2.$$

As above, $c_{\mathrm{b},\mathcal{C}^0} \leq c_{\mathrm{b},\mathcal{C}}$ ensures the positivity of the constant and the proof is complete. □

Convergence estimates

The convergence theorem presented in this section makes use of two main ideas, following the proof for truncated trigonometric polynomials in [102, Paper 5]. One is the first Strang lemma in Lemma 2.40, giving a connection between the error made by discretizing the partial differential equation and the errors produced by changing the bilinear form and linear form. The second is the approximation error in the ansatz space, handled by Lemma 2.24. We concentrate on the Lippmann-Schwinger equation (LS) and give a sketch for the proof in case of the variational formulation (VE). The following theorem generalizes the results in [102] to anisotropic patterns and extends it to spaces of translates.

Theorem 3.10. *Let $\mathcal{C} \in \mathrm{SSym}_d\big(\mathcal{W}^{b,\infty}(\mathbb{T}^d)\big) \cap \mathrm{SSym}_d\big(\mathcal{A}(\mathbb{T}^d)\big)$ for $b \in \mathbb{N}$ with $b > \frac{d}{2}$, let $\mathcal{C}^0 \in \mathrm{SSym}_d\big(\mathbb{R}\big)$ such that the conditions on boundedness and ellipticity in Lemma 3.9 are fulfilled. Further, let $\mathcal{V}^f_{\mathbf{M}}$ be a space of translates of the function f, where $f = \mathrm{I}_{\mathbf{M}}$ is a fundamental interpolant where the translates $\mathcal{T}(\mathbf{M})f$ are orthonormal. Let $\mathrm{I}_{\mathbf{M}}$ fulfill the*

Strang-Fix conditions of Definition 2.22 for a regular matrix $\mathbf{M} \in \mathbb{Z}^{d\times d}$ *with* $\|\mathbf{M}\| \geq 2$, *Lebesgue index* $q = 2$, *order* $s \geq 0$, *and parameter* $a = b$. *Let in addition* $r \coloneqq \min\{s, b\}$.

Let $\varepsilon \in \mathcal{E}(\mathbb{T}^d)$ *solve the continuous formulation of the Lippmann-Schwinger equation* (LS) *given by*

$$\Big\langle \varepsilon + \Gamma^0\big(\mathcal{C} - \mathcal{C}^0\big) : \big(\varepsilon + \varepsilon^0\big), \gamma \Big\rangle_2 = 0$$

for all $\gamma \in \mathrm{Sym}_d\big(\mathcal{L}^2(\mathbb{T}^d)\big)$.

Let $\varepsilon_{\mathbf{M}} \in \mathcal{E}^f_{\mathbf{M}}(\mathbb{T}^d)$ *solve the discretized formulation of the Lippmann-Schwinger equation* (3.9) *given via*

$$\Big\langle \varepsilon_{\mathbf{M}} + \Gamma^0\, \mathrm{L}_{\mathbf{M}}\Big(\big(\mathcal{C} - \mathcal{C}^0\big) : \big(\varepsilon_{\mathbf{M}} + \varepsilon^0\big)\Big), \gamma_{\mathbf{M}} \Big\rangle_2 = 0$$

for all $\gamma_{\mathbf{M}} \in \mathrm{Sym}_d\big(\mathcal{V}^f_{\mathbf{M}}\big)$.

Then, the solution $\varepsilon_{\mathbf{M}}$ *of the discretized problem, compared to the solution* ε *of the continuous problem, behaves like*

$$\|\varepsilon - \varepsilon_{\mathbf{M}}\|_2 \leq \|\mathbf{M}\|^{-r} \kappa_{\mathbf{M}}^b \big(c_1 + c_2 \kappa_{\mathbf{M}}^b\big) \|\varepsilon^0\|_2,$$

where the constants c_1 *and* c_2 *are independent of* $\mathbf{M}$.

Proof. Consider the Lippmann-Schwinger equation (LS), which is equivalent to a variational problem of the form: find $\varepsilon \in \mathcal{E}(\mathbb{T}^d) \subset \mathrm{Sym}_d\big(\mathcal{L}^2(\mathbb{T}^d)\big)$ such that

$$B(\varepsilon, \gamma) = F(\gamma)$$

for all $\gamma \in \mathrm{Sym}_d\big(\mathcal{L}^2(\mathbb{T}^d)\big)$. The bilinear form $B : \mathrm{Sym}_d\big(\mathcal{L}^2(\mathbb{T}^d)\big) \times \mathrm{Sym}_d\big(\mathcal{L}^2(\mathbb{T}^d)\big) \to \mathbb{R}$ is given by

$$B(\varepsilon, \gamma) \coloneqq \Big\langle \varepsilon + \Gamma^0\big(\mathcal{C} - \mathcal{C}^0\big) : \varepsilon, \gamma \Big\rangle_2, \quad \varepsilon, \gamma \in \mathrm{Sym}_d\big(\mathcal{L}^2(\mathbb{T}^d)\big)$$

and the linear form $F : \mathrm{Sym}_d\big(\mathcal{L}^2(\mathbb{T}^d)\big) \to \mathbb{R}$ is defined via

$$F(\gamma) \coloneqq \Big\langle -\Gamma^0\big(\mathcal{C} - \mathcal{C}^0\big)\varepsilon^0, \gamma \Big\rangle_2, \quad \gamma \in \mathrm{Sym}_d\big(\mathcal{L}^2(\mathbb{T}^d)\big).$$

The discretized Lippmann-Schwinger equation from (3.10) can be written as follows: find a strain $\varepsilon_{\mathbf{M}} \in \mathcal{E}^f_{\mathbf{M}}(\mathbb{T}^d)$ such that

$$B_{\mathbf{M}}(\varepsilon_{\mathbf{M}}, \gamma_{\mathbf{M}}) = F_{\mathbf{M}}(\gamma_{\mathbf{M}})$$

for all $\gamma_{\mathbf{M}} \in \mathrm{Sym}_d\big(\mathcal{V}^f_{\mathbf{M}}\big)$. The discretized bilinear form $B_{\mathbf{M}} : \mathrm{Sym}_d\big(\mathcal{V}^f_{\mathbf{M}}\big) \times \mathrm{Sym}_d\big(\mathcal{V}^f_{\mathbf{M}}\big) \to \mathbb{R}$ and the linear form $F_{\mathbf{M}} : \mathrm{Sym}_d\big(\mathcal{V}^f_{\mathbf{M}}\big) \to \mathbb{R}$ are given by

$$B_{\mathbf{M}}(\varepsilon_{\mathbf{M}}, \gamma_{\mathbf{M}}) = \Big\langle \varepsilon_{\mathbf{M}} + \Gamma^0\, \mathrm{L}_{\mathbf{M}}\Big(\big(\mathcal{C} - \mathcal{C}^0\big) : \varepsilon_{\mathbf{M}}\Big), \gamma_{\mathbf{M}} \Big\rangle_2, \quad \varepsilon_{\mathbf{M}}, \gamma_{\mathbf{M}} \in \mathrm{Sym}_d\big(\mathcal{V}^f_{\mathbf{M}}\big),$$

and

$$F_{\mathbf{M}}(\gamma_{\mathbf{M}}) = \Big\langle \Gamma^0\, \mathrm{L}_{\mathbf{M}}\Big(\big(\mathcal{C} - \mathcal{C}^0\big) : \varepsilon^0\Big), \gamma_{\mathbf{M}} \Big\rangle_2, \quad \gamma_{\mathbf{M}} \in \mathrm{Sym}_d\big(\mathcal{V}^f_{\mathbf{M}}\big),$$

respectively.

Let $\mathcal{C}$ be bounded with constant $c_{\mathrm{b},\mathcal{C}}$ and elliptic with constant $c_{\mathrm{e},\mathcal{C}}$. Let further $\mathcal{C}^0$ be bounded with constant $c_{\mathrm{b},\mathcal{C}^0}$ and elliptic with constant $c_{\mathrm{e},\mathcal{C}^0}$.

By Theorem 2.38, the bilinear form B is elliptic and bounded with bound $c_{\mathrm{b},B}$, and the linear form F is bounded. By Lemma 3.9, the bilinear form $B_{\mathbf{M}}$ is bounded and uniformly elliptic with the constant of ellipticity $c_{\mathrm{e},B_{\mathbf{M}}}$, and the linear form $F_{\mathbf{M}}$ is bounded. The constants are given as

$$\begin{aligned} c_{\mathrm{b},B} &\coloneqq 1 + \frac{c_{\mathrm{b},\mathcal{C}^0}}{c_{\mathrm{e},\mathcal{C}^0}^2}(c_{\mathrm{b},\mathcal{C}} - c_{\mathrm{b},\mathcal{C}^0}), \\ c_{\mathrm{e},B_{\mathbf{M}}} &\coloneqq 1 + \frac{c_{\mathrm{e},\mathcal{C}^0}}{c_{\mathrm{b},\mathcal{C}^0}^2}(c_{\mathrm{e},\mathcal{C}} - c_{\mathrm{e},\mathcal{C}^0}). \end{aligned}$$

Further, the inclusion $\mathrm{Sym}_d\big(\mathcal{V}_{\mathbf{M}}^f\big) \subset \mathrm{Sym}_d\big(\mathcal{L}^2(\mathbb{T}^d)\big)$ holds and therefore the first Strang lemma from Lemma 2.40 is applicable. This lemma yields the estimate

$$\begin{aligned} \|\varepsilon - \varepsilon_{\mathbf{M}}\|_2 \leq& \Big(1 + \frac{c_{\mathrm{b},B}}{c_{\mathrm{e},B_{\mathbf{M}}}}\Big) \inf_{\varphi_{\mathbf{M}} \in \mathrm{Sym}_d(\mathcal{V}_{\mathbf{M}}^f)} \|\varepsilon - \varphi_{\mathbf{M}}\|_2 \\ &+ \frac{1}{c_{\mathrm{e},B_{\mathbf{M}}}} \inf_{\varphi_{\mathbf{M}} \in \mathrm{Sym}_d(\mathcal{V}_{\mathbf{M}}^f)} \sup_{\eta_{\mathbf{M}} \in \mathrm{Sym}_d(\mathcal{V}_{\mathbf{M}}^f)} \frac{|B(\varphi_{\mathbf{M}}, \eta_{\mathbf{M}}) - B_{\mathbf{M}}(\varphi_{\mathbf{M}}, \eta_{\mathbf{M}})|}{\|\eta_{\mathbf{M}}\|_2} \\ &+ \frac{1}{c_{\mathrm{e},B_{\mathbf{M}}}} \sup_{\eta_{\mathbf{M}} \in \mathrm{Sym}_d(\mathcal{V}_{\mathbf{M}}^f)} \frac{|F(\eta_{\mathbf{M}}) - F_{\mathbf{M}}(\eta_{\mathbf{M}})|}{\|\eta_{\mathbf{M}}\|_2}. \end{aligned}$$

We insert the definitions of the bilinear forms B and $B_{\mathbf{M}}$ and the linear forms F and $F_{\mathbf{M}}$ into the above estimate and apply the Cauchy-Schwarz theorem. This results in

$$\begin{aligned} \|\varepsilon - \varepsilon_{\mathbf{M}}\|_2 \leq& \Big(1 + \frac{c_{\mathrm{b},B}}{c_{\mathrm{e},B_{\mathbf{M}}}}\Big) \inf_{\varphi_{\mathbf{M}} \in \mathrm{Sym}_d(\mathcal{V}_{\mathbf{M}}^f)} \|\varepsilon - \varphi_{\mathbf{M}}\|_2 \\ &+ \frac{1}{c_{\mathrm{e},B_{\mathbf{M}}}} \inf_{\varphi_{\mathbf{M}} \in \mathrm{Sym}_d(\mathcal{V}_{\mathbf{M}}^f)} \Big\| \Gamma^0 \mathcal{C}^0 \big(\mathcal{C}^0\big)^{-1} \Big(\mathcal{C} : \varphi_{\mathbf{M}} - \mathrm{L}_{\mathbf{M}}\big(\mathcal{C} : \varphi_{\mathbf{M}}\big)\Big) \Big\|_2 \\ &+ \frac{1}{c_{\mathrm{e},B_{\mathbf{M}}}} \Big\| \Gamma^0 \mathcal{C}^0 \big(\mathcal{C}^0\big)^{-1} \Big(\mathcal{C} : \varepsilon^0 - \mathrm{L}_{\mathbf{M}}\big(\mathcal{C} : \varepsilon^0\big)\Big) \Big\|_2. \end{aligned}$$

The expressions with $\mathcal{C}^0$ vanish, because the functions $\varphi_{\mathbf{M}}$ are elements of $\mathrm{Sym}_d(\mathcal{V}_{\mathbf{M}}^f)$, the reference stiffness $\mathcal{C}^0$ is constant, and thus approximation with $\mathrm{L}_{\mathbf{M}}$ has no effect.

The infima are bounded from above by inserting approximations $\varphi_{\mathbf{M}} = \mathrm{L}_{\mathbf{M}}\,\varepsilon$ into the respective expressions. This leads to

$$\begin{aligned} \|\varepsilon - \varepsilon_{\mathbf{M}}\|_2 \leq& \Big(1 + \frac{c_{\mathrm{b},B}}{c_{\mathrm{e},B_{\mathbf{M}}}}\Big) \|\varepsilon - \mathrm{L}_{\mathbf{M}}\,\varepsilon\|_2 \\ &+ \frac{1}{c_{\mathrm{e},B_{\mathbf{M}}}} \Big\| \Gamma^0 \mathcal{C}^0 \big(\mathcal{C}^0\big)^{-1} \Big(\mathcal{C} : \mathrm{L}_{\mathbf{M}}\,\varepsilon - \mathrm{L}_{\mathbf{M}}\big(\mathcal{C} : \mathrm{L}_{\mathbf{M}}\,\varepsilon\big)\Big) \Big\|_2 \\ &+ \frac{1}{c_{\mathrm{e},B_{\mathbf{M}}}} \Big\| \Gamma^0 \mathcal{C}^0 \big(\mathcal{C}^0\big)^{-1} \Big(\mathcal{C} : \varepsilon^0 - \mathrm{L}_{\mathbf{M}}\big(\mathcal{C} : \varepsilon^0\big)\Big) \Big\|_2. \end{aligned}$$

Bounds on $\Gamma^0\mathcal{C}^0\big(\mathcal{C}^0\big)^{-1}$ established in Lemma 3.9 give

$$\begin{aligned}\|\varepsilon-\varepsilon_{\mathbf{M}}\|_2 \leq& \Big(1+\frac{c_{\mathrm{b},B}}{c_{\mathrm{e},B_{\mathbf{M}}}}\Big)\|\varepsilon-\mathrm{L}_{\mathbf{M}}\,\varepsilon\|_2\\ &+\frac{c_{\mathrm{b},\mathcal{C}^0}}{c_{\mathrm{e},\mathcal{C}^0}c_{\mathrm{e},B_{\mathbf{M}}}}\Big\|\mathcal{C}:\mathrm{L}_{\mathbf{M}}\,\varepsilon-\mathrm{L}_{\mathbf{M}}\big(\mathcal{C}:\mathrm{L}_{\mathbf{M}}\,\varepsilon\big)\Big\|_2\\ &+\frac{c_{\mathrm{b},\mathcal{C}^0}}{c_{\mathrm{e},\mathcal{C}^0}c_{\mathrm{e},B_{\mathbf{M}}}}\Big\|\mathcal{C}:\varepsilon^0-\mathrm{L}_{\mathbf{M}}\big(\mathcal{C}:\varepsilon^0\big)\Big\|_2.\end{aligned}$$

By assumption, the stiffness distribution has smoothness b with $\mathcal{C}\in\mathrm{SSym}_d\big(\mathcal{W}^{b,\infty}(\mathbb{T}^d)\big)$. By Lemma 2.39, the strain ε also has smoothness b with $\varepsilon\in\mathrm{Sym}_d\big(\mathcal{W}^{b,2}(\mathbb{T}^d)\big)$ and there exists a constant c_{smooth} such that

$$\|\varepsilon\|_{b,2}\leq c_{\mathrm{smooth}}\|C\|_{b,\infty}\|\varepsilon^0\|_2. \tag{3.22}$$

With $\mathcal{W}^{b,\infty}(\mathbb{T}^d)\subset\mathcal{W}^{b,2}(\mathbb{T}^d)$ by Lemma 2.2 e), the approximation estimate from Lemma 2.24 in the form for the Lebesgue space $\mathcal{L}^2(\mathbb{T}^d)$ in Corollary 2.25 is applicable. We denote the constant with respect to the approximation by c_{approx} and obtain the estimate

$$\begin{aligned}\|\varepsilon-\varepsilon_{\mathbf{M}}\|_2 \leq& \Big(1+\frac{c_{\mathrm{b},B}}{c_{\mathrm{e},B_{\mathbf{M}}}}\Big)c_{\mathrm{approx}}\kappa_{\mathbf{M}}^b\|M\|^{-r}\|\varepsilon\|_{b,2}\\ &+\frac{c_{\mathrm{b},\mathcal{C}^0}}{c_{\mathrm{e},\mathcal{C}^0}^2c_{\mathrm{e},B_{\mathbf{M}}}}c_{\mathrm{approx}}\kappa_{\mathbf{M}}^b\|M\|^{-r}\|\mathcal{C}:\mathrm{L}_{\mathbf{M}}\,\varepsilon\|_{b,2}\\ &+\frac{c_{\mathrm{b},\mathcal{C}^0}}{c_{\mathrm{e},\mathcal{C}^0}^2c_{\mathrm{e},B_{\mathbf{M}}}}c_{\mathrm{approx}}\kappa_{\mathbf{M}}^b\|M\|^{-r}\|\mathcal{C}:\varepsilon^0\|_{b,2}\\ \leq& \Big(1+\frac{c_{\mathrm{b},B}}{c_{\mathrm{e},B_{\mathbf{M}}}}\Big)c_{\mathrm{approx}}\kappa_{\mathbf{M}}^b\|M\|^{-r}\|\varepsilon\|_{b,2}\\ &+\frac{c_{\mathrm{b},\mathcal{C}^0}}{c_{\mathrm{e},\mathcal{C}^0}^2c_{\mathrm{e},B_{\mathbf{M}}}}c_{\mathrm{approx}}\kappa_{\mathbf{M}}^b\|M\|^{-r}c_{\mathrm{b},\mathcal{C}}\|\mathrm{L}_{\mathbf{M}}\,\varepsilon\|_{b,2}\\ &+\frac{c_{\mathrm{b},\mathcal{C}^0}}{c_{\mathrm{e},\mathcal{C}^0}^2c_{\mathrm{e},B_{\mathbf{M}}}}c_{\mathrm{approx}}\kappa_{\mathbf{M}}^b\|M\|^{-r}c_{\mathrm{b},\mathcal{C}}\|\varepsilon^0\|_{b,2},\end{aligned}$$

using the boundedness of $\mathcal{C}$. A special case of the approximation result in Corollary 2.25 is if the interpolated function is measured in the same norm as the original function, i.e. if in the corollary $a=b$. Together with the triangle inequality, a bound on the operator $\mathrm{L}_{\mathbf{M}}$ in $\mathcal{W}^{b,2}(\mathbb{T}^d)$ is given by

$$\begin{aligned}\|\mathrm{L}_{\mathbf{M}}\,\varepsilon\|_{b,2}&\leq\|\mathrm{L}_{\mathbf{M}}\,\varepsilon-\varepsilon\|_{b,2}+\|\varepsilon\|_{b,2}\\ &\leq\tilde{c}_{\mathrm{approx}}\kappa_{\mathbf{M}}^b\|M\|^{b-b}\|\varepsilon\|_{b,2}+\|\varepsilon\|_{b,2}\\ &\leq\big(1+\tilde{c}_{\mathrm{approx}}\kappa_{\mathbf{M}}^b\big)\|\varepsilon\|_{b,2}.\end{aligned}$$

Here, $\tilde{c}_{\mathrm{approx}}$ is the constant from Corollary 2.25, depending on the smoothness b of ε and the smoothness of the space in which we are measuring the error, which is also

b. Thus, $\tilde{c}_{\text{approx}}$ differs from c_{approx}. Further, considering ε^0 as a constant function, $\|\varepsilon^0\|_{b,2} = \|\varepsilon^0\|_2$.

Then, the error $\|\varepsilon - \varepsilon_{\mathbf{M}}\|_2$ is bounded, using Equation (3.22) and Remark 2.23, by

$$\begin{aligned}\|\varepsilon - \varepsilon_{\mathbf{M}}\|_2 \leq &\Big(1 + \frac{c_{\mathrm{b},B}}{c_{\mathrm{e},B_{\mathbf{M}}}}\Big) c_{\text{approx}} \kappa_{\mathbf{M}}^b \|M\|^{-r} c_{\text{smooth}} \|C\|_{b,\infty} \|\varepsilon^0\|_2 \\ &+ \frac{c_{\mathrm{b},\mathcal{C}^0}}{c_{\mathrm{e},\mathcal{C}^0}^2 c_{\mathrm{e},B_{\mathbf{M}}}} c_{\text{approx}} \kappa_{\mathbf{M}}^b \|M\|^{-r} c_{\mathrm{b},\mathcal{C}} \big(1 + \tilde{c}_{\text{approx}} \kappa_{\mathbf{M}}^b\big) c_{\text{smooth}} \|C\|_{b,\infty} \|\varepsilon^0\|_2 \\ &+ \frac{c_{\mathrm{b},\mathcal{C}^0}}{c_{\mathrm{e},\mathcal{C}^0}^2 c_{\mathrm{e},B_{\mathbf{M}}}} c_{\text{approx}} \kappa_{\mathbf{M}}^b \|M\|^{-r} c_{\mathrm{b},\mathcal{C}} \|\varepsilon^0\|_2.\end{aligned}$$

The constants c_{approx} and $\tilde{c}_{\text{approx}}$ are independent of $\mathbf{M}$ by Lemma 2.26. The constant c_{smooth} is also independent of $\mathbf{M}$ by definition.

We collect the parts independent of $\mathbf{M}$ and ε^0 in

$$\begin{aligned}c_1 &:= c_{\text{approx}} \Bigg(\Big(1 + \frac{c_{\mathrm{b},B}}{c_{\mathrm{e},B_{\mathbf{M}}}}\Big) c_{\text{smooth}} \|\mathcal{C}\|_{b,\infty} + \\ &\qquad \frac{c_{\mathrm{b},\mathcal{C}^0}}{c_{\mathrm{e},\mathcal{C}^0}^2 c_{\mathrm{e},B_{\mathbf{M}}}} c_{\text{smooth}} c_{\mathrm{b},\mathcal{C}} \|\mathcal{C}\|_{b,\infty} + \frac{c_{\mathrm{b},\mathcal{C}^0}}{c_{\mathrm{e},\mathcal{C}^0}^2 c_{\mathrm{e},B_{\mathbf{M}}}} c_{\mathrm{b},\mathcal{C}} \Bigg), \\ c_2 &:= c_{\text{approx}} \frac{c_{\mathrm{b},\mathcal{C}^0}}{c_{\mathrm{e},\mathcal{C}^0}^2 c_{\mathrm{e},B_{\mathbf{M}}}} c_{\mathrm{b},\mathcal{C}} \tilde{c}_{\text{approx}} c_{\text{smooth}} \|\mathcal{C}\|_{b,\infty}.\end{aligned}$$

This yields

$$\|\varepsilon - \varepsilon_{\mathbf{M}}\|_2 \leq \|\mathbf{M}\|^{-r} \kappa_{\mathbf{M}}^b \big(c_1 + c_2 \kappa_{\mathbf{M}}^b\big) \|\varepsilon^0\|_2$$

and completes the proof. □

In the following, we state the respective convergence result for the variational equation. It uses the same technical assumptions as the result for the Lippmann-Schwinger equation and results in an estimate with the same order of convergence, yet slightly different expressions for the constants. We give here only an outline of the proof and state the differences to the proof of Theorem 3.10.

Theorem 3.11. *Let $\mathcal{C} \in \mathrm{SSym}_d\big(\mathcal{W}^{b,\infty}(\mathbb{T}^d)\big) \cap \mathrm{SSym}_d\big(\mathcal{A}(\mathbb{T}^d)\big)$ for $b \in \mathbb{N}$ with $b > \frac{d}{2}$, let $\mathcal{C}^0 \in \mathrm{SSym}_d\big(\mathbb{R}\big)$ such that the conditions on boundedness and ellipticity in Lemma 3.9 are fulfilled. Further, let $\mathcal{V}_{\mathbf{M}}^f$ be a space of translates of the function f, where $f = \mathrm{I}_{\mathbf{M}}$ is a fundamental interpolant where the translates $\mathcal{T}(\mathbf{M})f$ are orthonormal. Let $\mathrm{I}_{\mathbf{M}}$ fulfill the Strang-Fix conditions of Definition 2.22 for a regular matrix $\mathbf{M} \in \mathbb{Z}^{d\times d}$ with $\|\mathbf{M}\| \geq 2$, Lebesgue index $q = 2$, order $s \geq 0$, and parameter $a = b$. Let in addition $r \coloneqq \min\{s, b\}$.*

Let $\varepsilon \in \mathcal{E}(\mathbb{T}^d)$ solve the continuous formulation of the variational equation (VE) *given by*

$$\Big\langle \mathcal{C}^0\Gamma^0\mathcal{C} : \big(\varepsilon + \varepsilon^0\big), \gamma \Big\rangle_2 = 0$$

for all $\gamma \in \mathrm{Sym}_d\big(\mathcal{L}^2(\mathbb{T}^d)\big)$.

Let $\varepsilon_{\mathbf{M}} \in \mathcal{E}_{\mathbf{M}}^f(\mathbb{T}^d)$ solve the discretized formulation of the variational equation (3.15) *given via*

$$\Big\langle \mathcal{C}^0\Gamma^0\,\mathrm{L}_{\mathbf{M}}\Big(\mathcal{C} : \big(\varepsilon_{\mathbf{M}} + \varepsilon^0\big)\Big), \gamma_{\mathbf{M}} \Big\rangle_2 = 0$$

for all $\gamma_{\mathbf{M}} \in \mathrm{Sym}_d\big(\mathcal{V}_{\mathbf{M}}^f\big)$.

Then, the solution $\varepsilon_{\mathbf{M}}$ of the discretized problem, compared to the solution ε of the continuous problem, behaves like

$$\|\varepsilon - \varepsilon_{\mathbf{M}}\|_2 \leq \|\mathbf{M}\|^{-r}\kappa_{\mathbf{M}}^b\big(c_1 + c_2\kappa_{\mathbf{M}}^b\big)\|\varepsilon^0\|_2,$$

where the constants c_1 and c_2 are independent of $\mathbf{M}$.

Proof. With the same reasoning as in Lemma 3.9, the bilinear forms and linear forms for the variational equation are bounded and elliptic. The functions are given via

$$\begin{aligned}
B(\varepsilon,\gamma) &\coloneqq \Big\langle \mathcal{C}^0\Gamma^0\mathcal{C} : \varepsilon, \gamma \Big\rangle_2, && \varepsilon,\gamma \in \mathrm{Sym}_d\big(\mathcal{L}^2(\mathbb{T}^d)\big),\\
F(\gamma) &\coloneqq \Big\langle -\mathcal{C}^0\Gamma^0\mathcal{C} : \varepsilon^0, \gamma \Big\rangle_2, && \gamma \in \mathrm{Sym}_d\big(\mathcal{L}^2(\mathbb{T}^d)\big),\\
B_{\mathbf{M}}(\varepsilon_{\mathbf{M}},\gamma_{\mathbf{M}}) &\coloneqq \Big\langle \mathcal{C}^0\Gamma^0\,\mathrm{L}_{\mathbf{M}}\big(\mathcal{C} : \varepsilon_{\mathbf{M}}\big), \gamma_{\mathbf{M}} \Big\rangle_2, && \varepsilon_{\mathbf{M}},\gamma_{\mathbf{M}} \in \mathrm{Sym}_d\big(\mathcal{V}_{\mathbf{M}}^f\big),\\
F_{\mathbf{M}}(\gamma_{\mathbf{M}}) &\coloneqq \Big\langle \mathcal{C}^0\Gamma^0\,\mathrm{L}_{\mathbf{M}}\big(\mathcal{C} : \varepsilon^0\big), \gamma_{\mathbf{M}} \Big\rangle_2, && \gamma_{\mathbf{M}} \in \mathrm{Sym}_d\big(\mathcal{V}_{\mathbf{M}}^f\big).
\end{aligned}$$

The upper and lower bounds are then given by

$$\begin{aligned}
|B(\varepsilon,\gamma)| &\leq \frac{c_{\mathrm{b},\mathcal{C}^0}\,c_{\mathrm{b},\mathcal{C}}}{c_{\mathrm{e},\mathcal{C}^0}}\|\varepsilon\|_2\|\gamma\|_2, && \varepsilon,\gamma \in \mathrm{Sym}_d\big(\mathcal{L}^2(\mathbb{T}^d)\big),\\
|B(\gamma,\gamma)| &\geq \frac{c_{\mathrm{e},\mathcal{C}^0}\,c_{\mathrm{e},\mathcal{C}}}{c_{\mathrm{b},\mathcal{C}^0}}\|\gamma\|_2^2, && \gamma \in \mathrm{Sym}_d\big(\mathcal{L}^2(\mathbb{T}^d)\big),\\
|F(\gamma)| &\leq \frac{c_{\mathrm{b},\mathcal{C}^0}\,c_{\mathrm{b},\mathcal{C}}}{c_{\mathrm{e},\mathcal{C}^0}}\|\varepsilon^0\|_2\|\gamma\|_2, && \gamma \in \mathrm{Sym}_d\big(\mathcal{L}^2(\mathbb{T}^d)\big).
\end{aligned}$$

The same bounds with the same constants also hold for the discrete bilinear and linear forms $B_{\mathbf{M}}$ and $F_{\mathbf{M}}$. We further define the constants

$$c_{\mathrm{b},B} \coloneqq \frac{c_{\mathrm{b},\mathcal{C}^0} c_{\mathrm{b},\mathcal{C}}}{c_{\mathrm{e},\mathcal{C}^0}},$$
$$c_{\mathrm{e},B_{\mathbf{M}}} \coloneqq \frac{c_{\mathrm{e},\mathcal{C}^0} c_{\mathrm{e},\mathcal{C}}}{c_{\mathrm{b},\mathcal{C}^0}}.$$

The above bounds make the first Strang lemma in Lemma 2.40 applicable and similarly to the proof of Theorem 3.10 this gives after we insert $\mathrm{L}_{\mathbf{M}}\,\varepsilon$ the estimate

$$\begin{aligned}\|\varepsilon - \varepsilon_{\mathbf{M}}\|_2 \leq &\Big(1 + \frac{c_{\mathrm{b},B}}{c_{\mathrm{e},B_{\mathbf{M}}}}\Big)\|\varepsilon - \mathrm{L}_{\mathbf{M}}\,\varepsilon\|_2 \\ &+ \frac{1}{c_{\mathrm{e},B_{\mathbf{M}}}}\Big\|\mathcal{C}^0\Gamma^0\Big(\mathcal{C} : \mathrm{L}_{\mathbf{M}}\,\varepsilon - \mathrm{L}_{\mathbf{M}}\big(\mathcal{C} : \mathrm{L}_{\mathbf{M}}\,\varepsilon\big)\Big)\Big\|_2 \\ &+ \frac{1}{c_{\mathrm{e},B_{\mathbf{M}}}}\Big\|\mathcal{C}^0\Gamma^0\Big(\mathcal{C} : \varepsilon^0 - \mathrm{L}_{\mathbf{M}}\big(\mathcal{C} : \varepsilon^0\big)\Big)\Big\|_2.\end{aligned}$$

We apply the above bounds on the operators and get

$$\begin{aligned}\|\varepsilon - \varepsilon_{\mathbf{M}}\|_2 \leq &\Big(1 + \frac{c_{\mathrm{b},B}}{c_{\mathrm{e},B_{\mathbf{M}}}}\Big)\|\varepsilon - \mathrm{L}_{\mathbf{M}}\,\varepsilon\|_2 \\ &+ \frac{c_{\mathrm{b},\mathcal{C}^0}}{c_{\mathrm{e},\mathcal{C}^0}^2 c_{\mathrm{e},B_{\mathbf{M}}}}\Big\|\mathcal{C} : \mathrm{L}_{\mathbf{M}}\,\varepsilon - \mathrm{L}_{\mathbf{M}}\big(\mathcal{C} : \mathrm{L}_{\mathbf{M}}\,\varepsilon\big)\Big\|_2 \\ &+ \frac{c_{\mathrm{b},\mathcal{C}^0}}{c_{\mathrm{e},\mathcal{C}^0}^2 c_{\mathrm{e},B_{\mathbf{M}}}}\Big\|\mathcal{C} : \varepsilon^0 - \mathrm{L}_{\mathbf{M}}\big(\mathcal{C} : \varepsilon^0\big)\Big\|_2.\end{aligned}$$

The remainder of the proof is identical to the proof of Theorem 3.10 and is thus omitted. □

The convergence estimates in this section show that the smoothness of the coefficients and the regularity of the functions in the space of translates carry over to the order of convergence of the discretizations. Further, the regularities of the solution and the ansatz space have to "fit together", i.e. increasing the regularity in one does not yield any gain on the quality of the approximation without also increasing the other.

3.5 Numerical solution algorithms

In [74], the authors solve the Lippmann-Schwinger equation (3.10) in case of $d = 3$ and a diagonal pattern matrix $\mathbf{M}$ using the Dirichlet kernel $f_{\mathrm{D}_{\mathbf{M}}}$ by means of a fixed-point iteration. This is equivalent to solving an according Neumann series. We transfer this approach to solve the Lippmann-Schwinger equation to the setting of Equation (3.10) with anisotropic spaces of translates in arbitrary dimensions.

A second possibility to solve the quasi-static equation of linear elasticity in homogenization is to solve the variational equation (3.16) using a Krylov subspace method like

the conjugate gradient method. The convergence proof for this solver goes back to [112] and is generalized to anisotropic patterns with translation invariant spaces generated by the Dirichlet kernel in the second part of this section.

A solution using a Neumann-Series approach has the advantage of a small memory footprint: it iterates purely on the discretized strain $\varepsilon_{\mathbf{M}}$, requiring no additional variables to be stored. The disadvantage of the fixed-point iteration method is its linear convergence. In contrast, the conjugate gradients method converges quadratically, however, it internally stores three times as much data as the Neumann-Series approach. Especially with very large numbers of data points, like obtained from computer tomography images, this is an issue.

Solution by a fixed-point iteration

The Lippmann-Schwinger equation can be solved by a fixed-point iteration on the coefficients $\mathbf{E}_{\mathbf{y}}$ with $\mathbf{y} \in \mathcal{P}(\mathbf{M})$ of the discretized Lippmann-Schwinger equation (3.10), see [74] for tensor product grids. This is equivalent to solving the equation using a Neumann series approach. This section first shows that the appropriate operator is invertible and then lists the iterative algorithm and states convergence criteria.

Consider the Lippmann-Schwinger equation (3.9)

$$\left\langle \varepsilon_{\mathbf{M}} + \Gamma^0 \mathrm{L}_{\mathbf{M}}\Big(\big(\mathcal{C} - \mathcal{C}^0\big) : \big(\varepsilon_{\mathbf{M}} + \varepsilon^0\big)\Big), \gamma \right\rangle_2 = 0, \quad \gamma \in \mathrm{Sym}_d\big(\mathcal{V}_{\mathbf{M}}^f\big),$$

and define a new discretized strain $\tilde{\varepsilon}_{\mathbf{M}} \coloneqq \varepsilon_{\mathbf{M}} + \varepsilon^0$. Then, the Lippmann-Schwinger equation can be rearranged to read

$$\left\langle \tilde{\varepsilon}_{\mathbf{M}} + \Gamma^0 \mathrm{L}_{\mathbf{M}}\Big(\big(\mathcal{C} - \mathcal{C}^0\big) : \tilde{\varepsilon}_{\mathbf{M}}\Big), \gamma \right\rangle_2 = \big\langle \varepsilon^0, \gamma \big\rangle_2, \quad \gamma \in \mathrm{Sym}_d\big(\mathcal{V}_{\mathbf{M}}^f\big).$$

In terms of linear operators, this is equal to

$$\Big\langle \big(\mathrm{Id} - \mathcal{Q}\big) : \tilde{\varepsilon}_{\mathbf{M}}, \gamma \Big\rangle_2 = \big\langle \varepsilon^0, \gamma \big\rangle_2, \quad \gamma \in \mathrm{Sym}_d\big(\mathcal{V}_{\mathbf{M}}^f\big)$$

with

$$\mathcal{Q} : \tilde{\varepsilon}_{\mathbf{M}} \coloneqq -\Gamma^0 \mathrm{L}_{\mathbf{M}}\Big(\big(\mathcal{C} - \mathcal{C}^0\big) : \tilde{\varepsilon}_{\mathbf{M}}\Big).$$

For the operator $\mathrm{Id} - \mathcal{Q}$ to be invertible, $\|\mathcal{Q}\| < 1$ has to hold in operator norm, for which the conditions are shown in the following. For the continuous case, see a similar proof in [69, Section 14.6].

Theorem 3.12. *Let the translates of the fundamental interpolant $\mathrm{I}_{\mathbf{M}}$ be orthonormal, and let $\mathcal{C}^0 \in \mathrm{SSym}_d\big(\mathbb{R}\big)$ be a constant reference stiffness constant. Let $\mathcal{C}^0$ be elliptic with constant $c_{e,\mathcal{C}^0}$ and bounded with constant $c_{b,\mathcal{C}^0}$. Let further the stiffness distribution $\mathcal{C}$ be elliptic and bounded with constants $c_{b,\mathcal{C}}$ and $c_{e,\mathcal{C}}$, respectively.*

Then, the operator

$$\mathcal{Q} : \tilde{\varepsilon}_{\mathbf{M}} \coloneqq -\Gamma^0 \mathrm{L}_{\mathbf{M}}\Big(\big(\mathcal{C} - \mathcal{C}^0\big) : \tilde{\varepsilon}_{\mathbf{M}}\Big), \quad \tilde{\varepsilon}_{\mathbf{M}} \in \mathrm{Sym}_d\big(\mathcal{V}_{\mathbf{M}}^f\big)$$

fulfills $\|\mathcal{Q}\|_2 < 1$ *if* $c_{e,\mathcal{C}^0} > \frac{c_{b,\mathcal{C}}}{2}$. *If, in addition,* $c_{e,\mathcal{C}^0} = c_{b,\mathcal{C}^0} = \frac{c_{e,\mathcal{C}}+c_{b,\mathcal{C}}}{2}$, *then the norm* $\|\mathcal{Q}\|_2$ *is minimal.*

Proof. First, observe that the operator $\mathcal{C}^0$ is constant and that the interpolation operator $\mathrm{L}_\mathbf{M}$ acts componentwise and is linear. Therefore, $\mathcal{C}^0$ and $\mathrm{L}_\mathbf{M}$ commute. This equates the expressions

$$\mathcal{Q} = -\Gamma^0 \mathrm{L}_\mathbf{M}(\mathcal{C} - \mathcal{C}^0) = \Gamma^0\mathcal{C}^0 \mathrm{L}_\mathbf{M}\Big(\mathrm{Id} - \big(\mathcal{C}^0\big)^{-1}\mathcal{C}\Big).$$

The operator $\Gamma^0\mathcal{C}^0$ is a projection operator, see Lemma 2.32 c), and by [89, Lemma 3.2] even an orthogonal one, implying that $\left\|\Gamma^0\mathcal{C}^0\right\|_2 = 1$. Further, the interpolation operator $\mathrm{L}_\mathbf{M}$ is also an orthogonal projection, provided the translates of the fundamental interpolant $\mathrm{I}_\mathbf{M}$ are orthonormal, which we assume here. Therefore, $\left\|\mathrm{L}_\mathbf{M}\right\|_2 = 1$ holds.

This leads together with the submultiplicativity of the norm to

$$\|\mathcal{Q}\|_2 = \left\|\Gamma^0\mathcal{C}^0 \mathrm{L}_\mathbf{M}\Big(\mathrm{Id} - \big(\mathcal{C}^0\big)^{-1}\mathcal{C}\Big)\right\|_2 \leq \left\|\mathrm{Id} - \big(\mathcal{C}^0\big)^{-1}\mathcal{C}\right\|_2.$$

By [109, Section VII.3], the operators $\mathcal{C}$, $\mathcal{C}^0$, and $\big(\mathcal{C}^0\big)^{-1}$ are self-adjoint. Further, for a bounded self-adjoint operator $\mathcal{O}$, its norm is written as

$$\|\mathcal{O}\|_2 = \sup_{\|\mathbf{x}\|\leq 1} \big|\langle \mathcal{O}\mathbf{x}, \mathbf{x}\rangle_2\big|.$$

For the operator $\mathrm{Id} - \big(\mathcal{C}^0\big)^{-1}\mathcal{C}$ this amounts to checking its eigenvalues with

$$\left\|\mathrm{Id} - \big(\mathcal{C}^0\big)^{-1}\mathcal{C}\right\| = \max\Big\{|l| : l \text{ is an eigenvalue of } \mathrm{Id} - \big(\mathcal{C}^0\big)^{-1}\mathcal{C}\Big\}.$$

Considering the upper and lower bounds of $\mathcal{C}^0$ and $\mathcal{C}$, this expression can be bounded from above by

$$\left\|\mathrm{Id} - \big(\mathcal{C}^0\big)^{-1}\mathcal{C}\right\| \leq \max\left\{\left|\frac{c_{\mathrm{b},\mathcal{C}}}{c_{\mathrm{b},\mathcal{C}^0}} - 1\right|, \left|\frac{c_{\mathrm{e},\mathcal{C}}}{c_{\mathrm{e},\mathcal{C}^0}} - 1\right|, \left|\frac{c_{\mathrm{b},\mathcal{C}}}{c_{\mathrm{e},\mathcal{C}^0}} - 1\right|, \left|\frac{c_{\mathrm{e},\mathcal{C}}}{c_{\mathrm{b},\mathcal{C}^0}} - 1\right|\right\}.$$

For $\left\|\mathrm{Id} - \big(\mathcal{C}^0\big)^{-1}\mathcal{C}\right\| < 1$ to hold, and considering $c_{\mathrm{e},\mathcal{C}^0} \leq c_{\mathrm{b},\mathcal{C}^0}$ and $c_{\mathrm{e},\mathcal{C}} \leq c_{\mathrm{b},\mathcal{C}}$, the condition $2c_{\mathrm{e},\mathcal{C}^0} < c_{\mathrm{b},\mathcal{C}}$ has to be fulfilled and thus the first part of the theorem is proven.

For the second part, [69, Section 14.6] shows that the estimate above is minimized by $c_{\mathrm{e},\mathcal{C}^0} = c_{\mathrm{b},\mathcal{C}^0} = \frac{c_{\mathrm{e},\mathcal{C}}+c_{\mathrm{b},\mathcal{C}}}{2}$, resulting in an upper bound

$$\left\|\mathrm{Id} - \big(\mathcal{C}^0\big)^{-1}\mathcal{C}\right\| \leq \left(\frac{c_{\mathrm{b},\mathcal{C}}}{c_{\mathrm{e},\mathcal{C}}} - 1\right)\left(\frac{c_{\mathrm{b},\mathcal{C}}}{c_{\mathrm{e},\mathcal{C}}} + 1\right) < 1 \tag{3.23}$$

and the proof is finished. □

With the convergence proof at hand, the algorithm solving the Lippmann-Schwinger equation via a fixed-point iteration is described in Algorithm 1. This algorithm is also called basic-scheme. It starts in space domain and applies the term $\mathcal{C}_\mathbf{y} - \mathcal{C}^0$ as a pointwise

operation on the coefficients $\mathbf{E}_\mathbf{y}$. Then, it switches to frequency domain by means of the discrete Fourier transform. There, the operator Γ^p is a multiplicative operator and can be applied pointwise. After setting the average of the function, a switch back to the space domain completes an iteration. Therefore, the algorithm is dominated by the discrete Fourier transformation, which amounts to $\mathcal{O}(m \log m)$ computations with $m = |\det(\mathbf{M})|$. The operators $\mathcal{C} - \mathcal{C}^0$ and Γ^p can be applied with $\mathcal{O}(m)$ operations and do not contribute to the asymptotic complexity of the basic-scheme.

An optimal choice of the reference stiffness $\mathcal{C}^0$ according to Theorem 3.12 guarantees a convergence rate given by

$$\left\| \left(\mathbf{E}_\mathbf{y}^{(n+1)} - \mathbf{E}_\mathbf{y}^{(n)} \right)_{\mathbf{y} \in \mathcal{P}(\mathbf{M})} \right\|_2 \leq c^{n+1} \|\varepsilon^0\|_2,$$

where c is the upper bound from Equation (3.23). It follows that a Cauchy criterion is a sensible choice to detect convergence and is therefore used in this thesis.

The stopping criterion suggested in [73, 74] is based on the residuum

$$\left\| {\nabla_\mathrm{Sym}}^\mathrm{T} \mathcal{C} : \varepsilon^{(n+1)} \right\|_2.$$

In contrast to the Cauchy criterion, a simplified stopping criterion is suggested in [42]. Instead of having to keep the strain $\mathbf{E}_\mathbf{y}^{(n)}$ in memory, the authors use the expression

$$\frac{\left| \left\| \left(\mathbf{E}_\mathbf{y}^{(n+1)} \right)_{\mathbf{y} \in \mathcal{P}(\mathbf{M})} \right\|_2^2 - \left\| \left(\mathbf{E}_\mathbf{y}^{(n)} \right)_{\mathbf{y} \in \mathcal{P}(\mathbf{M})} \right\|_2^2 \right|^{\frac{1}{2}}}{\|\varepsilon^0\|} \tag{3.24}$$

for testing convergence. Convergence with regards to the criterion (3.24), however, does not imply convergence of the Cauchy sequence. This can be immediately seen by the reverse triangle inequality which gives

$$\frac{\left| \left\| \left(\mathbf{E}_\mathbf{y}^{(n+1)} \right)_{\mathbf{y} \in \mathcal{P}(\mathbf{M})} \right\|_2^2 - \left\| \left(\mathbf{E}_\mathbf{y}^{(n)} \right)_{\mathbf{y} \in \mathcal{P}(\mathbf{M})} \right\|_2^2 \right|^{\frac{1}{2}}}{\|\varepsilon^0\|} \leq \left\| \left(\mathbf{E}_\mathbf{y}^{(n+1)} - \mathbf{E}_\mathbf{y}^{(n)} \right)_{\mathbf{y} \in \mathcal{P}(\mathbf{M})} \right\|_2.$$

Solution by the conjugate gradients method

The solution of the variational formulation via the conjugate gradient method for truncated trigonometric polynomials was first investigated numerically in [112] and then theoretically in [105]. It is not immediately clear, however, that the resulting linear system fulfills the assumptions for the conjugate gradient method to converge, i.e. that the system matrix is symmetric and positive definite. The convergence is proven by using that the operator $\Gamma^0 \mathcal{C}^0$ is a projection operator, thus generating a suitable Krylov subspace [87, Section 6.7]. This projection property is the reason, why the conjugate gradient method is not applicable to general spaces of translates. There, the operator $\Gamma^\mathrm{p} \mathcal{C}^0$ is in general not a projection operator and thus the proof of [105] fails in these cases.

Algorithm 1 Fixed-point algorithm on patterns.

$\mathbf{E}_{\mathbf{y}}^{(0)} \leftarrow \epsilon^0, \quad \mathbf{y} \in \mathcal{P}(\mathbf{M})$
$n \leftarrow 0$
repeat
  $\mathbf{E}_{\mathbf{y}}^{(n+1)} \leftarrow \left(\mathcal{C}(\mathbf{y}) - \mathcal{C}^0\right) : \mathbf{E}_{\mathbf{y}}^{(n)}, \quad \mathbf{y} \in \mathcal{P}(\mathbf{M})$
  $\left(\hat{\mathbf{E}}_{\mathbf{h}}^{(n+1)}\right)_{\mathbf{h}\in\mathcal{G}(\mathbf{M}^{\mathrm{T}})} \leftarrow \mathcal{F}(\mathbf{M})\left(\mathbf{E}_{\mathbf{y}}^{(n+1)}\right)_{\mathbf{y}\in\mathcal{P}(\mathbf{M})}$
  $\hat{\mathbf{E}}_{\mathbf{h}}^{(n+1)} \leftarrow \hat{\Gamma}_{\mathbf{h}}^{\mathrm{p}} \hat{\mathbf{E}}_{\mathbf{h}}^{(n+1)}, \quad \mathbf{h} \in \mathcal{G}(\mathbf{M}^{\mathrm{T}})$
  $\hat{\mathbf{E}}_{\mathbf{0}}^{(n+1)} \leftarrow \varepsilon^0$
  $\left(\mathbf{E}_{\mathbf{y}}^{(n+1)}\right)_{\mathbf{y}\in\mathcal{P}(\mathbf{M})} \leftarrow \mathcal{F}(\mathbf{M})^{-1}\left(\hat{\mathbf{E}}_{\mathbf{h}}^{(n+1)}\right)_{\mathbf{h}\in\mathcal{G}(\mathbf{M}^{\mathrm{T}})}$
  $n \leftarrow n + 1$
until a convergence criterion is reached

Theorem 3.13. *Let $\mathcal{V}_{\mathbf{M}}^{f} = \mathcal{V}_{\mathbf{M}}^{f_{\mathrm{D}_{\mathbf{M}}}}$ be the space generated by translates of the Dirichlet kernel $f_{\mathrm{D}_{\mathbf{M}}}$. Then the variational equation* (3.16) *can be solved by the conjugate gradient method for any initial solution $\mathbf{E}_{\mathbf{y}}^{(0)} \in \mathrm{Sym}_d(\mathbb{R})$ with $\mathbf{y} \in \mathcal{P}(\mathbf{M})$.*

Proof. The proof in case of a diagonal matrix $\mathbf{M}$ can be found in [105, Lemma 13] and can be applied directly to the anisotropic pattern case. □

The iterative algorithm known as the basic-scheme which is introduced in [74] is applicable to the discretizations introduced in the chapter, as well. The optimal choice for the reference stiffness $\mathcal{C}^0$ is the same for all admissible spaces of translates $\mathcal{V}_{\mathbf{M}}^{f}$, i.e. where the translates of the fundamental interpolant are orthonormal. A solution by the conjugate gradient method introduced for this kind of equation in [112] is not feasible for spaces which are not generated by the Dirichlet kernel $f_{\mathrm{D}_{\mathbf{M}}}$. There, the Krylov space cannot be generated by the Green operator $\Gamma^{\mathrm{p}}\mathcal{C}^0$ for it is not a projection operator.

4 Numerics

In this chapter we study the influence of the pattern and the space of translates separately on example geometries. We verify the convergence theory and introduce composite voxels and their effect on high-resolution voxel images.

The geometries we use are described in the first section of this chapter. They consist each of two structures in two and in three dimensions. Section 4.2 introduces the implementations used to compute the numerical results, followed by a study of the influence of the pattern matrix for the Dirichlet kernel in Section 4.3. Then, we compute the equations of elasticity using different ansatz functions for the space of translates. We validate the convergence theory on the spline geometry. Finally, the composite voxel technique is introduced and demonstrated on the polycrystalline geometry.

The contents of Sections 4.3 and 4.4 are based on [6] and [8], respectively. The contents of Sections 4.6 and 4.7 are based on [46].

4.1 Example problem geometries

The example geometries we use in this thesis consist of two- and three-dimensional structures. The two-dimensional structures are the generalized Hashin structure, where the strain ε and the effective stiffness matrix $\mathcal{C}^{\text{eff}}$ can be expressed analytically. We use

analytic descriptions to study effects in the strain field and errors in the effective stiffness. The spline geometry — also a two-dimensional example — has coefficients with a defined smoothness and is suited best for the verification of the convergence analysis.

The three-dimensional geometries consist of a single fiber geometry and a polycrystalline structure. We use the single fiber geometry with its dominant fiber direction to determine the effects of different patterns. The polycrystalline structure has many material interfaces where the anisotropic materials differ only in orientation. We use the geometry to demonstrate the composite voxel technique.

The generalized Hashin structure

The generalized Hashin structure is based on the idea to construct an inclusion embedded in a matrix material that behaves neutrally with respect to a specific macroscopic strain [39]. Such an inclusion does not disturb the surrounding stress field. In its simpler form, such a structure that behaves neutrally is given by a circular core surrounded by a concentric ring embedded in a surrounding matrix material. All stiffnesses are isotropic, see [69, Section 7] and [46, Section 4.1].

In this section, we detail a more general structure exhibiting an anisotropic behavior. It is built from an ellipsoid with a confocal ellipsoidal coating embedded in a matrix material. The ellipsoid can be oriented in arbitrary directions, thus allowing studies depending on the principal directions of the pattern [6]. The structure aligned with the coordinate axes is described in [69, Section 7.7 ff] and the rotation can be achieved by an application of [69, Section 8.3]. In this form, the generalized Hashin structure is also explained in [6, Section 4.2]. Given a specific macroscopic strain ε^0, the strain field ε and the average stress $\mathcal{C}^{\text{eff}}\varepsilon^0$ are known and described in the following. In Figure 4.1, a schematic of the generalized Hashin structure is shown.

Consider confocal ellipsoidal coordinates which are given for $\mathbf{x} = (x_1, x_2, x_3)^{\mathrm{T}} \in \mathbb{R}^d$ by

$$\sum_{i=1}^{3} \frac{x_i^2}{c_i^2 + a} = 1. \tag{4.1}$$

The constants $c_1, c_2, c_3 \in \mathbb{R}$ with $0 \leq c_1 \leq c_2 \leq c_3 \leq \infty$ determine the relative lengths of the semi-axes of the ellipsoid whose shortest semi-axis $l_1(a)$ is aligned with the x_1-axis. The number $a \in \mathbb{R}$ with $a \geq -c_1^2$ is the generalized radius of the ellipsoid and the above equation ensures confocality of the ellipsoids for all a. The lengths of the semi-axes are then given by $l_i(a) \coloneqq \sqrt{c_i^2 + a}$ for $i = 1, 2, 3$. Given a point on the ellipsoid, the according ellipsoidal radius a is uniquely determined by the largest solution of (4.1) and $a \geq -c_1^2$ follows. In this thesis, we only consider the special case of an elliptic cylinder with $c_3 = \infty$. The so-called depolarization factors are given by

$$\begin{aligned} d_1(a) &\coloneqq \big(l_1(a) + l_2(a)\big)^{-1} l_2(a) \\ d_2(a) &\coloneqq \big(l_1(a) + l_2(a)\big)^{-1} l_1(a) \\ d_3(a) &\coloneqq 0 \end{aligned}$$

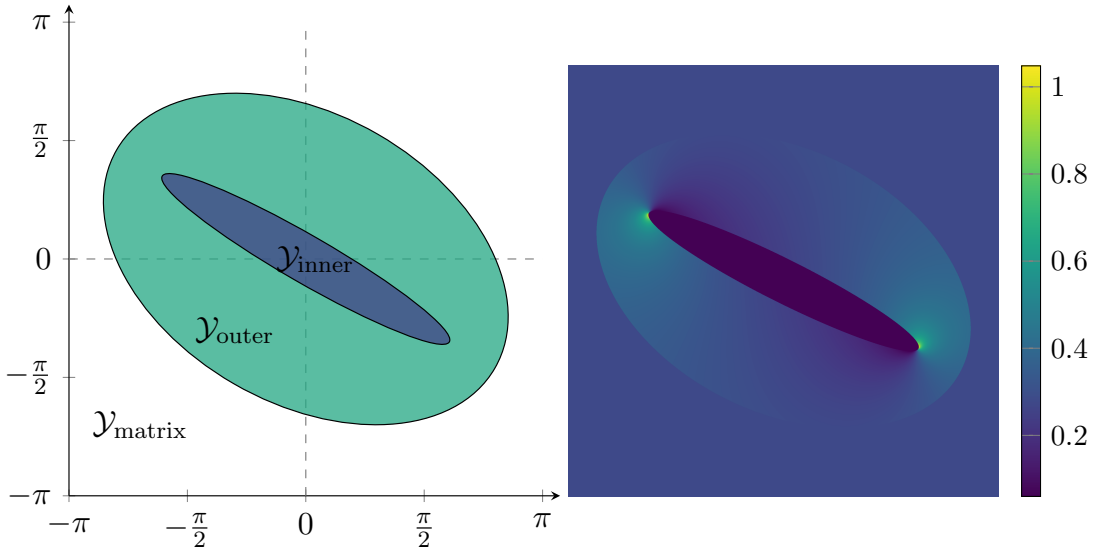

Figure 4.1. A schematic of the generalized Hashin structure (left) and the analytic solution for 11-component of the strain ε (right).

and are collected in a matrix

$$\mathbf{D}(a) \coloneqq \operatorname{diag}\big(d_i(a)\big)_{i=1,2,3}.$$

Choose radii a_{inner} for the inner ellipsoid and a_{outer} for the outer one. The resulting ellipsoids have to be completely contained in the unit cube $[-\pi,\pi)^3$ which is guaranteed by the choice $-c_1 < a_{\text{inner}} < a_{\text{outer}}$ with $l_2(a_{\text{outer}}) < \pi$. The direction the ellipsoid faces is parametrized by a normalized vector $\mathbf{n} = (n_1, n_2, n_3)^{\mathrm{T}} \in \mathbb{R}^3$ with $\|n\| = 1$, which signifies the direction of the shortest semi-axis. The according rotation matrix $\mathbf{R}$ transforming the vector $(1,0,0)^{\mathrm{T}}$ into $\mathbf{n}$ is defined by

$$\mathbf{R} \coloneqq \begin{pmatrix} 1 & -n_2 & -n_3 \\ n_2 & 1 & 0 \\ n_3 & 0 & 1 \end{pmatrix} + \frac{1-n_1}{\|(n_2,n_3)^{\mathrm{T}}\|} \begin{pmatrix} -n_2^2-n_3^2 & 0 & 0 \\ 0 & -n_2^2 & -n_2n_3 \\ 0 & -n_2n_3 & -n_3^2 \end{pmatrix}.$$

With this at hand, we define the core, coating, and the surrounding material on the sets

$$\begin{aligned} \mathcal{Y}_{\text{inner}} &\coloneqq \big\{\mathbf{x} \in \mathbb{R}^d : a(\mathbf{R}^{-1}\mathbf{x}) \le a_{\text{inner}}\big\} \\ \mathcal{Y}_{\text{outer}} &\coloneqq \big\{\mathbf{x} \in \mathbb{R}^d : a_{\text{inner}} < a(\mathbf{R}^{-1}\mathbf{x}) \le a_{\text{outer}}\big\} \\ \mathcal{Y}_{\text{matrix}} &\coloneqq [-\pi,\pi)^3 \setminus \big(\mathcal{Y}_{\text{inner}} \cup \mathcal{Y}_{\text{outer}}\big), \end{aligned}$$

respectively. The volume of an ellipsoid with radius a is given by the formula $v(a) \coloneqq \sqrt{(c_1^2+a)(c_2^2+a)}$ and therefore the volume fraction of the core $\mathcal{Y}_{\text{inner}}$ in the coated ellipsoid is $f(a_{\text{outer}})$ with $f(a) \coloneqq v(a_{\text{inner}})v(a)^{-1}$.

In this thesis, we further assume that the core and coating ellipsoids have isotropic stiffnesses. The matrix material is an anisotropic stiffness tensor. To lighten the burden on the reader, we break here with the convention regarding the use of greek letters and use instead the traditional symbols for the stiffness parameters. Thus, assume that the stiffness tensors have the form $\mathcal{C}_{ijkl} = \lambda\delta_{ij}\delta_{kl} + \mu(\delta_{ik}\delta_{jl} + \delta_{il}\delta_{jk})$ for $i, j, k, l = 1, \dots, 3$, where λ is Lamé's first parameter and $\mu \geq 0$ is the shear modulus. For the core and coating we then denote their respective parameters by λ_{inner}, λ_{outer}, and μ_{inner}, μ_{outer}, respectively. Further, let the bulk moduli of the core and coating be given by $\kappa_{\text{inner}} \coloneqq \lambda_{\text{inner}} + \frac{2}{3}\mu_{\text{inner}}$ and $\kappa_{\text{outer}} \coloneqq \lambda_{\text{outer}} + \frac{2}{3}\mu_{\text{outer}}$, respectively.

Prescribe a macroscopic strain $\varepsilon^0 \in \mathrm{Sym}_d(\mathbb{R})$ with

$$\varepsilon^0 \coloneqq \mathbf{R}\left(\frac{3\kappa_{\text{outer}} + 4\mu_{\text{outer}}}{9\big(\kappa_{\text{inner}} - \kappa_{\text{outer}}\big)}\mathbf{Id}_3 + \big(1 - f(a_{\text{outer}})\big)\mathbf{S}\right)\mathbf{R}^{\mathrm{T}},$$

where

$$\mathbf{S} \coloneqq \big(1 - f(a_{\text{outer}})\big)^{-1}\big(\mathbf{D}(a_{\text{inner}}) - f(a_{\text{outer}})\mathbf{D}(a_{\text{outer}})\big).$$

The coated ellipsoid is constructed in such a way, that it is neutral, i.e. that it does not affect the stress field $\mathcal{C} : \varepsilon$. Therefore, the action $\mathcal{C}^{\text{eff}} : \varepsilon^0$ of the effective stiffness matrix on the macroscopic strain coincides with the actions of the stiffness of the matrix material to ε^0. This results in a tensor

$$\begin{aligned}\mathcal{C}^{\text{eff}} : \varepsilon^0 \coloneqq &\mathbf{R}\left(\frac{\kappa_{\text{outer}}}{\kappa_{\text{inner}} - \kappa_{\text{outer}}}\left(\kappa_{\text{inner}} + \frac{4}{3}\mu_{\text{outer}}\right) + \frac{4}{3}\mu_{\text{outer}} f(a_{\text{outer}})\right)\mathbf{Id}_{3,\text{Sym}}\mathbf{R}^{\mathrm{T}} \\ &+\mathbf{R}\frac{2}{3}\mu_{\text{outer}}\big(1 - f(a_{\text{outer}})\big)\big(3\mathbf{S} - \mathbf{Id}_{3,\text{Sym}}\big)\mathbf{R}^{\mathrm{T}}.\end{aligned}$$

The resulting strain field ε is constant in the core $\mathcal{Y}_{\text{inner}}$ and in the matrix $\mathcal{Y}_{\text{matrix}}$. In the coating $\mathcal{Y}_{\text{outer}}$ the behavior of the strain is nonlinear. Thus, the strain field is given by

$$\varepsilon(\mathbf{x}) \coloneqq \mathbf{R}\frac{3\kappa_{\text{outer}} + 4\mu_{\text{outer}}}{9(\kappa_{\text{inner}} - \kappa_{\text{outer}})},$$

for $\mathbf{x} \in \mathcal{Y}_{\text{inner}}$,

$$\begin{aligned}\varepsilon(\mathbf{x}) \coloneqq &\mathbf{R}\Big(\tfrac{3\kappa_{\text{outer}}+4\mu_{\text{outer}}}{9(\kappa_{\text{inner}}-\kappa_{\text{outer}})}\,\mathrm{Id}_{3,\text{Sym}} + \mathbf{D}(a_{\text{inner}}) - f\big(a(\mathbf{R}^{-1}\mathbf{x})\big)\mathbf{D}\big(a(\mathbf{R}^{-1}\mathbf{x})\big)\Big)\mathbf{R}^{\mathrm{T}} \\ &+ \mathbf{R}\Big(\tfrac{v(a_{\text{inner}})}{2}\mathbf{q}(\mathbf{R}^{-1}\mathbf{x})\,\nabla^{\mathrm{T}}_{\mathbf{R}^{-1}\mathbf{x}}\,a(\mathbf{R}^{-1}\mathbf{x})\Big)\mathbf{R}^{\mathrm{T}}\end{aligned}$$

for $\mathbf{x} \in \mathcal{Y}_{\text{outer}}$, and

$$\varepsilon(\mathbf{x}) \coloneqq \varepsilon^0$$

for $\mathbf{x} \in \mathcal{Y}_{\text{matrix}}$. We set

$$\begin{aligned}\big(\mathbf{q}(\mathbf{x})\big)_i &\coloneqq \frac{x_i}{\big(c_i^2 + a(\mathbf{x})\big)v\big(a(\mathbf{x})\big)}, \\ \big(\nabla_{\mathbf{x}}\,a(\mathbf{x})\big)_i &\coloneqq \frac{2x_i}{c_i^2 + a(\mathbf{x})}\left(\sum_{j=1}^{2}\frac{x_j}{c_j^2 + a(\mathbf{x})}\right)^{-1}\end{aligned}$$

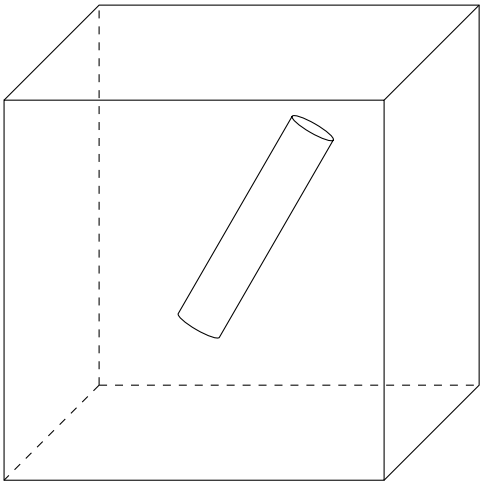

Figure 4.2. A single fiber geometry.

for $\mathbf{x} = (x_1, x_2, x_3)^{\mathrm{T}} \in \mathbb{T}^d$ and $i = 1, 2$, and $\big(\mathbf{q}(\mathbf{x})\big)_3 = \big(\nabla_{\mathbf{x}}\, a(\mathbf{x})\big)_3 \coloneqq 0$. With $a(\mathbf{x})$ we denote the unique solution of (4.1) for a.

In this thesis we use the geometry parametrized by the parameters $\mathbf{n} \coloneqq (0.5, 1, 0)^{\mathrm{T}}$, $c_1 \coloneqq 0.1\pi$, $c_2 \coloneqq 0.7\pi$, $c_3 \coloneqq \infty$, $a_{\text{inner}} \coloneqq 0$, $a_{\text{outer}} \coloneqq 0.36\pi^2$, $E_{\text{inner}} \coloneqq 10$, $E_{\text{outer}} \coloneqq 1$, $\nu_{\text{inner}} \coloneqq 0.3$, and $\nu_{\text{outer}} \coloneqq 0.3$, with $\lambda = \frac{E\nu}{(1+\nu)(1-2\nu)}$ and $\mu = \frac{E}{2(1+\nu)}$. The analytic solution for the 11-component of the strain ε is shown in Figure 4.1 (right).

A single fiber geometry

In addition to the two-dimensional generalized Hashin structure, we investigate a more realistic geometry, consisting of a single short fiber that is rotated in space [8]. Let $a > 0$ be the radius, let $l > 0$ be the length, and let $\mathbf{n} \in \mathbb{R}^3$ with $\|n\| = 1$ be the direction the fiber is pointing to. Let further $\mathcal{C}_{\text{fiber}}$ and $\mathcal{C}_{\text{matrix}}$ be isotropic materials. Then the stiffness distribution of the single fiber geometry is given by

$$\mathcal{C}(\mathbf{x}) \coloneqq \begin{cases} \mathcal{C}_{\text{fiber}}, & \text{for } \mathbf{R}^{-1}\mathbf{x} \in \mathcal{Y}_{\text{fiber}}, \\ \mathcal{C}_{\text{matrix}}, & \text{else,} \end{cases}$$

for $\mathbf{x} = (x_1, x_2, x_3)^{\mathrm{T}} \in \mathbb{T}^3$, where

$$\mathcal{Y}_{\text{fiber}} \coloneqq \Big\{ \mathbf{x} \in \mathbb{T}^3 : \big\|(0, x_2, x_3)^{\mathrm{T}}\big\| \leq a,\ |x_1| \leq l \Big\}.$$

In this thesis, we use the geometry parametrized by the parameters $\mathbf{n} \coloneqq (0.5, 1, 0)^{\mathrm{T}}$, $\varepsilon^0 \coloneqq \operatorname{diag}(1, 0, 0)$, $a \coloneqq 0.2\pi$, $l \coloneqq \pi$, $E_{\text{fiber}} \coloneqq 10$, $E_{\text{matrix}} \coloneqq 1$, $\nu_{\text{fiber}} \coloneqq 0.3$, and $\nu_{\text{matrix}} \coloneqq 0.3$, with $\lambda = \frac{E\nu}{(1+\nu)(1-2\nu)}$ and $\mu = \frac{E}{2(1+\nu)}$. This geometry is depicted in Figure 4.2.

The spline geometry

The third example geometry has a stiffness distribution with isotropic materials. This stiffness distribution, however, is not build using piecewise constant materials, but changes according to a given smoothness. This makes it ideal to verify the convergence result of Theorem 3.10.

Therefore, we assume that the stiffness distribution $\mathcal{C}(\mathbf{x})$ has for $\mathbf{x} \in \mathbb{T}^d$ the form

$$\mathcal{C}_{ijkl}(\mathbf{x}) \coloneqq \frac{E(\mathbf{x})\nu}{(1+\nu)(1-2\nu)}\delta_{ij}\delta_{kl} + \frac{E(\mathbf{x})}{2(1+\nu)}(\delta_{ik}\delta_{jl} + \delta_{il}\delta_{jk}),$$

where $\nu \coloneqq 0.3$ is Poisson's ratio and $E(\mathbf{x})$ is the Youngs modulus.

The Youngs modulus $E(\mathbf{x})$ is given as a spline with compact support in the set $\big[-\pi, \pi\big)^3$ defined as a tensor product function

$$E\Big(\frac{\mathbf{x}}{2\pi}\Big) \coloneqq \prod_{i=1}^{3} f(x_i)$$

for $\mathbf{x} = (x_1, x_2, x_3)^{\mathrm{T}}$.

The function $f(x)$ is composed of two polynomials $f_1(x)$ and $f_2(x)$ with

$$f(x) \coloneqq 5.0 + 5.0 \begin{cases} 1, & \text{for } x < -\frac{1}{4}, \\ f_1(x), & \text{for } -\frac{1}{4} \leq x < 0, \\ f_2(x), & \text{for } 0 \leq x < \frac{1}{4}, \\ 1, & \text{for } \frac{1}{4} \leq x. \end{cases}$$

The polynomials $f_1(x)$ and $f_2(x)$ are chosen as

$$\begin{aligned} f_1(x) &\coloneqq -768x^4 - 512x^3 - 96x^2 + 1, \\ f_2(x) &\coloneqq -768x^4 + 512x^3 - 96x^2 + 1, \end{aligned}$$

and the function satisfies $f(x) \in \mathcal{C}^2(\mathbb{T}^d) \setminus \mathcal{C}^3(\mathbb{T}^d)$.

Polycrystalline structure

The final example geometry we study is a three-dimensional polycrystalline structure [46, Section 4.4], see Figure 4.3. Its stiffness distribution consists of a single transversal isotropic material, i.e. a material that is directional and behaves isotropically orthogonal to this direction. The grains of the polycrystal differ only in the orientation of this material. The example was created with the software GeoDict[1] and has 16 different material orientations. The data is given on a tensor product grid with a diagonal pattern matrix $\mathbf{M} = \operatorname{diag}(2048, 2048, 2048)$. The material of the crystal is magnesium at 300 Kelvin and the components of the stiffness tensor are given as $\mathcal{C}_{1111} = \mathcal{C}_{2222} = 59.3\,\mathrm{GPa}$,

[1] Math2Market GmbH `http://www.geodict.de`, Accessed: 2017-12-20.

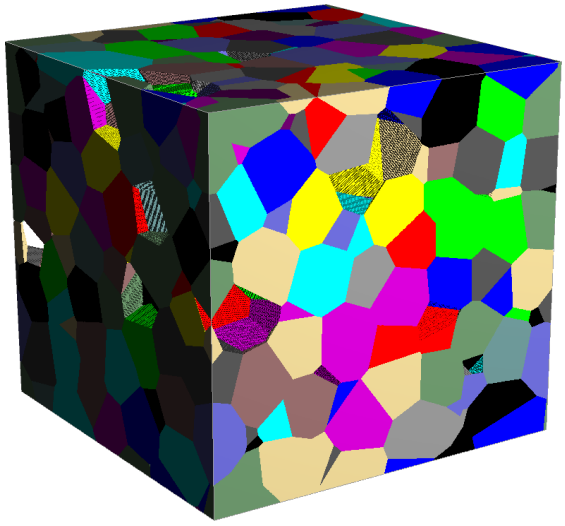

Figure 4.3. The polycrystalline geometry. Different colors signify areas of different orientation.

$\mathcal{C}_{1122} = 25.7\,\mathrm{GPa}$, $\mathcal{C}_{1133} = 21.4\,\mathrm{GPa}$, $\mathcal{C}_{3333} = 61.5\,\mathrm{GPa}$, $\mathcal{C}_{2323} = \mathcal{C}_{3131} = 16.4\,\mathrm{GPa}$, and $\mathcal{C}_{1212} = 16.8\,\mathrm{GPa}$, see [77]. The rest of the entries are given by the symmetry of $\mathcal{C}$ or are set to zero otherwise.

The reference solution for this geometry is computed using the diagonal pattern matrix $\mathbf{M} = \mathrm{diag}(1024, 1024, 1024)$ using laminate mixing.

4.2 Implementations

We use two implementations that handle different parts of the discretization techniques introduced throughout this thesis. Basis for the code on patterns and spaces of translates is the MPAWL library[2]. We adapted this code to Julia and built upon it a library to solve the equations of elasticity in homogenization. This code is written in a modular way such that the discretization pattern, the ansatz space, and the Green operator can be exchanged independently. This software is used to compute the solutions for the generalized Hashin structure, the spline geometry, and the single fiber geometry.

The other software used is FeelMath[3] by Fraunhofer ITWM. This product has a monolithic structure and is heavily parallelized and able to perform on clusters. It is used to compute the polycrystalline example and includes the code for composite voxels.

[2] Wolfram Library Archive: The multivariate periodic anisotropic wavelet Library (MPAWL) `http://library.wolfram.com/infocenter/MathSource/8761/`, Accessed: 2017-12-20.

[3] Fraunhofer ITWM: FeelMath `https://www.itwm.fraunhofer.de/de/abteilungen/sms/produkte-und-leistungen/feelmath.html`, Accessed: 2017-12-20

	Pattern basis	e_1	e_2	$e_{\text{eff}}(\mathbf{M})$
$\mathbf{M}_{7,0,0}$	$(1,0,0)^{\mathrm{T}}$, $(0,1,0)^{\mathrm{T}}$	128	128	$8 \cdot 10^{-4}$
$\mathbf{M}_{6,64,1}$	$(1,0,0)^{\mathrm{T}}$, $\left(1,\frac{1}{3},0\right)^{\mathrm{T}}$	64	256	$1.9 \cdot 10^{-4}$
$\mathbf{M}_{7,32,0}$	$(1,0,0)^{\mathrm{T}}$, $(1,-0.05,0)^{\mathrm{T}}$	32	512	$2.1 \cdot 10^{-4}$
$\mathbf{M}_{7,80,0}$	$(1,0,0)^{\mathrm{T}}$, $(1,0.011,0)^{\mathrm{T}}$	16	1024	$1.9 \cdot 10^{-4}$
$\mathbf{M}_{7,160,1}$	$(1,-1,0)^{\mathrm{T}}$, $(1,-0.95,0)^{\mathrm{T}}$	32	512	$2.0 \cdot 10^{-4}$

Table 4.1. Errors in the effective matrix e_{eff} for different matrices. For the pattern matrices, their rescaled pattern basis vectors with the respective elementary divisors are given.

4.3 The influence of the pattern matrix for the Dirichlet kernel

In this section we investigate the influence of the pattern matrix on the solution of the Lippmann-Schwinger equation. To this avail we take a step back and do not use nontrivial spaces of translates and restrict ourselves to the Dirichlet kernel $f_{\mathrm{D}_\mathbf{M}}$, i.e. to the standard discrete Fourier transform and spaces of truncated trigonometric series.

For the anisotropic Hashin structure we study matrices of the form

$$\mathbf{M}_{j,k,a} \coloneqq \begin{pmatrix} 2^j & ak & 0 \\ (1-a)k & 2^{14-j} & 0 \\ 0 & 0 & 1 \end{pmatrix}, \tag{4.2}$$

where $j = 5, \dots, 9$ with $a = 0, 1$ and $k = -512, -496, \dots, 512$. The patterns generated by these matrices have 2^{14} points. Changing k leads to a shearing of the pattern, which for $a = 1$ shears the x-coordinate and for $a = 0$ the y-coordinate.

In the following we look at the relative ℓ^2-error e_{ℓ^2} between the computed strain ε and the analytic solution $\tilde{\varepsilon}$ with

$$e_{\ell^2} \coloneqq \|\varepsilon - \tilde{\varepsilon}\|_2 \|\tilde{\varepsilon}\|_2^{-1}.$$

We measure the relative error e_{eff} in the effective stiffness $\mathcal{C}^{\text{eff}}$ with respect to the analytic effective stiffness tensor $\tilde{\mathcal{C}}^{\text{eff}}$ for a given macroscopic strain ε^0 by

$$e_{\text{eff}} \coloneqq \|\mathcal{C}^{\text{eff}}\varepsilon^0 - \tilde{\mathcal{C}}^{\text{eff}}\varepsilon^0\| \|\tilde{\mathcal{C}}^{\text{eff}}\varepsilon^0\|^{-1}.$$

In Figure 4.4 the effective error e_{eff} depending on k for different values of j and a is shown. There, we omit those curves, which give very large errors and only the ones resulting in small error remain. The errors belonging to the parameter $k = 0$, i.e. those based on a tensor product grid, are marked with crosses.

The error for the tensor product case is around $8 \cdot 10^{-4}$. This can be improved upon by shearing the pattern matrix, up to an error of about $2 \cdot 10^{-4}$. This error is reached for the pattern matrices $\mathbf{M}_{6,64,1}$, $\mathbf{M}_{7,32,0}$, $\mathbf{M}_{7,80,0}$, and $\mathbf{M}_{7,160,1}$. The rescaled pattern basis vectors for these matrices, via Definition 2.9, and their respective elementary divisors e_j from Lemma 2.8 are listed in Table 4.1.

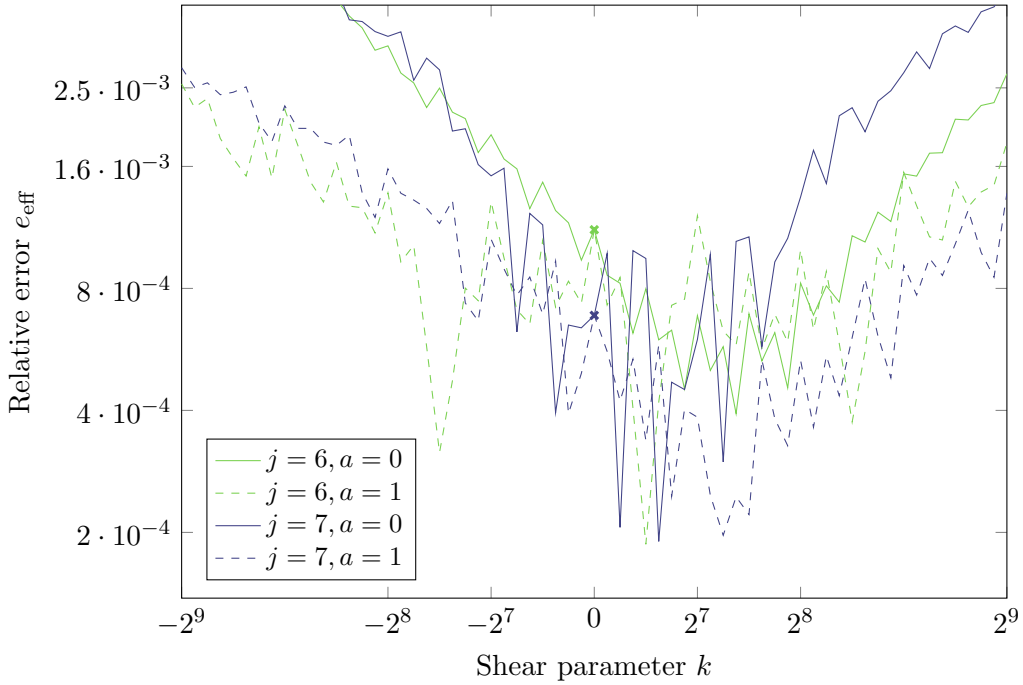

Figure 4.4. Effective error e_{eff} for the anisotropic Hashin structure with pattern matrices $\mathbf{M}_{j,k,a}$ from (4.2). The values belonging to $k = 0$ are marked with a cross.

These matrices, especially for $j = 7$ have in common, that their pattern basis vectors have a small angle between them. When looking at the elementary divisors, they are much larger for the second slightly sheared vector. This means that this vector is repeated much more often to produce the pattern $\mathcal{P}(\mathbf{M})$ than the first vector. The resulting pattern for $\mathbf{M}_{7,80,0}$, where only every 16-th point is shown, is displayed in Figure 4.5. The interferences between the points generated by the two pattern basis vectors, together with the modulo operation on the torus, produces a pattern that is almost aligned with the generalized Hashin structure.

We formalize this alignment by inserting lines into the pattern which intersect at least two points. These lines which intersect the most points are the "visually dominant" directions of the pattern and are in included in the picture.

In Figure 4.6 we show the ℓ^2-error and mark the error for $k = 0$ with a cross. The errors when using tensor product grids are around 0.04 and can be reduced to approximately 0.02. Such errors are achieved for the pattern matrices $\mathbf{M}_{7,k,1}$ for $192 \leq k \leq 384$ and — to a lesser extend — for the matrix $\mathbf{M}_{6,128,0}$. The pattern bases are given in Table 4.2 together with their respective elementary divisors and the ℓ^2-error. The error for the matrix $\mathbf{M}_{7,256,1}$ is with a value of 0.019 the lowest error displayed. There the pattern basis vector $(1, -0.5, 0)^{\mathrm{T}}$ is orthogonal to the direction of the smallest semi-axis of the ellipsoid given by $\mathbf{n} = (0.5, 1, 0)^{\mathrm{T}}$. This results in a good resolution of the high strains at the tips of the inner ellipsoid. Investing many sampling points and thus Fourier coefficients in this direction reduces the Gibbs phenomenon which yields smaller ℓ^2-errors.

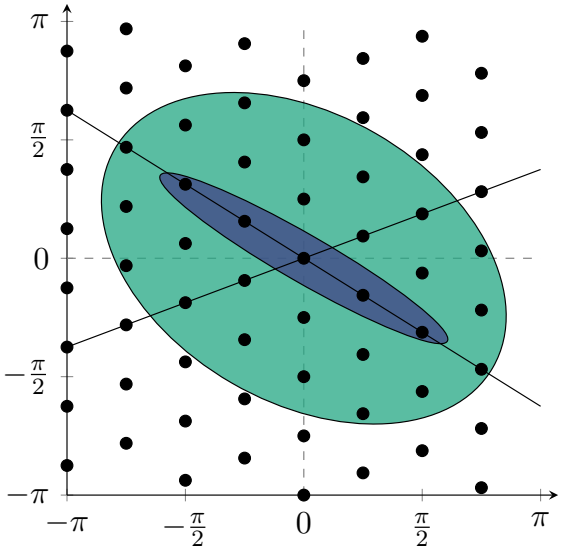

Figure 4.5. The generalized Hashin structure overlayed with the sampling points of the pattern $\mathcal{P}(\mathbf{M}_{7,80,0})$, where every 16-th point is drawn. The lines are the "visually dominant" directions of the pattern.

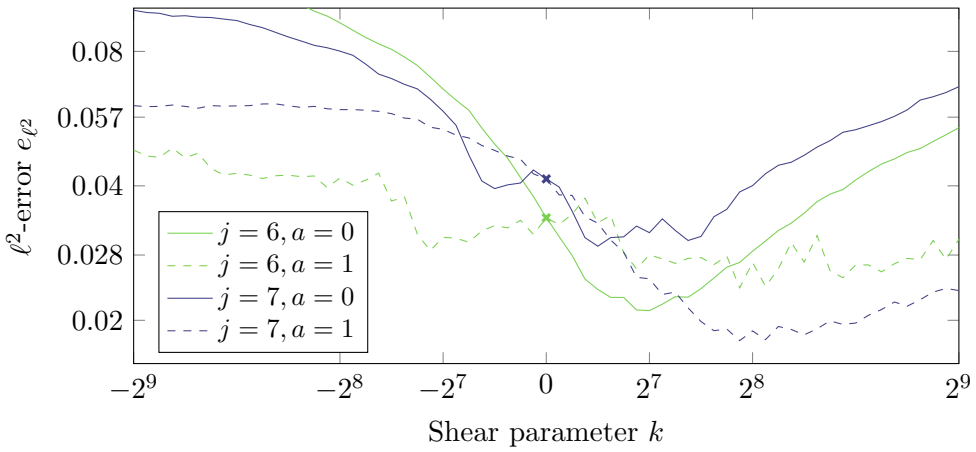

Figure 4.6. ℓ^2-error e_{ℓ^2} for the anisotropic Hashin structure with matrices $\mathbf{M}_{j,k,a}$ from (4.2). The values belonging to $k = 0$ are marked with a cross.

	Pattern basis	e_1	e_2	$e_{\ell^2}(\mathbf{M})$
$\mathbf{M}_{7,0,0}$	$(1,0,0)^{\mathrm{T}}$, $(0,1,0)^{\mathrm{T}}$	128	128	0.041
$\mathbf{M}_{7,192,1}$	$(1,-1,0)^{\mathrm{T}}$, $(1,-0.86,0)^{\mathrm{T}}$	64	256	0.020
$\mathbf{M}_{7,256,1}$	$(1,0,0)^{\mathrm{T}}$, $(1,-0.5,0)^{\mathrm{T}}$	128	128	0.019
$\mathbf{M}_{7,384,1}$	$(1,0,0)^{\mathrm{T}}$, $\left(1,-\frac{1}{3},0\right)^{\mathrm{T}}$	128	128	0.020
$\mathbf{M}_{6,128,0}$	$(1,0,0)^{\mathrm{T}}$, $(1,0.25,0)^{\mathrm{T}}$	64	256	0.021

Table 4.2. The errors e_{ℓ^2} for different matrices. For the pattern matrices, their rescaled pattern basis vectors with the respective elementary divisors are given.

For the single fiber structure we study matrices of the form

$$\mathbf{M} \coloneqq \begin{pmatrix} 32 & p_1 & p_2 \\ p_3 & 32 & p_4 \\ p_5 & p_6 & 32 \end{pmatrix}$$

with the parameters $p_i \in \{-32, -24, \dots, 32\}$ for $i = 1, \dots, 6$. The parameters fulfill the equations $p_1 p_3 = p_2 p_5 = p_4 p_6 = 0$ and we ensured that only matrices where the number of points is $m = |det(\mathbf{M})| = 32^3$ are taken into account. Of these matrices, we want to take a look at the following ones:

$$\mathbf{M}_1 \coloneqq \begin{pmatrix} 32 & 0 & 0 \\ 0 & 32 & 0 \\ 0 & 0 & 32 \end{pmatrix},$$

$$\mathbf{M}_2 \coloneqq \begin{pmatrix} 32 & 0 & 0 \\ 0 & 32 & 0 \\ 0 & -16 & 32 \end{pmatrix},$$

$$\mathbf{M}_3 \coloneqq \begin{pmatrix} 32 & 0 & 32 \\ -32 & 32 & 0 \\ 0 & -32 & 32 \end{pmatrix},$$

$$\mathbf{M}_4 \coloneqq \begin{pmatrix} 32 & 0 & 0 \\ -8 & 32 & 32 \\ 24 & 0 & 32 \end{pmatrix}.$$

The matrix $\mathbf{M}_1$ corresponds to a tensor product grid with 32 points in each direction. Matrix $\mathbf{M}_2$ is chosen in such a way that one pattern basis vector points in the direction of the fiber. The lowest ℓ^2-error is achieved for $\mathbf{M}_3$ and the error in the effective properties is lowest for $\mathbf{M}_4$. The errors together with the rescaled pattern bases can be found in Table 4.3.

Aligning the pattern for $\mathbf{M}_2$ with the direction of the fiber reduces the error in the effective properties slightly. This results in a reduction of the effective error by 5 percent, while the ℓ^2-error stays the same. The best ℓ^2-error is achieved for $\mathbf{M}_3$ with $4.5 \cdot 10^{-2}$, which is 15 percent smaller than computing on a tensor product grid. The effective error is reduced by $\mathbf{M}_4$ from $3.7 \cdot 10^{-4}$ to $1.3 \cdot 10^{-4}$.

	Pattern basis	$e_{\text{eff}}(\mathbf{M})$	$e_{\ell^2}(\mathbf{M})$
$\mathbf{M}_1$	$(1,0,0)^{\mathrm{T}}$, $(0,1,0)^{\mathrm{T}}$, $(0,0,1)^{\mathrm{T}}$	$3.7 \cdot 10^{-4}$	$5.3 \cdot 10^{-2}$
$\mathbf{M}_2$	$(0,1,0)^{\mathrm{T}}$, $(1,2,0)^{\mathrm{T}}$, $(0,2,1)^{\mathrm{T}}$	$3.5 \cdot 10^{-4}$	$5.3 \cdot 10^{-2}$
$\mathbf{M}_3$	$(1,0,0)^{\mathrm{T}}$, $(0,1,0)^{\mathrm{T}}$, $(1,1,-1)^{\mathrm{T}}$	$4.7 \cdot 10^{-4}$	$\mathbf{4.5 \cdot 10^{-2}}$
$\mathbf{M}_4$	$(1,0,0)^{\mathrm{T}}$, $(4,1,0)^{\mathrm{T}}$, $(4,0,1)^{\mathrm{T}}$	$\mathbf{1.3 \cdot 10^{-4}}$	$5.7 \cdot 10^{-2}$

Table 4.3. Effective errors e_{eff} and ℓ^2-errors for the single fiber geometry. $\mathbf{M}_1$ corresponds to a tensor product grid, $\mathbf{M}_2$ has a pattern basis vector aligned with the fiber, $\mathbf{M}_3$ gives the smallest ℓ^2-error and $\mathbf{M}_4$ the smallest effective error found. Together with the matrices, their respective rescaled pattern basis vectors are stated. The smallest errors in their respecive category are in boldface.

4.4 The influence of the space of translates

In this section we study the influence of the space of translates on the solution of the equation of elasticity in homogenization. For the Hashin structure we use the pattern matrices $\mathbf{M}_1 \coloneqq \mathbf{M}_{7,0,0}$, $\mathbf{M}_2 \coloneqq \mathbf{M}_{7,80,0}$,and $\mathbf{M}_3 \coloneqq \mathbf{M}_{7,256,1}$, using (4.2). The matrix $\mathbf{M}_1$ corresponds to the tensor product grid, $\mathbf{M}_2$ is the matrix with the smallest effective error e_{eff}, and $\mathbf{M}_3$ produces the smallest ℓ^2-error in the study in Section 4.3.

In Figure 4.7, the logarithmic error in the 11-component of the strain ε is displayed. If $\tilde{\varepsilon}$ is the analytic strain, then we compute the error by $\log(1 + |\varepsilon_{11} - \tilde{\varepsilon}_{11}|)$ for the purposes of visualization. We solve the generalized Hashin structure for the matrices $\mathbf{M}_1$, $\mathbf{M}_2$, and $\mathbf{M}_3$. These pattern matrices are combined with the Dirichlet kernel $f_{\mathrm{D}_{\mathbf{M}}}$, the de la Vallée Poussin kernel $f_{\mathbf{M},a}$ with $a = 0.25$, and a Box spline kernel $f_{\mathbf{M},\mathcal{X}}$ with

$$\mathcal{X} \coloneqq \{\mathbf{p}_1, \mathbf{p}_1, \mathbf{p}_1, \mathbf{p}_1, \mathbf{p}_2, \mathbf{p}_2, \mathbf{p}_2, \mathbf{p}_2\}$$

with $\mathbf{p}_1 \coloneqq (1,0,0)^{\mathrm{T}}$ and $\mathbf{p}_2 \coloneqq (0,1,0)^{\mathrm{T}}$. This constructs a Box spline that is three times differentiable.

The solutions for the Dirichlet kernel show the Gibbs phenomenon radiating from the interfaces. The de la Vallée Poussin kernel is better localized in space which leads to a fast decay of the Gibbs phenomenon. The solution is thus visually smoother and the effective stiffness can be reproduced better. The ℓ^2-error gets slightly larger. The solution for the Box spline shows a strong aliasing effect. The Box spline has an infinite support in Fourier space and the periodized Green operator Γ^{p} is approximated, leading to the visible artifacts. While having no compact support in frequency domain, the Box spline has compact support in space and is regular. This leads to a good reproduction of the effective stiffness. The aliasing effects, however, have a negative impact on the ℓ^2-error.

For the single fiber geometry, the relative ℓ^2-errors e_{ℓ^2} and the relative errors in the effective properties e_{eff} are listed in Table 4.4. There, we use the Dirichlet kernel $f_{\mathrm{D}_{\mathbf{M}}}$ and the de la Vallée Poussin kernel $f_{\mathbf{M},a}$ for $a = 0.1, 0.25, 0.4$. The pattern matrices are the same as in the previous section, where $\mathbf{M}_1$ gives a tensor product grid, $\mathcal{P}(\mathbf{M}_2)$ is aligned with the fiber, $\mathbf{M}_3$ gives the smallest ℓ^2-error, and $\mathbf{M}_4$ yields the smallest error in the effective stiffness.

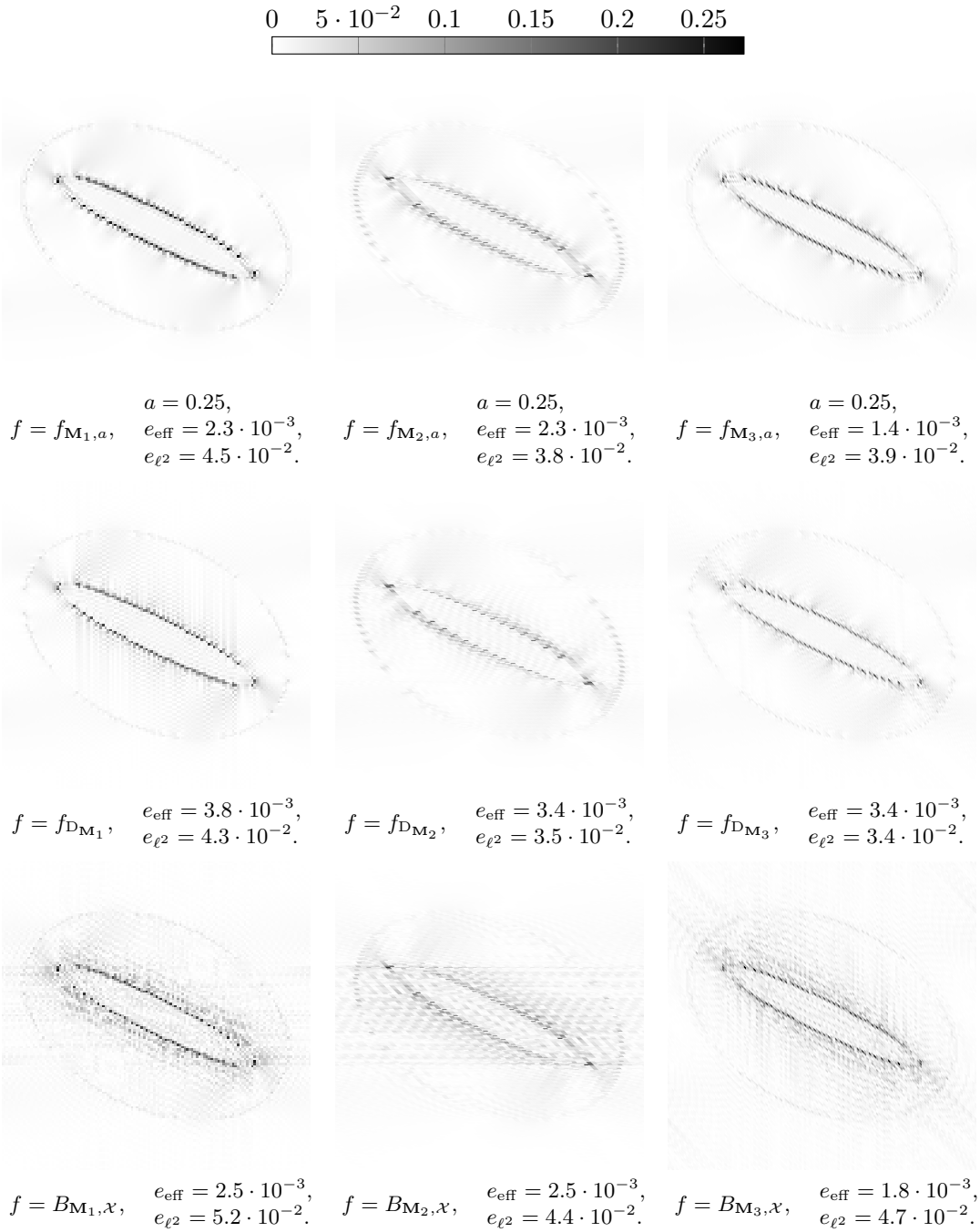

$f = f_{\mathbf{M}_1,a}$, $a = 0.25$, $e_{\text{eff}} = 2.3 \cdot 10^{-3}$, $e_{\ell^2} = 4.5 \cdot 10^{-2}$.
$f = f_{\mathbf{M}_2,a}$, $a = 0.25$, $e_{\text{eff}} = 2.3 \cdot 10^{-3}$, $e_{\ell^2} = 3.8 \cdot 10^{-2}$.
$f = f_{\mathbf{M}_3,a}$, $a = 0.25$, $e_{\text{eff}} = 1.4 \cdot 10^{-3}$, $e_{\ell^2} = 3.9 \cdot 10^{-2}$.

$f = f_{\mathrm{D}_{\mathbf{M}_1}}$, $e_{\text{eff}} = 3.8 \cdot 10^{-3}$, $e_{\ell^2} = 4.3 \cdot 10^{-2}$.
$f = f_{\mathrm{D}_{\mathbf{M}_2}}$, $e_{\text{eff}} = 3.4 \cdot 10^{-3}$, $e_{\ell^2} = 3.5 \cdot 10^{-2}$.
$f = f_{\mathrm{D}_{\mathbf{M}_3}}$, $e_{\text{eff}} = 3.4 \cdot 10^{-3}$, $e_{\ell^2} = 3.4 \cdot 10^{-2}$.

$f = B_{\mathbf{M}_1,\mathcal{X}}$, $e_{\text{eff}} = 2.5 \cdot 10^{-3}$, $e_{\ell^2} = 5.2 \cdot 10^{-2}$.
$f = B_{\mathbf{M}_2,\mathcal{X}}$, $e_{\text{eff}} = 2.5 \cdot 10^{-3}$, $e_{\ell^2} = 4.4 \cdot 10^{-2}$.
$f = B_{\mathbf{M}_3,\mathcal{X}}$, $e_{\text{eff}} = 1.8 \cdot 10^{-3}$, $e_{\ell^2} = 4.7 \cdot 10^{-2}$.

Figure 4.7. The logarithmic error of the 11-component of the strain field ε using the color bar at the top. We use the pattern matrices $\mathbf{M}_1$ (left column), $\mathbf{M}_2$ (middle column), and $\mathbf{M}_3$ (right column) combined with the de la Vallée Poussin kernel $f_{\mathbf{M},a}$ with $a = 0.25$ (top row), the Dirichlet kernel $f_{\mathrm{D}_\mathbf{M}}$ (middle row), and the Box spline $f_{\mathbf{M},\mathcal{X}}$ (bottom row).

		$\mathbf{M}_1$	$\mathbf{M}_2$	$\mathbf{M}_3$	$\mathbf{M}_4$
$f_{\mathrm{D_M}}$	$e_{\mathrm{eff}}(\mathbf{M})$	$\mathbf{3.7 \cdot 10^{-4}}$	$\mathbf{3.5 \cdot 10^{-4}}$	$\mathbf{4.4 \cdot 10^{-4}}$	$\mathbf{1.3 \cdot 10^{-4}}$
	$e_{\ell^2}(\mathbf{M})$	$5.3 \cdot 10^{-2}$	$5.3 \cdot 10^{-2}$	$5.9 \cdot 10^{-2}$	$5.7 \cdot 10^{-2}$
$f_{\mathbf{M},0.1}$	$e_{\mathrm{eff}}(\mathbf{M})$	$4.6 \cdot 10^{-4}$	$4.4 \cdot 10^{-4}$	$5.4 \cdot 10^{-4}$	$2.5 \cdot 10^{-4}$
	$e_{\ell^2}(\mathbf{M})$	$5.2 \cdot 10^{-2}$	$5.2 \cdot 10^{-2}$	$5.8 \cdot 10^{-2}$	$5.6 \cdot 10^{-2}$
$f_{\mathbf{M},0.25}$	$e_{\mathrm{eff}}(\mathbf{M})$	$6.0 \cdot 10^{-4}$	$6.6 \cdot 10^{-4}$	$7.5 \cdot 10^{-4}$	$4.6 \cdot 10^{-4}$
	$e_{\ell^2}(\mathbf{M})$	$5.0 \cdot 10^{-2}$	$5.1 \cdot 10^{-2}$	$5.6 \cdot 10^{-2}$	$5.4 \cdot 10^{-2}$
$f_{\mathbf{M},0.4}$	$e_{\mathrm{eff}}(\mathbf{M})$	$8.3 \cdot 10^{-4}$	$1.0 \cdot 10^{-3}$	$1.0 \cdot 10^{-3}$	$7.2 \cdot 10^{-4}$
	$e_{\ell^2}(\mathbf{M})$	$\mathbf{5.0 \cdot 10^{-2}}$	$\mathbf{5.0 \cdot 10^{-2}}$	$\mathbf{5.5 \cdot 10^{-2}}$	$\mathbf{5.3 \cdot 10^{-2}}$

Table 4.4. Error in the effective properties and in ℓ^2 for the single fiber geometry on a 32^3 lattice using different ansatz functions compared to a solution on a 256^3 lattice using the Dirichlet kernel. The bold numbers are the lowest errors in the respective category.

The smallest effective errors e_{eff} are achieved for the Dirichlet kernel. These errors increase for the de la Vallée Poussin kernel with increasing support and go from $3.7 \cdot 10^{-4}$ to $8.3 \cdot 10^{-4}$ for the tensor product grid $\mathbf{M}_1$ and increase by a factor of 5 for the pattern matrix $\mathbf{M}_4$.

The relative ℓ^2-errors are smallest for the de la Vallée Poussin means $f_{\mathbf{M},0.4}$ when the support of the kernel is largest. The error drops by 6 to 8 percent compared to the Dirichlet kernel solution.

4.5 Convergence study

The convergence result in Theorem 3.10 predicts that the discretization of the Lippmann-Schwinger equation has a speed of convergence in $\mathbf{M}$ which is the minimum of the smoothness of the coefficients and the ansatz functions. In this section we verify this result numerically using the spline geometry. There, the stiffness distribution fulfills $\mathcal{C} \in \mathrm{SSym}_d\big(\mathcal{C}^2(\mathbb{T}^d) \setminus \mathcal{C}^3(\mathbb{T}^d)\big)$. We solve the spline geometry on tensor product grids $\mathbf{M} = \mathrm{diag}(n, n, 1)$ for $n = 16, 32, \ldots, 128$ and compare the strain field with a solution on a tensor product grid with $n = 256$.

The convergence theorem requires for $d = 3$ that the smoothness b of the coefficients fullfills $b > \frac{d}{2}$. Therefore, the spline geometry has with $b = 2$ the lowest smoothness for which the theorem is applicable. Further, by Lemma 2.27, the Box splines of orders 4 and 5 fulfill the periodic Strang-Fix conditions with parameters $s = 3$, $a = 2$, and $s = 4$, $a = 2$, respectively. For them, the assumption $b = a$ in the convergence theorem is satisfied.

The error curves for these Box splines are shown in Figure 4.8 together with the line for quadratic convergence. By Theorem 3.10, the ℓ^2-error converges with $\|\mathbf{M}\|^{-2}$ for the Box spline of order 4, which is verified by the plot. The higher smoothness of the fifth-order Box spline does not increase the speed of convergence, because the regularity of the coefficients saturates the parameter r in the theorem.

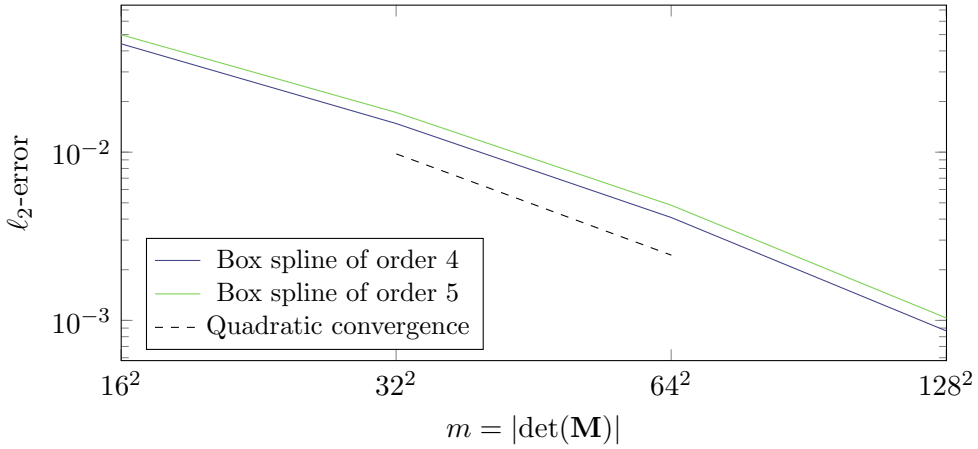

Figure 4.8. The ℓ^2-errors for Box splines of order 4 and 5 for coefficients which are twice continuously differentiable, but not three times. The black line corresponds to quadratic convergence.

4.6 Anisotropic subsampling with composite voxels

High-resolution voxel images are often found as the result of a computer tomography of composite materials. Such images, while catching the features of the geometry in great detail, are difficult to handle numerically due to the enormous amount of data. Methods of data reduction based on using the coefficients on a sublattice are not optimal as they leave the additional information unused. The same problem arises when we are given an analytic description of a geometry. Sampling does evaluate geometry at certain points and does not take into account features on a subvoxel scale. We call voxels, which consist of more than one material on a finer level, *composite voxels*.

This section introduces methods to incorporate information on a finer sampling grid into the computation of the equation of elasticity in homogenization. The method we show here does not increase the required memory and can be implemented as a preprocessing step. In case of a tensor product grid, this method is introduced for the heat equation in [64–66] and for elasticity in [46]. In this thesis, we generalize the approach to anisotropic patterns. Extensions to nonlinear problems [44], hyperelasticity at finite strains [47], and inelastic problems [45] are available.

In case of tensor product grids, [18] suggest a formula to treat interface voxels, i.e. voxels which contain a discontinuity in the stiffness distribution $\mathcal{C}$. Let $\mathcal{W}_\mathbf{y} \subset \mathbb{T}^d$ be such an interface voxel with volume $|\mathcal{W}_\mathbf{y}|$ belonging to the sampling point $\mathbf{y} \in \mathcal{P}(\mathbf{M})$. The authors choose the sampled stiffness $\mathcal{C}_\mathbf{y}$ by the formula

$$\left(\mathcal{C}_\mathbf{y} - \mathcal{C}^0\right)^{-1} = \frac{1}{|\mathcal{W}|} \int_\mathcal{W} \left(\mathcal{C}(\mathbf{x}) - \mathcal{C}^0\right)^{-1} \mathrm{d}\mathbf{x}.$$

This formula ensures that the discretization approach derived from on an energy-based formulation using constant finite elements allows to compute bounds on the effective properties.

General mixing rules for the sampling of the stiffness distribution have to be bounded and be consistent with the discretization, as explained in the following definition.

Definition 4.1. *Let $\mathcal{C}$ be a stiffness distribution that is bounded and elliptic with constants c_b and c_e, respectively, according to Definition 2.28. Let $\mathbf{M} \in \mathbb{Z}^{d\times d}$ be regular and let n_{min} be its smallest eigenvalue. To a point $\mathbf{y} \in \mathcal{P}(\mathbf{M})$ assign the surrounding voxel $\big(\mathcal{W}_\mathbf{M}\big)_\mathbf{y}$ by*

$$\big(\mathcal{W}_\mathbf{M}\big)_\mathbf{y} \coloneqq \left\{\mathbf{y} + \mathbf{x} : \mathbf{x} \in \mathbf{M}^{-1}\Big[-\frac{1}{2}, \frac{1}{2}\Big)^d\right\}$$

with volume $|\mathcal{W}_\mathbf{M}\big)_\mathbf{y}|$. Consider a mixing rule that leads to a stiffness $\big(\mathcal{C}_\mathbf{M}\big)_\mathbf{y}$ for all $\mathbf{y} \in \mathcal{P}(\mathbf{M})$ and define the voxelwise constant stiffness distribution

$$\mathcal{C}^{mix}_\mathbf{M}(\mathbf{x}) \coloneqq \big(\mathcal{C}_\mathbf{M}\big)_\mathbf{y}$$

if $\mathbf{x} \in \big(\mathcal{W}_\mathbf{M}\big)_\mathbf{y}$. A mixing rule is consistent *if*

a) the stiffness $\mathcal{C}^{mix}$ is bounded and elliptic with the same constants c_b and c_e as $\mathcal{C}$, and if

b) the stiffness $\mathcal{C}^{mix}(\mathbf{x}) \to \mathcal{C}(\mathbf{x})$ for almost all $\mathbf{x} \in \mathbb{T}^d$ and $n_{min} \to \infty$.

The first condition ensures that the mixing does not influence the speed of convergence of the basic scheme, see Theorem 3.12. The second one ensures convergence of the discrete mixing rule as the maximal distance between adjacent grid points goes to zero.

We consider three mixing rules in this section. The first two are motivated by the Voigt [101] and Reuss [83] bounds giving an upper and lower bound, respectively, for the elasticity of the composite voxel.

Definition 4.2. *Let the voxel $\big(\mathcal{W}_\mathbf{M}\big)_\mathbf{y}$ surrounding the point $\mathbf{y} \in \mathcal{P}(\mathbf{M})$ be defined as in Definition 4.1. The mixing rule that assigns the stiffness*

$$\big(\mathcal{C}^{Voigt}_\mathbf{M}\big)_\mathbf{y} \coloneqq \frac{1}{|\big(\mathcal{W}_\mathbf{M}\big)_\mathbf{y}|}\int_{\big(\mathcal{W}_\mathbf{M}\big)_\mathbf{y}} \mathcal{C}(\mathbf{x})\,\mathrm{d}\mathbf{x} \tag{4.3}$$

to the voxel $\big(\mathcal{W}_\mathbf{M}\big)_\mathbf{y}$ for $\mathbf{y} \in \mathcal{P}(\mathbf{M})$ is called Voigt mixing. *The mixing rule*

$$\big(\mathcal{C}^{Reuss}_\mathbf{M}\big)_\mathbf{y} \coloneqq \left(\frac{1}{|\big(\mathcal{W}_\mathbf{M}\big)_\mathbf{y}|}\int_{\big(\mathcal{W}_\mathbf{M}\big)_\mathbf{y}} \mathcal{C}(\mathbf{x})^{-1}\,\mathrm{d}\mathbf{x}\right)^{-1} \tag{4.4}$$

is called Reuss mixing.

These mixing rules are consistent due to the continuity of the integral operator.

Such mixing rules are very simple as they take into account the volume fractions of the different stiffnesses in the composite voxels. They, however, ignore any spacial

information about the coefficients. Consider a stiffness distribution with a laminate structure given by

$$\mathcal{C}(\mathbf{x}) \coloneqq \begin{cases} \mathcal{C}^{\text{left}}, & \text{for } x_1 < 0, \\ \mathcal{C}^{\text{right}}, & \text{for } x_1 \geq 0, \end{cases}$$

for $\mathbf{x} = (x_1, x_2)^{\mathrm{T}} \in \mathbb{T}^2$. Such a structure can be seen in Figure 4.9. We sample the geometry by a pattern $\mathcal{P}(\mathbf{M})$ with $\mathbf{M} \coloneqq \left(\begin{smallmatrix} 5 & 0 \\ 0 & 5 \end{smallmatrix}\right)$ and get a layer of composite voxels in the middle. We choose a mixing rule of the form

$$\left(\mathcal{C}_{\mathbf{M}}^{\text{laminate}}\right)_{\mathbf{y}} \coloneqq \begin{cases} \mathcal{C}^{\text{left}}, & \text{for } y_1 < -\frac{\pi}{5}, \\ \mathcal{C}^{\text{right}}, & \text{for } y_1 \geq \frac{\pi}{5}, \\ \mathcal{C}^{\text{laminate}}, & \text{else}, \end{cases}$$

for $\mathbf{y} = (y_1, y_2)^{\mathrm{T}} \in \mathcal{P}(\mathbf{M})$ with an unknown stiffness tensor $\mathcal{C}^{\text{laminate}}$.

The question arises how to choose the stiffness matrix $\mathcal{C}^{\text{laminate}}$ such that the effective matrix $\mathcal{C}^{\text{eff}}$ of the continuous problem is the same as the stiffness matrix of the numerical problem $\left(\mathcal{C}_{\mathbf{M}}^{\text{laminate}}\right)^{\text{eff}}$. For the heat equation this problem is solved in [64].

Theorem 4.3. *The effective stiffnesses $\mathcal{C}^{\text{eff}} = \left(\mathcal{C}_{\mathbf{M}}^{laminate}\right)^{\text{eff}}$ coincide if and only if the stiffness in the laminate is chosen as the effective stiffness with $\mathcal{C}^{laminate} = \mathcal{C}^{\text{eff}}$.*

Proof. The effective properties for a laminate are given analytically in [69, Section 9.5]. The proof is performed by considering the voxelized structure including the composite voxel layer as a laminate with three constituents. Then, we equate the formulas for the effective stiffness of the three-layer and the two-layer laminate and solve for the composite layer. □

This simple example is our motivation for laminate voxels: we assume, that internally the subvoxel geometry is given by a laminate, where the direction of lamination $\mathbf{n}$ is arbitrary. For such a laminate, the effective stiffness matrix $\left(\mathcal{C}_{\mathbf{M}}^{\text{laminate}}\right)_{\mathbf{y}}^{\text{eff}}$ for a voxel associated with the point $\mathbf{y} \in \mathcal{P}(\mathbf{M})$ is in three dimensions given by the equation

$$\begin{aligned} &\left(\mathcal{H} + a\Big(\left(\mathcal{C}_{\mathbf{M}}^{\text{laminate}}\right)_{\mathbf{y}}^{\text{eff}} - a\,\mathrm{Id}\Big)^{-1}\right)^{-1} = \\ &\qquad \frac{1}{\left|\left(\mathcal{W}_{\mathbf{M}}\right)_{\mathbf{y}}\right|} \int_{\left(\mathcal{W}_{\mathbf{M}}\right)_{\mathbf{y}}} \left(\mathcal{H} + a\Big(\mathcal{C}(\mathbf{x}) - a\,\mathrm{Id}\Big)^{-1}\right)^{-1} \mathrm{d}\mathbf{x} \end{aligned} \tag{4.5}$$

for $a \in \mathbb{R}$. The fourth-order tensor $\mathcal{H}$ is given by

$$\mathcal{H}_{ijkl} \coloneqq \frac{1}{2}\big(n_i\delta_{jk}n_l + n_i\delta_{jl}n_k + n_j\delta_{ik}n_l + n_j\delta_{il}n_k\big) + n_in_jn_kn_l$$

for $i, j, k, l = 1, \ldots, 3$ and $\mathbf{n} = (n_1, n_2, n_3) \in \mathbb{R}^3$ is the normal of the laminate interface. The operator Id is the symmetric fourth-order identity tensor. Let c_{b} be the upper bound on $\mathcal{C}$, then [46, Appendix] proves that $a > c_{\mathrm{b}}$ ensures that the equation (4.5) can be

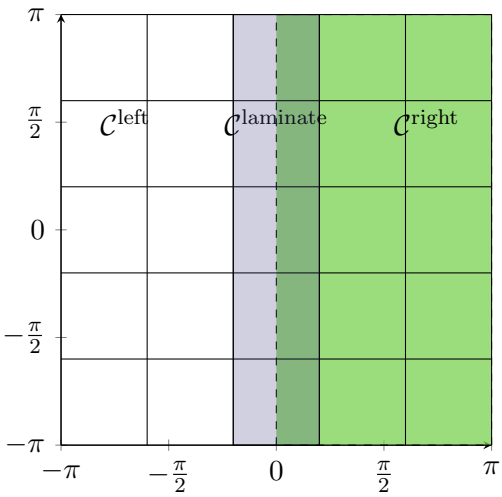

Figure 4.9. An example of a structure that consists of two materials in form of a laminate. This structure is divided into voxels for a tensor product grid with 5×5 voxels.

solved. The formula is directly applicable to anisotropic lattices, because the necessary transformations of the coordinate system [69, Section 8.3] cancel out. The stiffness chosen by the laminate formula is anisotropic, even if the constituing materials are isotropic themselves. This mixing rule is consistent.

For the laminate mixing rule we assume that the interface in the composite voxel is linear. This assumption is justified, if the material boundary is smooth and the grid is fine enough that a voxelwise linearization is possible.

An application of the laminate mixing rule requires an estimate for the normal of the interface in a composite voxel $\left(\mathcal{W}_{\mathbf{M}}\right)_{\mathbf{y}}$. We compute the unweighted center of mass of the composite voxel and the unweighted center of mass of the material $\mathcal{C}^{\text{dominant}}$, which has the largest volume s in the voxel. Then an estimate for the normal $\mathbf{n}$ is given by

$$\mathbf{n} \coloneqq \int_{\left(\mathcal{W}_{\mathbf{M}}\right)_{\mathbf{y}}} \frac{\mathbf{x}\mathbb{1}_{\mathcal{C}^{\text{dominant}}}\left(\mathcal{C}(\mathbf{x})\right)}{s} - \frac{x}{|\left(\mathcal{W}_{\mathbf{M}}\right)_{\mathbf{y}}|}\,\mathrm{d}\mathbf{x} \tag{4.6}$$

and $\mathbb{1}_{\mathcal{C}^{\text{dominant}}}$ is the characteristic function of the dominant material.

In the discrete case we assume, that we have stiffness data on a very fine pattern $\mathcal{P}(\mathbf{M})$ and we compute on a subpattern $\mathcal{P}(\mathbf{N})$ in the sense of Lemma 2.3. Then there is a regular matrix $\mathbf{J} \in \mathbb{Z}^{d\times d}$ such that $\mathbf{M} = \mathbf{JN}$. An enumeration of the points of the fine pattern $\mathcal{P}(\mathbf{M})$ in a voxel associated to $\mathbf{y} \in \mathcal{P}(\mathbf{N})$ is given by the decomposition in Lemma 2.4. The same decomposition can also be used to compute the volume fractions of each material. The integrals in Equations (4.3), (4.4), (4.5), and (4.6) can be replaced by finite sums over the points of the fine pattern $\mathcal{P}(\mathbf{M})$. For analytic descriptions of the geometry, we can either compute the integrals exactly or we sample first on a fine grid and then follow the above procedure.

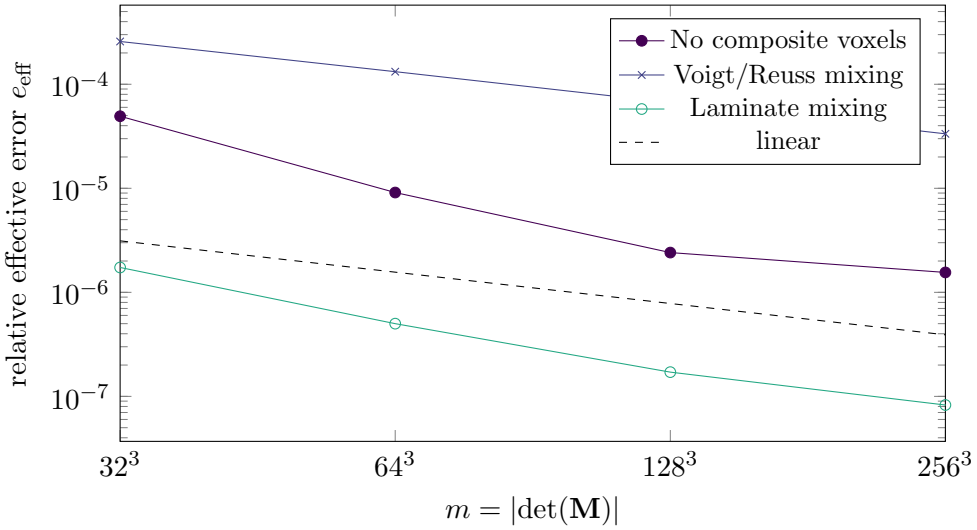

Figure 4.10. A convergence study for the polycrystalline structure using different mixing rules on a tensor product grid. The effective properties are compared to a solution on 1024^3 voxels using laminate mixing.

4.7 The effect of composite voxels

Composite voxels work best on structures, which have many linear interfaces. Such a structure is the polycrystalline geometry on which we compare the different mixing rules using the software FeelMath.

In Figure 4.10, the effective error is plotted for different resolutions. The effective property is compared to a solution on 1024^3 voxels computed using laminate mixing. The error when using the Voigt and Reuss mixing — their errors coincide — is around 10^{-4} for all resolutions and decays linearly. Using no composite voxels gives an error of $5 \cdot 10^{-5}$ for a resolution of $m = 32^3$ voxels and is reduced to $2 \cdot 10^{-5}$ for $m = 256^3$. Laminate mixing gives the smallest error throughout all resolutions. This error is smaller by a factor of 10 compared to using no composite voxels. When we use laminate mixing, we can therefore reduce the number of voxels by a factor of 64 and get the same quality of the effective stiffness as when using no composite voxels.

We use the solution with laminate voxels as the reference solution because it gives the most accurate effective stiffness. This can be seen when comparing to the solution using no composite voxels on $m = 1024^3$. There, the error using laminate mixing gets constant as it surpasses the reference solution in its accuracy.

A computation using the software FeelMath consists of subsampling the high-resolution stiffness image. During the downsampling, the volume fractions of the materials and the estimated normal on the interface are computed. During the computation, every time the stiffness of a composite voxel is to be evaluated, the laminate formula (4.5) is solved. This approach yields an efficient solution of the Lippmann-Schwinger equation. The bottleneck when computing large-scale problems is not the workload of the CPU,

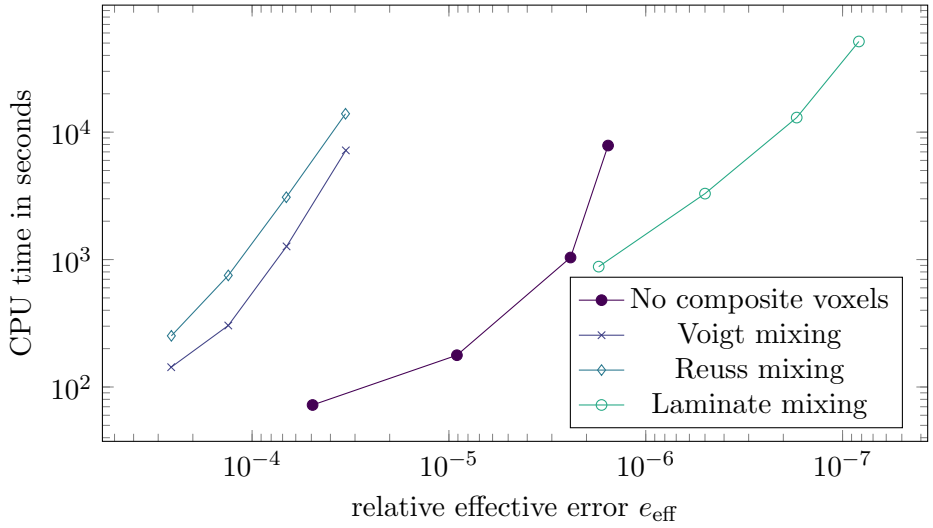

Figure 4.11. A comparison of the ratio between the time required to downsample and compute the solution for the polycrystalline structure using different mixing rules on a tensor product grid. The effective properties are compared to a solution on 1024^3 voxels using laminate mixing.

but the access times for the RAM. Therefore, the inversions in the laminate formula do not increase the computing time.

Figure 4.11 plots the error e_{eff} in the effective properties against the computing time in seconds. This time includes the downsampling and the time to solve the linear system. Voigt and Reuss mixing give the worst ratio between the error and the computing time. Reuss mixing (4.4) fares a little bit worse than Voigt mixing (4.3) because of the inversions necessary to compute the stiffness.

Using no composite voxels does not require the computation of volume fractions and normal vectors and the evaluation of the stiffness matrix is trivial. It yields for the same computing time an error which is 10 to 15 times smaller than using Voigt and Reuss mixing.

The laminate mixing gives the best error to computing time ratio. Even for very small resolutions it requires a lot computations for downsampling and for evaluating the stiffness matrix. For $m = 32^3$ voxels this time is 10 times larger than using no composite voxels. This is counterbalanced by a very low error in the effective stiffness matrix. Computing on 32^3 voxels using laminate mixing is therefore comparable to computing on 128^3 voxels without using the composite voxel technique.

5 Summary

In this thesis we generalize the discretization of the Lippmann-Schwinger equation and the variational formulation [105] to anisotropic lattices [6]. Anisotropic patterns are used to adjust the sampling grid to the geometry and invest more sampling points in the direction of interfaces. For a proper choice of the sampling lattice, this leads to much smaller errors for the effective stiffness tensor and can reduce the ℓ^2-error. Alignment of the Sine functions with material interfaces reduces the Gibbs phenomenon and regions of high stresses are resolved with more accuracy. Subsampling of data on tensor product grids combined with composite voxels [46] makes this approach also available to tensor product grids with a high resolution.

We extend and unify the Dirichlet kernel approach with constant finite elements as ansatz functions to periodic anisotropic spaces of translates [5, 9]. These ansatz spaces motivate the periodized Green operator Γ^{p}, see [8]. The truncated Fourier series emerge as a special case as they produce a Green operator which is a projection and coincides with the Green operator of Moulinec and Suquet. For truncated Fourier series, the solutions of the Lippmann-Schwinger equation and the variational formulation are the same. This is not the case for general spaces of translates, where the Green operator is not a projection operator. We use approximation results on spaces of translates to establish a convergence rate for the discretization. The speed of convergence depends not only on the smoothness of the coefficients, but also on the regularity of the ansatz function generating the space of translates. The periodic Strang-Fix conditions [9] measure the degree of trigonometric polynomials which can be reproduced exactly by the functions in the ansatz space and control the speed of convergence, which we demonstrate numerically. The periodized Green operator can be used with de la Vallée Poussin means and Box splines. The former reduce the Gibbs phenomenon in the solution giving more exact strain fields. The latter have compact support in space and can reproduce the effective stiffness well. However, the solution suffers from aliasing effects, caused by approximating the periodized Green operator Γ^{p}, which has noncompact support.

Stiffness fields which are given on a fine voxel grid can be subsampled on anisotropic sampling lattices [4]. The loss of information from subsampling may be greatly reduced by using mixing rules that compute a new stiffness tensor from subvoxel data [46]. Such mixing rules take into account the volume fractions of the materials contained in an interface voxels, which leads to Voigt [101] and Reuss mixing [83]. In addition, laminate mixing uses an estimate for the direction of a linear interface present in the voxel. For smooth material boundaries and sufficiently small voxels such an approach is reasonable. With laminate mixing, the number of voxels for a polycrystal structure can be reduced by a factor of 64 giving the same error for the effective stiffness as when using no composite voxels. The advantage of the reduced error exceeds the additional computing time,

including the downsampling as a preprocessing step.

An open problem regarding the anisotropic lattices is an automated choice of the sampling matrix depending on the geometry of the problem. This choice may be sensitive to errors.

Finite elements with nontrivial quadrature rules can also be incorporated in this framework. For them, the evaluation of the periodized Green operator is costly and the performance of the algorithm has to be investigated in detail.

Translation invariant spaces are used as the basis for a periodic multiresolution analysis. The framework presented in this thesis can be extended to wavelet spaces in order to exploit sparsity properties of given data. This is also a point of future research.

Bibliography

[1] K. Åhlander and H. Munthe-Kaas. "Applications of the Generalized Fourier Transform in Numerical Linear Algebra". In: *BIT Numerical Mathematics* 45.4 (2005), pp. 819–850. ISSN: 1572-9125. DOI: 10.1007/s10543-005-0030-3.

[2] B. Anglin, R. Lebensohn, and A. Rollett. "Validation of a numerical method based on Fast Fourier Transforms for heterogeneous thermoelastic materials by comparison with analytical solutions". In: *Computational Materials Science* 87 (2014), pp. 209–217. DOI: 10.1016/j.commatsci.2014.02.027.

[3] K. Atkinson and W. Han. *Theoretical numerical analysis*. Vol. 39. Springer, 2005. ISBN: 978-1-4419-0457-7.

[4] R. Bergmann. "The fast Fourier transform and fast wavelet transform for patterns on the torus". In: *Applied and Computational Harmonic Analysis* 35.1 (2013), pp. 39–51. DOI: 10.1016/j.acha.2012.07.007.

[5] R. Bergmann. "Translationsinvariante Räume multivariater anisotroper Funktionen auf dem Torus". German. Dissertation. Universität zu Lübeck, 2013. URL: http://www.math.uni-luebeck.de/mitarbeiter/bergmann/publications/diss_bergmann.pdf. Similarily: Shaker Verlag, ISBN 978-3844022667, 2013.

[6] R. Bergmann and D. Merkert. "A framework for FFT-based homogenization on anisotropic lattices". In: *Computers & Mathematics with Applications* 76.1 (2018), pp. 125–140. DOI: 10.1016/j.camwa.2018.04.008.

[7] R. Bergmann and D. Merkert. "Approximation of periodic PDE solutions with anisotropic translation invariant spaces". In: *Sampling Theory and Applications (SampTA), 2017 International Conference on*. IEEE. 2017, pp. 396–399. URL: https://arxiv.org/abs/1705.00879.

[8] R. Bergmann and D. Merkert. "FFT-based homogenization on periodic anisotropic translation invariant spaces". In: *Applied and Computational Harmonic Analysis* (2018). DOI: 10.1016/j.acha.2018.05.003.

[9] R. Bergmann and J. Prestin. "Multivariate Anisotropic Interpolation on the Torus". In: *Approximation Theory XIV: San Antonio 2013*. Springer International Publishing, 2014, pp. 27–44. DOI: 10.1007/978-3-319-06404-8_3.

[10] R. Bergmann and J. Prestin. "Multivariate Periodic Wavelets of de la Vallée Poussin Type". In: *Journal of Fourier Analysis and Applications* 21.2 (2014), pp. 342–369. DOI: 10.1007/978-3-319-06404-8_3.

[11] G. Bonnet. "Effective properties of elastic periodic composite media with fibers". In: *Journal of the Mechanics and Physics of Solids* 55.5 (2007), pp. 881–899. DOI: 10.1016/j.jmps.2006.11.007.

[12] C. de Boor, K. Höllig, and S. D. Riemenschneider. "Bivariate cardinal interpolation by splines on a three-direction mesh". In: *Illinois Journal of Mathematics* 29.4 (1985), pp. 533–566. URL: http://www.dtic.mil/docs/citations/ADA127939.

[13] C. de Boor, K. Höllig, and S. Riemenschneider. *Box Splines*. New York: Springer-Verlag, 1993. ISBN: 0-387-94101-0. DOI: 10.1007/978-1-4757-2244-4.

[14] C. Boutin. "Microstructural effects in elastic composites". In: *International Journal of Solids and Structures* 33.7 (1996), pp. 1023–1051. DOI: 10.1016/0020-7683(95)00089-5.

[15] R. P. Boyer and W. M. Goh. "Generalized Gibbs phenomenon for Fourier partial sums and de la Vallée-Poussin sums". In: *Journal of Applied Mathematics and Computing* 37.1-2 (2011), pp. 421–442. DOI: 10.1007/s12190-010-0442-3.

[16] E. Breitenberger. "Uncertainty measures and uncertainty relations for angle observables". In: *Foundations of Physics* 15.3 (1985), pp. 353–364. DOI: 10.1007/BF00737323.

[17] R. Brenner. "Numerical computation of the response of piezoelectric composites using Fourier transform". In: *Physical Review B* 79.18 (2009), p. 184106. DOI: 10.1103/PhysRevB.79.184106.

[18] S Brisard and L Dormieux. "FFT-based methods for the mechanics of composites: A general variational framework". In: *Computational Materials Science* 49.3 (2010), pp. 663–671. DOI: 10.1016/j.commatsci.2010.06.009.

[19] S. Brisard. "Overview of FFT-based homogenization techniques from the Galerkin point of view". In: *Conférence Internationale de Géotechnique, des Ouvrages et Structures (CIGOS 2015)*. 2015.

[20] S. Brisard. "Reconstructing displacements from the solution to the periodic Lippmann-Schwinger equation discretized on a uniform grid". In: *International Journal for Numerical Methods in Engineering* 109.4 (2017), pp. 459–486. DOI: 10.1002/nme.5263.

[21] S. Brisard and L. Dormieux. "Combining Galerkin approximation techniques with the principle of Hashin and Shtrikman to derive a new FFT-based numerical method for the homogenization of composites". In: *Computer Methods in Applied Mechanics and Engineering* 217 (2012), pp. 197–212. DOI: 10.1016/j.cma.2012.01.003.

[22] S. Brisard and F. Legoll. *Periodic homogenization using the Lippmann–Schwinger formalism*. 2014. arXiv: 1411.0330v1.

[23] C. K. Chui and C. Li. "A general framework of multivariate wavelets with duals". In: *Applied and Computational Harmonic Analysis* 1.4 (1994), pp. 368–390. DOI: 10.1006/acha.1994.1023.

[24] P. G. Ciarlet and J.-L. Lions. *Handbook of Numerical Analysis Vol II: Finite Element Methods Part 1*. North-Holland, 1991. ISBN: 0-444-70365-9.

[25] D. Cioranescu and P. Donato. *Introduction to homogenization*. 2000. ISBN: 978-0-1985-6554-3.

[26] F. Dietrich, D. Merkert, and B. Simeon. *Derivation of higher-order terms in FFT-based numerical homogenization*. 2017. arXiv: 1712.05145.

[27] P. Eisenlohr et al. "A spectral method solution to crystal elasto-viscoplasticity at finite strains". In: *International Journal of Plasticity* 46 (2013), pp. 37–53. DOI: 10.1016/j.ijplas.2012.09.012.

[28] W. Erb. *Uncertainty principles on Riemannian manifolds*. Logos Verlag Berlin GmbH, 2011. ISBN: 978-3-8325-2744-0.

[29] L. C. Evans. *Partial Differential Equations: Second Edition*. American Mathematical Society, 2010. ISBN: 0-821-84974-3.

[30] D. Eyre and G. Milton. "A fast numerical scheme for computing the response of composites using grid refinement". In: *The European Physical Journal Applied Physics* 6.1 (1999), pp. 41–47. DOI: 10.1051/epjap:1999150.

[31] M. Frigo and S. G. Johnson. "The design and implementation of FFTW3". In: *Proceedings of the IEEE* 93.2 (2005), pp. 216–231. DOI: 10.1109/JPROC.2004.840301.

[32] E Galipeau and P. P. Castañeda. "Giant field-induced strains in magnetoactive elastomer composites". In: *Proceedings of the Royal Society A*. Vol. 469. The Royal Society. 2013, p. 20130385. DOI: 10.1098/rspa.2013.0385.

[33] E. Galipeau and P. P. Castañeda. "A finite-strain constitutive model for magnetorheological elastomers: magnetic torques and fiber rotations". In: *Journal of the Mechanics and Physics of Solids* 61 (4 2013), pp. 1065–1090. DOI: 10.1016/j.jmps.2012.11.007.

[34] L. Gélébart and R. Mondon-Cancel. "Non-linear extension of FFT-based methods accelerated by conjugate gradients to evaluate the mechanical behavior of composite materials". In: *Computational Materials Science* 77 (2013), pp. 430–439. DOI: 10.1016/j.commatsci.2013.04.046.

[35] L. Gélébart and F. Ouaki. "Filtering material properties to improve FFT-based methods for numerical homogenization". In: *Journal of Computational Physics* 294 (2015), pp. 90–95. DOI: 10.1016/j.jcp.2015.03.048.

[36] J. W. Gibbs. "Fourier's series". In: *Nature* 59.1522 (1898), p. 200. DOI: 10.1038/059606a0.

[37] S. S. Goh and T. N. Goodman. "Uncertainty principles and asymptotic behavior". In: *Applied and Computational Harmonic Analysis* 16.1 (2004), pp. 19–43. DOI: 10.1016/j.acha.2003.10.001.

[38] F. Grennerat et al. "Experimental characterization of the intragranular strain field in columnar ice during transient creep". In: *Acta Materialia* 60.8 (2012), pp. 3655–3666. DOI: 10.1016/j.actamat.2012.03.025.

[39] Z. Hashin and S. Shtrikman. "On some variational principles in anisotropic and nonhomogeneous elasticity". In: *Journal of the Mechanics and Physics of Solids* 10.4 (1962), pp. 335–342. DOI: 10.1016/0022-5096(62)90004-2.

[40] W. Heisenberg. "Über den anschaulichen Inhalt der quantentheoretischen Kinematik und Mechanik". In: *Zeitschrift für Physik* 43.3-4 (1927), pp. 172–198. DOI: 10.1007/BF01397280.

[41] E. Hewitt and R. E. Hewitt. "The Gibbs-Wilbraham phenomenon: an episode in Fourier analysis". In: *Archive for history of Exact Sciences* 21.2 (1979), pp. 129–160. URL: http://www.jstor.org/stable/41133555.

[42] M Kabel and H Andrä. "Fast numerical computation of precise bounds of effective elastic moduli". In: *Berichte des Fraunhofer ITWM* 224.224 (2012), pp. 1–16. URL: http://publica.fraunhofer.de/documents/N-225668.html.

[43] M. Kabel, T. Böhlke, and M. Schneider. "Efficient fixed point and Newton-Krylov solvers for FFT-based homogenization of elasticity at large deformations". In: *Computational Mechanics* 54.6 (2014), pp. 1497–1514. DOI: 10.1007/s00466-014-1071-8.

[44] M. Kabel et al. "Nonlinear composite voxels and FFT-based homogenization". In: *VII European Congress on Computational Methods in Applied Sciences and Engineering, Crete Island, Greece*. 2016. URL: https://www.eccomas2016.org/proceedings/pdf/5977.pdf.

[45] M. Kabel, A. Fink, and M. Schneider. "The composite voxel technique for inelastic problems". In: *Computer Methods in Applied Mechanics and Engineering* 322 (2017), pp. 396–418. DOI: 10.1016/j.cma.2017.04.025.

[46] M. Kabel, D. Merkert, and M. Schneider. "Use of composite voxels in FFT-based homogenization". In: *Computer Methods in Applied Mechanics and Engineering* 294 (2015), pp. 168–188. DOI: 10.1016/j.cma.2015.06.003.

[47] M. Kabel, F. Ospald, and M. Schneider. "A model order reduction method for computational homogenization at finite strains on regular grids using hyperelastic laminates to approximate interfaces". In: *Computer Methods in Applied Mechanics and Engineering* 309 (2016), pp. 476–496. DOI: 10.1016/j.cma.2016.06.021.

[48] L. Kämmerer, D. Potts, and T. Volkmer. "Approximation of multivariate periodic functions by trigonometric polynomials based on rank-1 lattice sampling". In: *Journal of Complexity* 31 (4 2015), pp. 543–576. DOI: 10.1016/j.jco.2015.02.004.

[49] L. Kämmerer, D. Potts, and T. Volkmer. "Approximation of multivariate periodic functions by trigonometric polynomials based on sampling along rank-1 lattice with generating vector of Korobov form". In: *Journal of Complexity* 31 (3 2015), pp. 424–456. DOI: 10.1016/j.jco.2014.09.001.

[50] A. Kanjarla et al. "Study of internal lattice strain distributions in stainless steel using a full-field elasto-viscoplastic formulation based on fast Fourier transforms". In: *Acta Materialia* 60.6 (2012), pp. 3094–3106. DOI: 10.1016/j.actamat.2012.02.014.

[51] E. Kröner. *Statistical Continuum Mechanics*. Springer-Verlag, Wien, 1971. DOI: 10.1007/978-3-7091-2862-6.

[52] N. Lahellec et al. "Analysis of inhomogeneous materials at large strains using fast Fourier transforms". In: *IUTAM symposium on computational mechanics of solid materials at large strains*. Springer. 2003, pp. 247–258. DOI: 10.1007/978-94-017-0297-3_22.

[53] D. Langemann and J. Prestin. "Multivariate periodic wavelet analysis". In: *Applied and Computational Harmonic Analysis* 28.1 (2010), pp. 46–66. DOI: 10.1016/j.acha.2009.07.001.

[54] R. Lebensohn et al. "Dilatational viscoplasticity of polycrystalline solids with intergranular cavities". In: *Philosophical Magazine* 91.22 (2011), pp. 3038–3067. DOI: 10.1080/14786435.2011.561811.

[55] R. A. Lebensohn, M. I. Idiart, and P. P. Castañeda. "Modeling microstructural effects in dilatational plasticity of polycrystalline materials". In: *Procedia IUTAM* 3 (2012), pp. 314–330. DOI: 10.1016/j.piutam.2012.03.020.

[56] R. A. Lebensohn, A. K. Kanjarla, and P. Eisenlohr. "An elasto-viscoplastic formulation based on fast Fourier transforms for the prediction of micromechanical fields in polycrystalline materials". In: *International Journal of Plasticity* 32 (2012), pp. 59–69. DOI: 10.1016/j.ijplas.2011.12.005.

[57] R. A. Lebensohn, A. D. Rollett, and P. Suquet. "Fast Fourier transform-based modeling for the determination of micromechanical fields in polycrystals". In: *JOM Journal of the Minerals, Metals and Materials Society* 63.3 (2011), pp. 13–18. DOI: 10.1007/s11837-011-0037-y.

[58] S.-B. Lee, R. Lebensohn, and A. D. Rollett. "Modeling the viscoplastic micromechanical response of two-phase materials using Fast Fourier Transforms". In: *International Journal of Plasticity* 27.5 (2011), pp. 707–727. DOI: 10.1016/j.ijplas.2010.09.002.

[59] G Lefebvre et al. "Accounting for local interactions in the prediction of roping of ferritic stainless steel sheets". In: *Modelling and Simulation in Materials Science and Engineering* 20.2 (2012), p. 024008. DOI: 10.1088/0965-0393/20/2/024008.

[60] A Liebscher et al. "Modelling open cell foams based on 3D image data". In: *20th International Conference on Composite Materials*. 2015. URL: http://iccm20.org/fullpapers/file?f=vvg2RO3nqw.

[61] A. Liebscher. "Stochastic Modelling of Foams". Dissertation. Technische Universität Kaiserslautern, 2014. ISBN: 978-3-8396-0789-3. URL: http://www.verlag.fraunhofer.de/bookshop/buch/Stochastic-Modelling-of-Foams/242168.

[62] B. A. Lippmann and J. Schwinger. "Variational principles for scattering processes. I". In: *Physical Review* 79.3 (1950), p. 469. DOI: 10.1103/PhysRev.79.469.

[63] B Liu et al. "Comparison of finite element and fast Fourier transform crystal plasticity solvers for texture prediction". In: *Modelling and Simulation in Materials Science and Engineering* 18.8 (2010), p. 085005. DOI: 10.1088/0965-0393/18/8/085005.

[64] D. Merkert. "Voxel-based fast solution of the Lippmann-Schwinger equation with smooth material interfaces". Master thesis. Technische Universität Kaiserslautern, 2013. URL: http://www.mathematik.uni-kl.de/fileadmin/AGs/das/Merkert/201309_masterarbeit.pdf.

[65] D. Merkert et al. "An Efficient Algorithm to Include Sub-Voxel Data in FFT-Based Homogenization for Heat Conductivity". In: *Recent Trends in Computational Engineering-CE2014*. Springer International Publishing, 2015, pp. 267–279. DOI: 10.1007/978-3-319-22997-3_16.

[66] D. Merkert et al. "Voxel-based fast solution of the Lippmann-Schwinger equation with smooth material interfaces". In: *PAMM* 14.1 (2014), pp. 579–580. DOI: 10.1002/pamm.201410277.

[67] J. Michel, H Moulinec, and P Suquet. "A computational method based on augmented Lagrangians and fast Fourier transforms for composites with high contrast". In: *Computer Modelling in Engineering & Sciences* 1.2 (2000), pp. 79–88. DOI: 10.3970/cmes.2000.001.239.

[68] J. Michel, H Moulinec, and P Suquet. "A computational scheme for linear and non-linear composites with arbitrary phase contrast". In: *International Journal for Numerical Methods in Engineering* 52.1-2 (2001), pp. 139–160. DOI: 10.1002/nme.275.

[69] G. W. Milton. *The theory of composites*. Vol. 6. Cambridge University Press, 2002. DOI: 10.1017/CBO9780511613357.

[70] N. Mishra, J. Vondřejc, and J. Zeman. "A comparative study on low-memory iterative solvers for FFT-based homogenization of periodic media". In: *Journal of Computational Physics* 321 (2016), pp. 151–168. DOI: 10.1016/j.jcp.2016.05.041.

[71] V. Monchiet. "Combining FFT methods and standard variational principles to compute bounds and estimates for the properties of elastic composites". In: *Computer Methods in Applied Mechanics and Engineering* 283 (2015), pp. 454–473. DOI: 10.1016/j.cma.2014.10.005.

[72] V. Monchiet and G. Bonnet. "Numerical homogenization of nonlinear composites with a polarization-based FFT iterative scheme". In: *Computational Materials Science* 79 (2013), pp. 276–283. DOI: 10.1016/j.commatsci.2013.04.035.

[73] H. Moulinec and P. Suquet. "A fast numerical method for computing the linear and nonlinear mechanical properties of composites". In: *Comptes rendus de l'Académie des sciences. Série II, Mécanique, Physique, Chimie, Astronomie* 318.11 (1994), pp. 1417–1423.

[74] H. Moulinec and P. Suquet. "A numerical method for computing the overall response of nonlinear composites with complex microstructure". In: *Computer Methods in Applied Mechanics and Engineering* 157.1-2 (1998), pp. 69–94. DOI: 10.1016/s0045-7825(97)00218-1.

[75] H. Moulinec and F. Silva. "Comparison of three accelerated FFT-based schemes for computing the mechanical response of composite materials". In: *International Journal for Numerical Methods in Engineering* 97.13 (2014), pp. 960–985. DOI: 10.1002/nme.4614.

[76] J. S. Nagra et al. "Efficient fast Fourier transform-based numerical implementation to simulate large strain behavior of polycrystalline materials". In: *International Journal of Plasticity* 98 (2017), pp. 65–82. DOI: 10.1016/j.ijplas.2017.07.001.

[77] A. Nikishin and D. Nikolaev. "Calculation of averaged elastic properties of materials having noncircular character of pole figures". In: *Crystallography Reports* 53.3 (2008), pp. 493–496. DOI: 10.1134/S1063774508030188.

[78] G. Pöplau. "Multivariate periodische Interpolation durch Translate und deren Anwendung". German. Dissertation. Universität Rostock, 1995.

[79] G. Poplau and F. Sprengel. "Some error estimates for periodic interpolation on full and sparse grids". In: *in Curves and Surfaces with Applications in CAGD*. 1997. URL: http://citeseerx.ist.psu.edu/viewdoc/summary?doi=10.1.1.45.5567.

[80] D. Potts and T. Volkmer. "Sparse high-dimensional FFT based on rank-1 lattice sampling". In: *Applied and Computational Harmonic Analysis* 41.3 (2016), pp. 713–748. DOI: 10.1016/j.acha.2015.05.002.

[81] A Prakash and R. Lebensohn. "Simulation of micromechanical behavior of polycrystals: finite elements versus fast Fourier transforms". In: *Modelling and Simulation in Materials Science and Engineering* 17.6 (2009), p. 064010. DOI: 10.1088/0965-0393/17/6/064010.

[82] J. Prestin and K. Selig. "Interpolatory and orthonormal trigonometric wavelets". In: *Signal and Image Representation in Combined Spaces*. Ed. by Y. Zeevi and R. Coifman. Vol. 7. Wavelet Analysis and Its Applications. Academic Press, 1998, pp. 201–255. DOI: 10.1016/S1874-608X(98)80009-5.

[83] A Reuss. "Berechnung der Fließgrenze von Mischkristallen auf Grund der Plastizitätsbedingung für Einkristalle." In: *ZAMM-Journal of Applied Mathematics and Mechanics/Zeitschrift für Angewandte Mathematik und Mechanik* 9.1 (1929), pp. 49–58. DOI: 10.1002/zamm.19290090104.

[84] C. Robert and C. Mareau. "A comparison between different numerical methods for the modeling of polycrystalline materials with an elastic-viscoplastic behavior". In: *Computational Materials Science* 103 (2015), pp. 134–144. DOI: 10.1016/j.commatsci.2015.03.028.

[85] A. Rollett et al. "Stress hot spots in viscoplastic deformation of polycrystals". In: *Modelling and Simulation in Materials Science and Engineering* 18.7 (2010), p. 074005. DOI: 10.1088/0965-0393/18/7/074005.

[86] W. Rudin. *Fourier analysis on groups*. Courier Dover Publications, 2017. ISBN: 978-0-4868-1365-3.

[87] Y. Saad. *Iterative methods for sparse linear systems*. SIAM, 2003. ISBN: 978-0-89871-534-7. DOI: 10.1137/1.9780898718003.

[88] M. Schneider. "An FFT-based fast gradient method for elastic and inelastic unit cell homogenization problems". In: *Computer Methods in Applied Mechanics and Engineering* 315 (2017), pp. 846–866. DOI: 10.1016/j.cma.2016.11.004.

[89] M. Schneider. "Convergence of FFT-based homogenization for strongly heterogeneous media". In: *Mathematical Methods in the Applied Sciences* 38.13 (2015), pp. 2761–2778. DOI: 10.1002/mma.3259.

[90] M. Schneider, D. Merkert, and M. Kabel. "FFT-based homogenization for microstructures discretized by linear hexahedral elements". In: *International Journal for Numerical Methods in Engineering* (2016). DOI: 10.1002/nme.5336.

[91] M. Schneider, F. Ospald, and M. Kabel. "Computational homogenization of elasticity on a staggered grid". In: *International Journal for Numerical Methods in Engineering* (2015). DOI: 10.1002/nme.5008.

[92] K. Selig. "Periodische Wavelet-Packets und eine gradoptimale Schauderbasis". German. Dissertation. Universität Rostock, 1998. ISBN: 978-3-8265-3491-1.

[93] W. Sickel and F. Sprengel. "Some error estimates for periodic interpolation of functions from Besov spaces". In: *convergence* 10 (1998).

[94] F. Sprengel. "A class of periodic function spaces and interpolation on sparse grids". In: *Numerical functional analysis and optimization* 21.1-2 (2000), pp. 273–293. DOI: 10.1080/01630560008816955.

[95] F. Sprengel. "Interpolation und Waveletzerlegung multivariater periodischer Funktionen". German. Dissertation. Universität Rostock, 1997.

[96] G. Strang. "Variational crimes in the finite element method". In: *The mathematical foundations of the finite element method with applications to partial differential equations* (1972), pp. 689–710. DOI: 10.1016/B978-0-12-068650-6.50030-7.

[97] G. Strang and G. Fix. "A Fourier analysis of the finite element variational method". In: *Constructive aspects of functional analysis* (2011), pp. 793–840. DOI: 10.1007/978-3-642-10984-3_7.

[98] T.-H. Tran, V. Monchiet, and G. Bonnet. "A micromechanics-based approach for the derivation of constitutive elastic coefficients of strain-gradient media". In: *International Journal of Solids and Structures* 49.5 (2012), pp. 783–792. DOI: 10.1016/j.ijsolstr.2011.11.017.

[99] H. Triebel. *Theory of Function Spaces*. Birkhäuser Basel, 1983. ISBN: 978-3-0346-0415-4. DOI: 10.1007/978-3-0346-0416-1.

[100] V Vinogradov and G. Milton. "An accelerated FFT algorithm for thermoelastic and non-linear composites". In: *International Journal for Numerical Methods in Engineering* 76.11 (2008), pp. 1678–1695. DOI: 10.1002/nme.2375.

[101] W. Voigt. "Ueber die Beziehung zwischen den beiden Elasticitätsconstanten isotroper Körper". In: *Annalen der Physik* 274.12 (1889), pp. 573–587. DOI: 10.1002/andp.18892741206.

[102] J Vondrejc. "FFT-based method for homogenization of periodic media: Theory and applications". PhD thesis. Czech Technical University in Prague, 2013. URL: https://pdfs.semanticscholar.org/5cf3/a69eedfb1e6ee260e30a02a28a899faaea46.pdf.

[103] J. Vondřejc. "Improved guaranteed computable bounds on homogenized properties of periodic media by the Fourier-Galerkin method with exact integration". In: *International Journal for Numerical Methods in Engineering* 107.13 (2016), pp. 1106–1135. DOI: 10.1002/nme.5199.

[104] J. Vondřejc and T. de Geus. *Energy-based comparison between Fourier-Galerkin and finite element method within numerical homogenisation*. 2017. arXiv: 1709.08477.

[105] J. Vondřejc, J. Zeman, and I. Marek. "An FFT-based Galerkin method for homogenization of periodic media". In: *Computers & Mathematics with Applications* 68.3 (2014), pp. 156–173. DOI: 10.1016/j.camwa.2014.05.014.

[106] J. Vondřejc, J. Zeman, and I. Marek. "Analysis of a fast Fourier transform based method for modeling of heterogeneous materials". In: *International Conference on Large-Scale Scientific Computing*. Springer. 2011, pp. 515–522. DOI: 10.1007/978-3-642-29843-1_58.

[107] J. Vondřejc, J. Zeman, and I. Marek. "Guaranteed upper–lower bounds on homogenized properties by FFT-based Galerkin method". In: *Computer Methods in Applied Mechanics and Engineering* 297 (2015), pp. 258–291. DOI: 10.1016/j.cma.2015.09.003.

[108] F. Willot. "Fourier-based schemes for computing the mechanical response of composites with accurate local fields". In: *Comptes Rendus Mécanique* 343.3 (2015), pp. 232–245. DOI: 10.1016/j.crme.2014.12.005.

[109] K. Yoshida. *Functional Analysis*. Classics in mathematics. World Publishing Company, 1980. ISBN: 978-0-3871-0210-8. URL: https://books.google.de/books?id=1zewQgAACAAJ.

[110] R. Zeller and P. Dederichs. "Elastic Constants of Polycrystals". In: *Physica status solidi A* 55.2 (1973), pp. 831–842. DOI: 10.1002/pssb.2220550241.

[111] J. Zeman et al. "A finite element perspective on nonlinear FFT-based micromechanical simulations". In: *International Journal for Numerical Methods in Engineering* (2017). DOI: 10.1002/nme.5481.

[112] J. Zeman et al. "Accelerating a FFT-based solver for numerical homogenization of periodic media by conjugate gradients". In: *Journal of Computational Physics* 229.21 (2010), pp. 8065–8071. DOI: 10.1016/j.jcp.2010.07.010.

Academic curriculum vitae

2008 **Abitur**, *Alfred-Amann-Gymnasium*, Bönnigheim.

2011 **Bachelor of Science**, *Technische Universität Kaiserslautern*, Department of Mathematics.
"Numerische Lösung von DAEs zur Modellierung mechanischer Systeme am Beispiel eines rückwärtsfahrenden Wagens mit Anhänger" supervised by Prof. Dr. Tobias Damm

2013 **Master of Science**, *Technische Universität Kaiserslautern*, Department of Mathematics.
"Voxel-based fast solution of the Lippmann-Schwinger equation with smooth material interfaces" supervised by Prof. Dr. Bernd Simeon

since 2013 **Research and teaching assistant**, *Technische Universität Kaiserslautern*, Department of Mathematics.

2018 **Dr. rer. nat.**, *Technische Universität Kaiserslautern*, Department of Mathematics.
Supervisor Prof. Dr. Bernd Simeon

Wissenschaftlicher Lebenslauf

2008 **Abitur**, *Alfred-Amann-Gymnasium*, Bönnigheim.

2011 **Bachelor of Science**, *Technische Universität Kaiserslautern*, Fachbereich Mathematik.
"Numerische Lösung von DAEs zur Modellierung mechanischer Systeme am Beispiel eines rückwärtsfahrenden Wagens mit Anhänger" betreut von Prof. Dr. Tobias Damm

2013 **Master of Science**, *Technische Universität Kaiserslautern*, Fachbereich Mathematik.
"Voxel-based fast solution of the Lippmann-Schwinger equation with smooth material interfaces" betreut von Prof. Dr. Bernd Simeon

seit 2013 **Wissenschaftlicher Mitarbeiter**, *Technische Universität Kaiserslautern*, Fachbereich Mathematik.

2018 **Dr. rer. nat.**, *Technische Universität Kaiserslautern*, Fachbereich Mathematik.
Betreuer Prof. Dr. Bernd Simeon